ISSN

INTERNATIONAL JOURNAL OF RESEARCH IN APPLIED SCIENCES

Vol. 2 Issue 1 (Jan-June)-2025

Research & Development Cell
GITA Autonomous College, Bhubaneswar
Badaraghunathpur, Odisha, India, 752054

INTERNATIONAL JOURNAL OF RESEARCH IN APPLIED SCIENCES

Published by

Research & Development Cell

GITA Autonomous College, Bhubaneswar

Badaraghunathpur, Odisha, India, 752054

Website : www.ijras.edu.in

Email : ijras@gita.edu.in

International Journal of Research in Applied Sciences

Vol 2 Issue 1 (January– June) 2025

EDITORIAL ADVISORY BOARD

Published by GITA R & D cell, on behalf GITA Autonomous College, Bhuhaneswar-752054. International Journal of Research in Applied Sciences is issued bimonthly by GITA R & D cell, GITA and assumes no responsibility for the statements and opinions advanced by the contributors. The editorial staff in the work of examining papers received for publication is assisted, in an honorary capacity, by a large number of distinguished scientists and engineers.

Communications regarding contributions for publication in the journal should be addressed to the Editor-in-Chief: International Journal of Research in Applied Sciences. GITA R & D Cell, GITA Autonomous College, Bhuhaneswar-752054. Correspondence regarding subscriptions and advertisement should he addressed to the Sales & Distribution Officer, GITA R & D Cell, GITA Autonomous College, Bhuhaneswar-752054. Badaraghunathpur, Bhubaneswar 752054. Annual subscription: Rs. 2000/- $290 Single Copy: Rs.300, $50 (inclusive of first-class mail). For inland outstation cheque, please add Rs. 50 /- and for foreign cheque, please add $ 10.00. Payment in respect of subscriptions and advertisements may be sent by cheque / bank draft, payable to GITA R & D Cell, GITA Autonomous College, Bhuhaneswar-752054, Badaraghunathpur. Bank charges shall be borne by subscriber.

Claims for missing numbers of the journal will be allowed only if received within 3 months of the date of issue of the journal plus the time normally required for postal delivery of the journals and the claim.

International Journal of Research in Applied Sciences
Vol. 2 Issue 1 (January -June) 2025

Editorial First Issue

With this first issue, we are very pleased to announce the launch of the International Journal of Research in Applied Sciences, sponsored by GITA Autonomous College, Bhubaneswar.

The International Journal of Research in Applied Sciences (IJRAS) aims to address this need and to be the main international forum for publishing papers on applied sciences and the journal intends to primarily publish papers from various disciplines illustrating different emerging technologies with real world applications.

The IJRIAS will be published bi-monthly. The abstracts of the published papers, and sometimes the full papers will be available on-line on the journal page of GITA website: www.ijras.in. The journal will contain original research papers on the topics listed in "Aims and Scope". Each paper will be thoroughly reviewed by independent reviewers.

Thanks are due to many people who have helped in starting up this new journal. We are particularly grateful to the Management of our institution, who provided us with a lot of support and advice. Further, we are also very much thankful to all our esteemed advisors, who will continue to Support us to represent the journal in their research areas. We are sure that their reputation and great expertise in the field will have a significant contribution in shaping up the journal and making IJRIAS a prestigious international journal.

It is also our great pleasure to welcome the members of the Editorial Board of IJRAS. We rely on their expertise for reviewing and accepting papers to the journal. Therefore, their contribution to the journal is invaluable and we are grateful to them for giving freely of their time to review papers for the journal. We hope they will continue to help us in the future.

We are convinced that with this unreserved support from such a prominent and large team of researchers the IJRIAS will become one of the most prestigious journals in the general area of applied sciences. We are fortunate to work with this team.

Finally, the Editors-in-chief wish to thank the authors who submitted papers to the first issue of IJRAS.
Any suggestion on how to improve our activity in order to deliver a better journal to the authors, readers and subscribers of this journal will be always very much appreciated.

Prof. (Dr.) Parimal Kumar Giri
June 2025, Editors-in-chief

International Journal of Research in Applied Sciences

Vol. 2 Issue 1 (January – June) 2025

CONTENTS

Editorial i

Papers

1. **Parametric Bianchi Type-III Spacetime with Cosmological Constant in the Context of General Relativity** 1
   Shantanu Kumar Biswal, Madhusmita Rout, Rohit Kumar Sarangi,

2. **Power Management Strategy in Solar Electric Vehicle** 9
   Dr. Pradeep Kumar Rautray,Chinmaya Sahoo, Soumya Ranjan Das,Soumya Ranjan Sahoo,Baikuntha Biswal

3. **An Empirical Analysis of UPI-Based Payment Adoption Behaviour Among Young Adults (GEN Z) in Odisha** 19
   Dusmant Kumar Sahoo, B.C.M. Patnaik, Ipseeta Satpathy, Prasanta Kumar Sahu, Shiva Ram Patnaik

4. **Geometric Insights Leveraging Machine Learning for Wheat Grain Identification** 29
   Lipsarani Jena, Subhadra Pradhan

5. **MR Image Segmentation Using the Hybrid k-Mean Graph Cut Method** 40
   Jyotiprakash Dash, Ravikant Turi, Rekhanjali Sahoo, RednamSSJyothi, Manoj Kumar Sahu

6. **Development of Bio-Concrete using Agricultural Wastes** 49
   Sujit Kumar Panda, Chinmayananda Sahoo, Pranakrushna Parida

7. **Optimization of SAG Structure** 55
   Dilip Kumar Nayak, Prabodha Kumar Dalai, ParthaSarathi Das, Pradosh Kumar Hota, Srilata Basu

8. **Pollution from Biomass Cooking: A Comprehensive Analysis of Emission Patterns** 62
   Chandrika Samal, Sushmita Dash, P. K Jena, A. S Dehury, Manmatha K. Roul, Manoj.K Pradahn

9. **Prevention of DDoS attack using blockchain** 71
   Laxminarayan Dash, Manaswinee Madhumita Panda, Vivek Priyadarshi Dash, Priya Paul

10. **The Intersection of Gender and Abolition: An Analysis of Feminism in the Narratives of Frederick Douglass** 79
    Rasabihari Mishra, Pranati Das, Sudarsan Sahoo,Lyndon Dominic Thomas,Pritish Bhanja

11. Transformation of Healthcare systems in Smart Cities using IoT and Big Data Analytics **86**
Debasish Pradhan, Mamata Rath, Arup Kumar Mohanty, Sudeep Kumar Gochhhayat, Jayanta Kumar Mishra

12. Solving Fuzzy Number Travelling Salesman Problems with Linear Ranking Function **95**

K.K. Mishra, Rabindra Panda, Bijaya Mishra

Bianchi Type-III Spacetime with Cosmological Constant in the Context of General Relativity

Shantanu Kumar Biswal, Madhusmita Rout, Rohit Kumar Sarangi,
Department of Physics, GITA Autonomous College, Bhubaneswar, Odisha, India
{shantanu.4u4@gmail.com, madhusmitarout088@gmail.com,rohitrules01@gmail.com}

Abstract:

We have examined higher-dimensional Bianchi type-III cosmological models within the framework of general relativity, incorporating a cosmological constant, strange quark matter, and a string cloud. By considering various functional forms for the metric potentials, we derived multiple solution classes. The analysis demonstrates that these models describe an expanding, shearing, and non-rotating universe. Furthermore, a detailed study of the physical and kinematic properties of the models was carried out.

Keywords: Five-dimensional Bianchi type-111, Space time, Quark Matter, Cosmic strings, General relativity, Cosmological Constant

1. Introduction

The study of higher-dimensional cosmological models has gained significant attention due to its potential to address fundamental questions in theoretical physics, particularly in string theory, brane-world scenarios, and early universe cosmology. In this context, strange quark matter (SQM), described by the Bag Model Equation of State, plays a critical role in understanding the nature of dense matter at extreme conditions, such as those present in the early universe or compact astrophysical objects like strange stars. SQM, composed of up, down, and strange quarks, is theorized to be the most stable form of hadronic matter under high density [1-7].

The string cloud, a collection of one-dimensional topological defects, has also emerged as a vital component in modeling the universe's initial stages. Strings are believed to have formed during symmetry-breaking phase transitions in the early universe, and their interaction with matter provides a profound insight into the structural evolution of spacetime [8]. The cosmological constant (Λ) plays a critical role in our understanding of the universe's expansion [9-10]. It represents a homogeneous energy density that drives the accelerated expansion of the universe. The introduction of Λ alters the relationship between matter density and the expansion rate, impacting our understanding of a matter-dominated universe and influencing the growth of cosmic structures [11].

Observations of Type Ia supernovae with redshifts up to $z \leq 1$ have provided evidence that we exist in a universe with low mass density, where the density parameter for non-relativistic matter (Ωm) is approximately 0.3. However, most of the matter in the universe is not directly observed, suggesting the presence of additional energy components sufficient to bring the total density parameter to Ω (total) ≈ 1. This leads to the hypothesis that the missing energy is associated with vacuum energy density, often attributed to the cosmological constant Theoretical models and observations continue to explore this dynamic behavior of Λ, aiming to reconcile the cosmological constant's small present value with its

potential origins in early universe physics [12]. These studies are critical for deepening our understanding of dark energy, the accelerated expansion of the universe, and the interplay between matter and energy across cosmic timescales.

In this paper, we investigate the behavior of strange quark matter coupled to a string cloud in a five-dimensional Bianchi type-III spacetime within the framework of general relativity. Bianchi type-III models, characterized by their anisotropy and spatial homogeneity, offer a versatile framework for exploring the dynamics of the universe beyond the standard isotropic cosmological models [13-22]. The five-dimensional extension introduces new degrees of freedom that could help bridge the gap between general relativity and higher-dimensional theories.

By assuming specific functional forms for the metric potentials, we derive different classes of solutions and examine their physical and kinematic characteristics. The resulting models reveal behaviors such as expansion, shear, and the absence of rotation. This study offers important insights into the interaction between quark matter, string clouds, and anisotropic spacetimes, enhancing our understanding of cosmological evolution in higher-dimensional frameworks.

2. The metric and field equations

We take up the space time of five-dimensional Bianchi type-III metric in the form

$$ds^2= dt^2 – A^2dx^2 – B^2 e^{2ax} dy^2 – C^2 dz^2 – D^2 d\Psi^2 \quad (1)$$

Here, A, B, C, and D are the functions of time ‘t’ only.

The energy momentum tensor for string cloud is given by

$$T_{ij}=\rho u_i u_j-\rho_s x_i x_j \quad (2)$$

Hereρ is the rest energy density for the cloud of strings with particles coupled to them and ρ_s is the string tension density. They are given by

$$\rho=\rho_p+\rho_s \quad (3)$$

Where ρ_p is the particle energy density.

The various vibrational modes of the string represent the various types of particles because these modes are seen as various masses or spins. Therefore, we will consider quarks as a substitute particle in the string cloud. Hence, wetake strange quark matter energy density in the string cloud. So, equation (3) becomes

$$\rho= \rho_q+\rho_s+ B_c \quad (4)$$

The velocity u^iexplains the cloud velocity and x^icorresponds to the direction of anisotropy. Here I have considered the first Co-ordinate is space like.

$$\text{Where } u^i= (1,0,0,0,0) \quad (5)$$

Without loss of generality, Iselect

$X^i = (0,0,0,1,0)$.(6)

We haveu^i and x^i with gratifyingconditions

$U_i = -x_i x^i = 1$ and $U^i X_i = 0$ (7)

The Einstein's field equation is given by

$$R_{ij} - \frac{1}{2} R g_{ij} = -T_{ij} + \delta_i^j \Lambda \quad (8)$$

Using the equations (2) – (8), the field equation for metric (1) can be written as.

$$\frac{A'B'}{AB} + \frac{A'C'}{AC} + \frac{A'D'}{AD} + \frac{B'C'}{BC} + \frac{B'D'}{BD} + \frac{C'D'}{CD} - \frac{a^2}{A^2} = \rho + \wedge \quad (9)$$

$$\frac{B''}{B} + \frac{C''}{C} + \frac{D''}{D} + \frac{B'C'}{BC} + \frac{B'D'}{BD} + \frac{C'D'}{CD} = 0 \quad (10)$$

$$\frac{A''}{A} + \frac{C''}{C} + \frac{D''}{D} + \frac{A'C'}{AC} + \frac{A'D'}{AD} + \frac{C'D'}{CD} = 0 \quad (11)$$

$$\frac{A''}{A} + \frac{B''}{B} + \frac{D''}{D} + \frac{A'B'}{AB} + \frac{A'D'}{AD} + \frac{B'D'}{BD} - \frac{a^2}{A^2} = \rho_s + \wedge \quad (12)$$

$$\frac{A''}{A} + \frac{B''}{B} + \frac{C''}{C} + \frac{A'B'}{AB} + \frac{A'C'}{AC} + \frac{B'C'}{BC} - \frac{a^2}{A^2} = 0 \quad (13)$$

$$\frac{A'}{A} = \frac{B'}{B} \quad (14)$$

3. Solutions of field Equations

From equation (14) it can be shown that A = μB, where μ is an arbitrary constant. Sowe have five equations in six unknowns. For destinies' solutions we need one statementwe shall explore physically significant solutions of the field equations (9) – (14) by taking a simplifying statement to the field variables A,B,C,D.

For cleanness, I take μ = 1 and get

$A = B$ (15)

Using equation (18), (12)-(16) reduce to

$$\left(\frac{A'}{A}\right)^2 + 2\frac{A'C'}{AC} + 2\frac{A'D'}{AD} + \frac{C'D'}{CD} - \frac{a^2}{A^2} = \rho + \wedge \quad (16)$$

$$\frac{A''}{A} + \frac{C''}{C} + \frac{D''}{D} + \frac{A'C'}{AC} + \frac{A'D'}{AD} + \frac{C'D'}{CD} = 0 \quad (17)$$

$$2\frac{A''}{A} + \frac{D''}{D} + \left(\frac{A'}{A}\right)^2 + 2\frac{A'D'}{AD} - \frac{a^2}{A^2} = \rho_s + \wedge (18)$$

$$2\frac{A''}{A} + \frac{C''}{C} + \left(\frac{A'}{A}\right)^2 + 2\frac{A'C'}{AC} - \frac{a^2}{A^2} = 0 \quad (19)$$

Now to obtain a certain solution, one extra condition is desired. Sowe suppose a relation between metric Co-efficient given by

$$C = A^n \quad (20)$$

Where n is a constant. With help of equation (20) and solving equation (19). We get

$$A = K_3 (K_1 t + K_2)^{\frac{1}{N+1}} \quad (21)$$

Where $K_3 = (N+1)^{\frac{1}{N+1}}$

And $N = \frac{n^2+n+1}{n+2}$

From equations (25) and (24) , I obtain

$$C = K_4 \ (K_1 t + K_2)^{\frac{n}{N+1}} \quad (22)$$

Where $K_4 = (K_3)^n$

With help of equations (21) , equation (17) becomes

$$(K_1 t + K_2)^2 D'' + \left(\frac{K_1}{N+1}\right)(n+1)) \ \ (K_1 t + K_2) D'$$

$$+ \frac{{K_1}^2}{(N+1)^2}(n^2 - nN - N)D = 0 \quad (23)$$

Which on integration yields

$$D = C_1 (K_1 t + K_2)^{\frac{(N-n)+\sqrt{(N+n)^2+4(N-n^2)}}{2(N+1)}} \quad (24)$$

Or $$D = C_2 (K_1 t + K_2)^{\frac{(N-n)-\sqrt{(n+N)^2+4(N-n^2)}}{2(N+1)}} \quad (25)$$

Now the above solutions give two different set of models.

4. Set – I

With help of equations (21), (22) and (24), the Bianchi type-III cosmological model for strange quark matter coupled to string cloud in general relativity can be written as

$$ds^2 = dt^2 - {K_3}^2 (K_1 t + K_2)^{\frac{2}{N+1}}(dx^2 + e^{2ax} dy^2) - {K_4}^2 (K_1 t + K_2)^{\frac{2n}{N+1}} dz^2$$

$$- {C_1}^2 (K_1 t + K_2)^{\frac{(N-n)+\sqrt{(n+N)^2+4(N-n)^2}}{(N+1)}} dy^2$$

(26) Through a suitable choice of co-ordinates and constants of integration, the above equation (26) reduces to

$$ds^2 = \frac{dT^2}{{K_1}^2} - {K_3}^2 (T)^{\frac{2}{N+1}}(dx^2 + e^{2ax} dy^2) - {K_4}^2 (T)^{\frac{2n}{N+1}} dz^2$$

$$-{C_1}^2(T)^{\frac{(N-n)+\sqrt{(n+N)^2+4(N-n^2)}}{(N+1)}}d\psi^2 \quad (27)$$

Using equations (21), (22) and (24) an equation (16) and (18), we obtain.,

Strong tension density,

$$\rho_s = \frac{(1+q-2N+2p){K_1}^2}{(N+1)^2T^2} - \frac{a^2}{{K_3}^2(T)^{\frac{2}{N+1}}} = \wedge \quad (28)$$

and String energy density,

$$\rho = \frac{(1-2n+2p+np){K_1}^2}{(N+1)^2T^2} - \frac{a^2}{{K_3}^2(T)^{\frac{2}{N+1}}} = \wedge \quad (29)$$

Where $P = \frac{(N+1)+\sqrt{(n+N)^2+4(N-n^2)}}{2}$

And $q = P\left[\frac{-(N+n+2)+\sqrt{(n+N)^2+4(N-n^2)}}{2}\right]$

Now Particle density

$$\rho_p = \rho - \rho_s = \frac{(2n+np-q+2N){K_1}^2}{(N+1)^2T^2} \quad (30)$$

Quark energy density

$$\rho_q = \frac{(2n+np-q+2N){K_1}^2}{(N+1)^2T^2} - B_c \quad (31)$$

Quark Pressure

$$p_q = \frac{(2n+np-q+2N){K_1}^2}{3(N+1)^2T^2} - \frac{B_c}{3} \quad (32)$$

Special Volume

$$V^3 = {K_3}^2K_4C_1(T)^{\frac{(4+n+N)+\sqrt{(n+N)^2+4(N-n^2)}}{2(N+1)}}e^{ax} \quad (33)$$

At T = 0, the string tension density, string energy, scalar expansion, and shear scalar all diverge, indicating the universe begins at this point with an initial singularity. However, as T increases, these singularities vanish, and the model described in equation (27) remains free of singularities. At the initial momentum (T = 0), both the quark pressure and density are infinite, but they decrease as TTT grows. The special volume VVV is zero at T = 0 and approaches infinity as T→ ∞.

5. Set – II

With help of equations (20) (21) and (25), the Bianchi type-III cosmological model for strange quark matter coupled to string cloud in general relatively can be written as.

$$ds^2 = dt^2 - {K_3}^2(K_1t + K_2)^{\frac{2}{N+1}}(dx^2 + e^{2ax}dy^2) - {K_4}^2(K_1t + K_2)^{\frac{2n}{N+1}}dz^2$$
$$-{C_2}^2(K_1t + K_2)^{\frac{(N-n)-\sqrt{(n+N)^2+4(N-n)^2}}{(N+1)}}dy^2 \quad (34)$$

Through a suitable choice of co-ordinates and constants of integration, the above equation (34) reduces to

$$ds^2 = \frac{dT^2}{{K_1}^2} - {K_3}^2(T)^{\frac{2}{N+1}}(dx^2 + e^{2ax}dy^2) - {K_4}^2(T)^{\frac{2n}{N+1}}dz^2$$
$$-{C_2}^2(T)^{\frac{(N-n)-\sqrt{(n+N)^2+4(N-n^2)}}{(N+1)}}d\psi^2 \quad (35)$$

Using equations (21), (22) and (25) in equations (16) and (18), we obtain.,

Strong tension density

$$\rho_s = \frac{(1+s-2N+2r){K_1}^2}{(N+1)^2T^2} - \frac{a^2}{{K_3}^2(T)^{\frac{2}{N+1}}} \wedge \quad (36)$$

and String energy density

$$\rho = \frac{(1+2n+2r+nr){K_1}^2}{(N+1)^2T^2} - \frac{a^2}{{K_3}^2(T)^{\frac{2}{N+1}}} \wedge \quad (37)$$

Where $r = \frac{(N-n)-\sqrt{(n+N)^2+4(N-n^2)}}{2}$

And$s = r\left[\frac{-(N+n+2)-\sqrt{(n+N)^2+4(N-n^2)}}{2}\right]$Now Particle density

$$\rho_p = \rho - \rho_s = \frac{(2n+nr-s+2N){K_1}^2}{(N+1)^2T^2} \quad (38)$$

Quark energy density

$$\rho_q = \frac{(2n+nr-s+2N){K_1}^2}{(N+1)^2T^2} - B_c \quad (39)$$

Quark Pressure

$$p_q = \frac{(2n+nr-s+2N){K_1}^2}{3(N+1)^2T^2} - \frac{B_c}{3} \quad (40)$$

Special Volume

$$V^3 = {K_3}^2K_4C_2(T)^{\frac{(4+n+N)-\sqrt{(n+N)^2+4(N-n^2)}}{2(N+1)}}e^{ax} \quad (41)$$

The string tension density, string energy, scalar expansion and shear scalar turn into infinite for T=0 which represents that the universe starts at T=0. So they possess preliminary singularity. However, as T increases these singularities disappear but the model (35) has no singularities. At preliminary momentum (T=0),

quark pressure and density are infinite, then both decreases as T increases. The special volume 'V' is zero when T=0 and turns into infinite when $T\rightarrow\infty$.

6. Conclusion

This paper presents cosmological solutions to Einstein's field equations that incorporate expansion, rotation, and shear rotation. The ratio for our proposed model is significantly higher than its current value of 10-3. Experimental findings support and validate the model, particularly in explaining the early stages of the universe's evolution. Notably, it is striking that as the temperature T increases, both the scalar expansion θ and the shear scalar $\sigma 2$ decrease, eventually reaching zero as $T\rightarrow\infty$.

References

[1.] Ellis, G. F. R. (1971). "Relativistic Cosmology." In General Relativity and Cosmology, ed. by P. G. Bergmann, V. de Sabbata. Plenum Press, New York.

[2.] Wald, R. M. (1984). General Relativity. University of Chicago Press.

[3.] Sahoo, P. K., and Behera, B. (2014). "String Cloud and Black Hole Solutions in Bianchi Type-III Spacetime," Astrophysics and Space Science, 352(1), 231-239.

[4.] Mohanty, S. S., Patnaik, P., and Biswal, S. K. (2018), "Dynamics Of Anisotropic Bianchi Universe With Bulk," Viscous International Journal of Recent Scientific Research, 9(4), 25899-25902.

[5.] Sharif, M., and Abbas, G. (2014). "Bianchi Type III Cosmological Models with String Cloud," International Journal of Modern Physics D, 23(9), 1450075.

[6.] Nzioki, A. M., and Kariuki, G. M. (2018). "Exact Solutions of Bianchi Type-III Spacetime in Five Dimensions with String Cloud," General Relativity and Gravitation, 50(12), 1-11.

[7.] Candelas, P., and Weinberg, E. (1984). "Spinor Fields in Higher-Dimensional Spacetimes," Physics Letters B, 144(5), 301-305.

[8.] Biswal, S.K. (2018), "De Sitter universe described by a binary mixture with a variable cosmological constant λ ," Astrophys. Space Sci., 363 (4), 78.

[9.] Biswal, S. K. (2017) "Unified Cosmological Models For Dark Energy," The African Review of Physics, 12(8), 61-66.

[10.] Mishra, B., and Biswal, S. K. (2014). "Five-Dimensional Bianchi Type V I0 Dark Energy Cosmological Model in General Relativity," The African Review of Physics, 9(12), 77-83.

[11.] Romero, C., and Mena, F. (1997). "String Clouds in Cosmology," Classical and Quantum Gravity, 14, 2041-2049.

[12.] Sharif, M., and Abbas, G. (2021). "Exact Solutions of the Einstein Field Equations in the Presence of String Clouds in Bianchi Type III Spacetime," Astrophysics and Space Science, 366(1), 1-7.

[13.] Abbas, G., and Sharif, M. (2021). "Bianchi Type-III Cosmological Models with String Cloud Matter and Their Gravitational and Cosmological Implications," International Journal of Modern Physics D, 30(10), 2150113.

[14.] Jana, S., and Saha, D. (2020). "String Cloud in Five-Dimensional Black Hole Spacetime and Their Thermodynamic Behavior," Modern Physics Letters A, 35(17), 2050179.

[15.] Nzioki, A. M., Kariuki, G. M., and Machaca, S. (2022). "Cosmological Models with String Cloud in Bianchi Type-III Spacetime and Its Physical Properties," Journal of Cosmology and Astroparticle Physics (JCAP), 2022(12), 010.

[16.] Gasperini, M., and Veneziano, G. (1993). "String Theory and Cosmology," Physics Reports 373, 1-92.
[17.] Sen, A. (1990). "String Theory and Classical Field Theory," Physical Review D, 41(10), 3035-3042.
[18.] Kaluza, T. (1921). "ZumUnitätsproblem der Physik," Sitzungsberichte der Preußischen Akademie der Wissenschaften.
[19.] Karam, R., and Sharif, M. (2013). "Exact Solutions of Einstein Field Equations in the Presence of String Clouds," General Relativity and Gravitation, 45, 2537-2550.
[20.] Afonso, V. I., and Figueiredo, R. P. (2020). "Black Hole Solutions in Five-Dimensional Spacetimes with String Cloud Matter," Physical Review D, 101(10), 104035.

Power Management Strategy in Solar Electric Vehicle

[1]Pradeep Kumar Rautray, [2]Chinmaya Sahoo, [3] Soumya Ranjan Das,[4]Soumya Ranjan Sahoo,[5]Baikuntha Biswal
GITA Autonomous College, Bhubaneswar, Odisha, India,
{pkrautray@gita.edu.in, chinmayasahoo6326@gmail.com, soumyaranjandas457@gmail.com, soumya9337243@gmail.com, biswalbaikunthaO@gmail.com}

Abstract

This article takes use of the improvements in smart car power management systems as well as the difficulties that come with seasonal and environmental changes. It will be an independent vehicle with no environmental problems if we install a 230V charging connection as a reserve for rainy and overcast seasons. The car's roof contains solar panels that can power the motor's drive and electrify the internal battery. In Solar electrical vehicles (SEV), further integrated functions including the software, GPS technology, and power windows are also modifiable. An overview of solar electric vehicles, their operation, power management systems (PMS), and charging techniques is provided in this study. This research aims to investigate the use of a further voltage source inverter in an efficient power control system to drive multiple motors. This lessens the influence of emission pollutants like SO2, CO2, and NO2 on slowing down global warming by reducing the number of hours that IC engine-based drives operate.

Keywords: Power management, solar electric Car, fuel cell electric car, hybrid electric vehicle

1. Introduction

The greenhouse gases like NO2 and CO2 are the cause of rising temperatures and ecological problems. As a result, the Govt. India is pursuing numerous preventive steps like BS regulations. The most recent car models include catalytic converters in their exhaust systems and adhere to BS6 regulations as of 2020. In addition to these steps, the burning of fuel in internal combustion engine cars will release greenhouse gases. Thus, by embracing EV & SEV, we may eradicate this issue [1-2]. There are several types of electric vehicles, such as FCEVs and HEV.However, SEVs are powered by solar energy, which is converted into electric energy and used to operate the motor and charge the battery. With the help of cutting-edge technology, [3] we can install an intuitive operating system and add new functions to make driving a seamless experience, especially on lengthy trips. Because Indian roads are a combination of level, incline, and declinate, this paper includes an efficient power management system to control the speed of the drive system using a brushless DC (BLDC) motor and a three-phase squirrel cage induction motor.

The induction method engines are utilized to move the pointed paths, whereas BLDC motors are utilized to handle the inclinations. In India, steep slopes are uncommon and are handled by internal combustion engines (ICs). This lowers the need for IC engines and thereby lowers the cost of crude oil and emissions of greenhouse gases. PMS is achieved more successfully as a consequence of this optimization than by any previous hybrid approaches used. This dissertation uses two test case studies—a solar electric vehicle with a BLDC motor and a solar electric vehicle with a 3-phase squirrel cage induction motor—to illustrate the power output methodologies involving P5 and an i3 machine for result simulation.

2. Overview on SEV

In order for SEVs to perform the functions given to them, they are either entirely powered by solar panels or, more importantly, all of the interior elements are properly coupled to the power source. Solar arrays use a charge controller to provide direct electrical power to the battery or the power management system. Solar electricity can power not just cars but also other forms of transportation, such as buses. A SEV is equipped with a variety of devices, including energy consumption monitoring units, communication, navigation, and security.

2.1 Overview of HEV

Because the vehicle may run in traffic zones with a combustion engine added for steep inclinations thanks to the electric motors. When the IC engine of this kind of car starts, the electric motor in it shuts off and its battery pack begins to charge via an alternator that is attached to the ICE. The Install hybrid electric automobile (PHEV) charging system uses a battery pack, and the internal combustion engine (IC engine) acts as a backup power source that kicks in if the battery runs completely flat. The PHEV also has a power converter that aids in efficient battery charging and discharging.

2.2. Comparison between SEV and HEV

In contrast to the HEV, which is made up of parts like a battery pack, an ICE, a DC-DC converter, a power converter, and other components, the SEV is made up of solar cells, a maximum power point (MPPT), an amount of charge, or SOC, converter, and other components like a motor drive and motor [5].

2.2.1Components of SEV Solar panel

Multifaceted solar panels are employed in SEV construction as an affordable and straightforward solution. We can infer from Figure 1 that a combination of 1000 watt solar panels will be installed in SEVs to aid in the direct conversion of solar radiation into electrical energy.

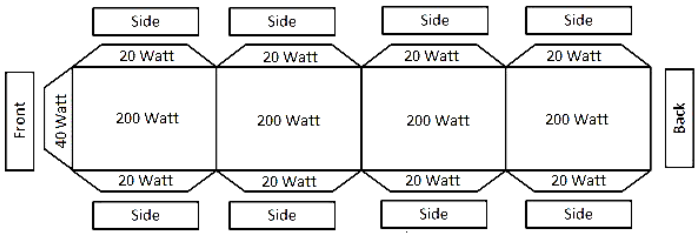

Fig-1 View of solar panel in SEV

MPPT & SOC

While the SOC controls battery charging and discharging, the MPPT is an electrical converter that aids in converting power and battery charge [6]. Maximum power point tracking, or MPPT, is typically utilized in HEVs [8] and electric vehicles [7].

Battery & Motor

Lithium ion batteries, sometimes referred to as battery packs because of their compact size and ability to lower temperatures, are used in SEVs. It requires a 48V, 20.83Ah battery in order to operate the car. SEVs typically use brushless DC motors (BLDC) to provide greater efficiency with decreased power usage [9].

2.2.2 Components of HEV

DC-DC Converter:

By momentarily retaining the input voltage and then releasing it at an output voltage that differs from the input, it transforms the direct current (DC) from a particular voltage to another [10]. There are two types of storage that are available: electric field storage and magnetic field storage.

Power converter

The power systems in EV [11] are separated and quasi-segregated converters. When there needs to be a minor ratio change in the voltage, the non-isolated kind is utilized. The five types of non-isolated converters are charge pump, buck, boost, buck-boost, and CUK. In an isolated converter, a high the frequency transformer is utilized.When the input and output must be totally separated, these converters are employed. Isolated power converters come in the form of half bridge, also known as full a bridge, fly-back, push pull, and forward converters. All converter is simultaneous with high step-up or step-down ratios.

3. Charging and operation of SEV

Typically, the solar panel mounted on the vehicle's roof provides power to SEVs [12–13]. The MPPT and SOC converters, which are coupled to a battery pack, are further connected to the polycrystalline solar panel utilized in SEVs. A type of DC-DC converter known as MPPT operates on the premise that altering the resistance of an identical load will also change the load's impedance. This DC converter can monitor changes in output due to the DC-duty motor's cycle. The fundamental MPPT network in this electrical framework is a BUCKS helicopter circuit, as seen in Figure 2. The following is the output of the Buck circuit:

Vout =D VinVin, Vout, and D, correspondingly, stand for input voltage, output voltage, and duty cycle.

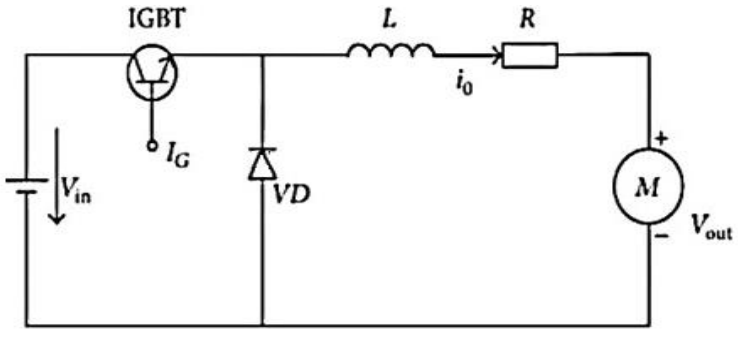

Fig-2 Buck chopper circuit

During the day, the solar panel can generate enough power to run the electric car [14–15] and charge the batteries at the same time. The vehicle's battery may discharge and provide electricity with the aid

of SOC. When there is a lack of sunshine, not only at night but also during overcast and rainy seasons, the pack of batteries can generate electricity by self-discharging. As an alternative source of power, we will install a 230V recharging socket [16], which aids in charging the car in the event that sunlight is unavailable for an extended amount of time. The air conditioning, electric window, GPS system, and movable seats are examples of interior features.

4. Power Management System & strategy

We provided a clear explanation of the power management system in this study using two test case studies. These two methodologies [17–18] for power management are linked to simple vehicle operating.

3.1 Test case-1 for SEV

We employed a forward conversion model with its simulation for a constant voltage output in this test scenario. This model can be used as an MPPT in the case of a SEV or as a DCDC converter in a HEV [19]. Figure 3 illustrates a forward rectifiers, which is used to enhance the conversion of power in DC-DC converters.

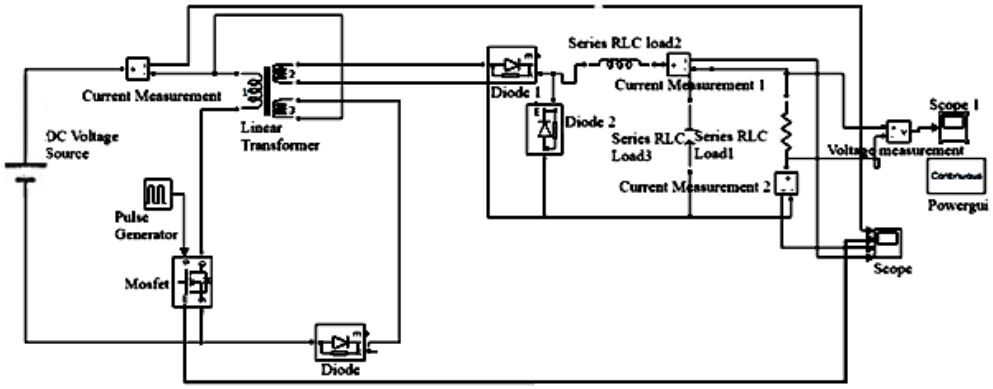

Fig-3 Simulink model of Forward Converter

Figure 4a shows the final result, or graph, for this conversion model and shows the voltage that is the production of the forward conversion, and Figure 4b shows the current output.

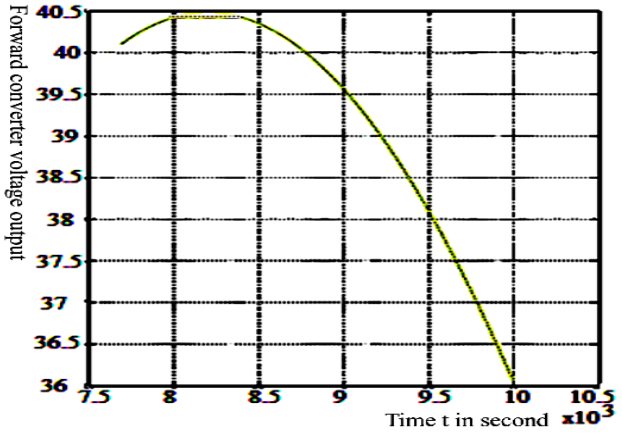

Fig.4a: Forward Converter Voltage Output

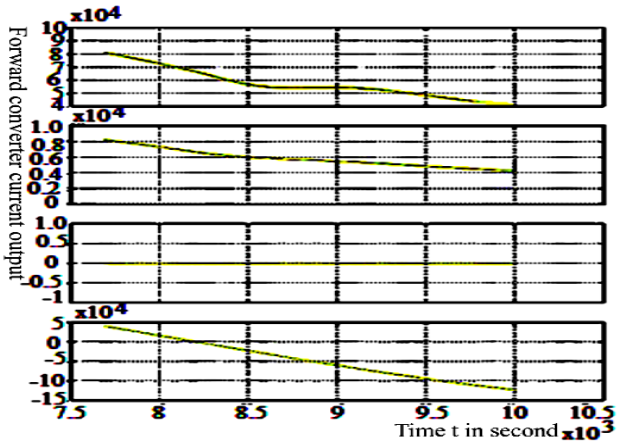

Fig.4b Forward converter's current output

SEV functions as a forward's converter when it uses a BLDC motor to provide strong torque at low power consumption. It can help with voltage input because it is essential to power conversion [20]. We can utilize forward converters in SEVs when variable / constant voltage is needed, just as they are used as DC-DC [21] converters of HEVs [22] for energy step upward and step down. It has the ability to accept power [23–25] from the battery as an input and supply the BLDC motor with a steady output voltage. Thus, test case 1 taught us that this model may be employed to obtain a constant voltage.

3.2 Test Case-2 for SEV

In order to convert DC to AC power and run a three-phase squirrels cage induction generator in a hybrid solar electric vehicle model, we used a DC / AC inverter modeling and its simulated graph in this test case study [26] (SEV). For all vehicles to operate on level tracks and heavily used routes, a strong engine with consistent torque is required. Figure 5 displays the Simulink model of the SEV inverter.

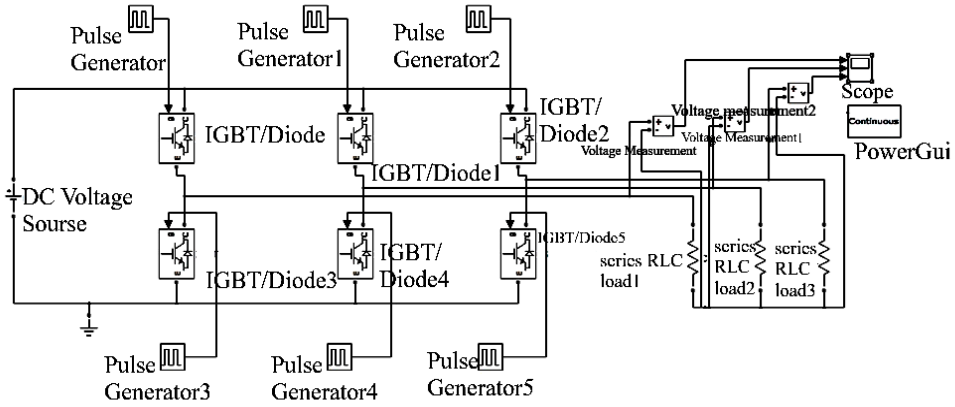

Fig-5 Simulink model of SEV inverter

This inverter model's output is presented in Figure 6.

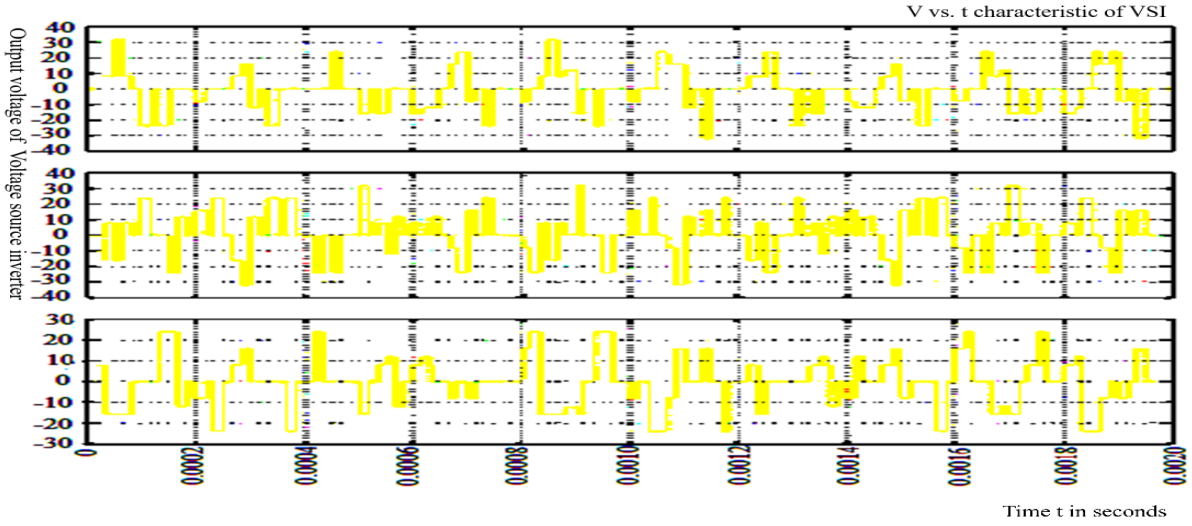

Fig.6 Output voltage of VSI

Installing this voltage supply inverter in a solar-powered electric vehicle with an induction motor coupled makes it easier for the vehicle to operate with less power consumption on uneven and steep terrain [27– 29]. When a SEV battery is discharged, the output DC power charges the voltage sensing instrument (VSI), which transforms DC to AC and charges the load. The solar panel is going to charge the battery in the presence of SOC. An induction motor produces a steady torque. Thus, with the aid of VSI, it is able to get a continuous AC input from the energy source and work more effectively than BLDC on flat tracks and Indian highways with significant traffic with little power consumption.

5. Result Analysis

Both of the test case studies yield two output outcomes. For level railways and levelled inclination roads, those are SEVs [30-33] with BLDC motors that use DC-DC converters in power management systems (PMS) [34-35]. They can provide better pickup and torque while using less energy. An additional one is a SEV with a 3-phase induction motor and an energy source converter in PSM for Indian tracks. This one may provide a steady torque for high-traffic areas or routes while consuming little electricity [36-38]. Furthermore, if both types of vehicles can be combined into a single SEV [39-41], the hybrid solar electric vehicle (HSEV) will be able to operate in any kind of road condition [42-44] without the need for outside assistance. For example, when the BLDC motor starts, whether it is powered by direct solar or a battery, the vehicle will move smoothly on level inclinations and other rough surfaces. When a traffic area or high-traffic route approaches, the driver can switch to the induction motor operating system, which will give the automobile continuous torque and stability while using the least amount of energy possible by preventing the BLDC motor at that point. Users can therefore readily accept this kind of contemporary, hybrid [45-47] SEVs.

6. Conclusion

There will inevitably be more EVs upon the road as smart cities proliferate. EV charging has become a difficult problem. All linked EVs can have their charging needs met with a solar-powered charging station that also has a battery storage system and extra grid support. By using a converter station, charge controller, and voltage source inverter (VSI) to keep the voltage on the DC bus constant for the station, required power can be achieved by voltage control. MATLAB/Simulink is used to clarify and validate the selected station's design and power management. This has a large power rating and can be used to power EV outlets at parking lots and workplaces. The case study using a simulation in Simulink to design a SEV with a hybrid concept that includes an IC engine, BLDC motor, converter, squirrel cage introduction motor, and VSI, among other components, shows that this is the best effortless vehicle for individuals with disabilities and that it has the best power management strategy, which contributes to green transportation. The foundation for largely reducing the use of fossil fuels to halt global warming is the constant speed, variable speed, and expedited speed for levelled tracks, inclined tracks, and steep hilly sections that are abundant in Indian road maps.

References

[1.] Tie, S. F., and Tan, C. W., "A Review of Power and Energy Management Strategies in Electric Vehicles," *2012 4th International Conference on Intelligent and Advanced Systems (ICIAS2012),* 2012, pp. 412–417.

[2.] Chen, H., Lu, F., and Guo, F., "Power Management System Design for Small Size Solar-Electric Vehicle," *2012 IEEE 7th International Power Electronics and Motion Control Conference - ECCE Asia*, 2012, pp. 2658–2662.

[3.] Ganji, B., and Kouzani, A. Z., "A Study on Look-ahead Control and Energy Management Strategies in Hybrid Electric Vehicles," *2010 8th IEEE International Conference on Control and Automation (ICCA)*, 2010, pp. 388–392.

[4.] Salmasi, F. R., "Control Strategies for Hybrid Electric Vehicles: Evolution, Classification, Comparison, and Future Trends," *IEEE Transactions on Vehicular Technology*, vol. 56, 2007, pp. 2393–2404.

[5.] Rosario, L., Luk, P. C. K., Economou, J. T., and White, B. A., "A Modular Power and Energy Management Structure for Dual-Energy Source Electric Vehicles," *IEEE Vehicle Power and Propulsion Conference*, 2006, pp. 1–6.

[6.] Iversen, E. B., Morales, J. M., and Madsen, H., "Optimal Charging of an Electric Vehicle Using a Markov Decision Process," *Applied Energy*, vol. 123, 2014, pp. 1–12.

[7.] Tsai, C.-S., and Ting, C.-H., "Evaluation of a Multi-Power System for an Electric Vehicle," *International Conference on Control, Automation and Systems 2010*, 2010, pp. 1308–1311.

[8.] Salazar, M., and Ertugrul, N., "Potential Enhancements for Vehicle Electrical Power Management Systems in Military Vehicles," *Australasian Universities Power Engineering Conference, AUPEC 2013*, 2013, pp. 1–6.

[9.] Tsai, M.-F., Tseng, C.-S., and Lin, Y.-H., "Power Management and Control of an Electric Vehicle with Auxiliary Fuel Cell and Wind Energies," *2013 IEEE Region 10 Conference (31194)*, 2013, pp. 1–4.

[10.] Choi, M.-E., Lee, J.-S., and Woo, S., "Real-time Optimization for Power Management Systems of a Battery/Supercapacitor Hybrid Energy Storage System in Electric Vehicles," *IEEE Transactions on Vehicular Technology*.

[11.] Xin, L., and Williamson, S. S., "Assessment of Efficiency Improvement Techniques for Future Power Electronics Intensive Hybrid Electric Vehicle Drive Trains," *Electrical Power Conference, 2007. EPC 2007. IEEE Canada*, 2007, pp. 268–273.

[12.] Nelson, L. J.-S., and Nelson, D. J., "Energy Management Power Converters in Hybrid Electric and Fuel Cell Vehicles," *Proceedings of the IEEE*, vol. 95, 2007, pp. 766–777.

[13.] Pisu, P., Koprubasi, K., and Rizzoni, G., "Energy Management and Drivability Control Problems for Hybrid Electric Vehicles," *44th IEEE Conference on Decision and Control, and the European Control Conference*, 2005, pp. 1824–1830.

[14.] Paganelli, G., Tateno, M., Brahma, A., Rizzoni, G., and Guezennec, Y., "Control Development for a Hybrid-electric Sport-Utility Vehicle: Strategy Implementation and Field Test Results," *Proc. American Control Conference, Arlington, VA*, 2001, pp. 5064–5069.

[15.] Paganelli, G., Ercole, G., Brahma, A., Guezennec, Y., and Rizzoni, G., "General Supervisory Control Policy for the Energy Optimization of Charge Sustaining Hybrid Electric Vehicles," *JSAE Review*, vol. 22, 2001, pp. 511–518.

[16.] Pisu, P., Musardo, C., Staccia, B., and Rizzoni, G., "A Comparative Study of Supervisory Control Strategies for Hybrid Electric Vehicles," *IEEE Transactions on Control Systems Technology*, vol. 15, no. 3, 2007, pp. 506–518.

[17.] Pisu, P., Rizzoni, G., and Calo', E., "Control Strategies for Parallel Hybrid Electric Vehicles," *IFAC'04, Salerno, Italy*, 19–23 Apr. 2004, pp. 508–513.

[18.] Malikopoulos, A. A., "Supervisory Power Management Control Algorithms for Hybrid Electric Vehicles: A Survey," *IEEE Transactions on Intelligent Transportation Systems*.

[19.] Malikopoulos, A. A., *Real-Time, Self-Learning Identification and Stochastic Optimal Control of Advanced Powertrain Systems*, Ann Arbor, MI, USA: ProQuest, Sep. 2011.

[20.] Cao, Y., Tang, S., Li, C., et al., "An Optimized EV Charging Model Considering TOU Price and SOC Curve," *IEEE Transactions on Smart Grid*, vol. 3, no. 1, 2011, pp. 388–393.

[21.] Guilbert, D., Gaillard, I. A., N'Diaye, A., and Djerdir, A., "Energy Efficiency and Fault Tolerance Comparison of DC/DC Converter Topologies for Fuel Cell Electric Vehicles," *Transportation Electrification Conference and Expo (ITEC)*, 2013 IEEE, pp. 1–7.

[22.] Xu, L.-F., Hua, J.-F., Li, X.-J., Meng, Q.-R., Li, J.-Q., and Ouyang, M. G., "Control Strategy Optimization of a Hybrid Fuel Cell Vehicle with Braking Energy Regeneration," *IEEE Vehicle Power and Propulsion Conference*, Sept. 3–5, Harbin, China, 2008.

[23.] Jiang, W., and Fahimi, B., "Active Current Sharing and Source Management in Fuel Cell-Battery Hybrid Power System," *IEEE Transactions on Industrial Electronics*, vol. 57, no. 2, Feb. 2010, pp. 752–761.

[24.] Clement, K., Haesen, E., and Driesen, J., "Coordinated Charging of Multiple Plug-in Hybrid Electric Vehicles in Residential Distribution Grids," *Proc. Power Systems Conference and Exposition*, 2009, pp. 1–7.

[25.] Chen, S., and Tong, L., "iEMS for Large Scale Charging of Electric Vehicles Architecture and Optimal Online Scheduling," *Proc. IEEE International Conference on Smart Grid Communications (SmartGridComm)*, Nov. 2012, pp. 629–634.

[26.] Bansal, N., Kimbrel, T., and Pruhs, K., "Speed Scaling to Manage Energy and Temperature," *Journal of the ACM (JACM)*, vol. 54, no. 1, 2007, pp. 1–39.

[27.] Alonso, M., Amaris, H., Germain, J. G., and Galan, J. M., "Optimal Charging Scheduling of Electric Vehicles in Smart Grids by Heuristic Algorithms," *Energies*, vol. 7, 2014, pp. 2449–2475.

[28.] Chen, N., and Quek, T. Q. S., "Optimal Charging of Electric Vehicles in Smart Grid: Characterization and Valley-Filling Algorithms," *IEEE Smart GridComm 2012 Symposium*, pp. 13–18.

[29.] Carli, G., and Williamson, S. S., "Technical Considerations on Power Conversion for Electric and Plug-in Hybrid Electric Vehicle Battery Charging in Photovoltaic Installations," *IEEE Transactions on Power Electronics*, vol. 28, no. 12, Dec. 2013, pp. 5784–5792.

[30.] Denholm, P., Kuss, M., and Margolis, R. M., "Co-benefits of Large Scale Plug-in Hybrid Electric Vehicle and Solar PV Deployment," *Journal of Power Sources*.

[31.] Taha, Z., Passarella, R., and Sah, J. M., "A Review on Energy Management System of Solar Car," *Proc. 9th Asia Pacific Industrial Engineering & Management Systems Conference*, Malaysia, 2008.

[32.] Kassakian, J. G., Wolf, H.-C., Miller, J. M., and Hurton, C. J., "Automotive Electrical Systems Circa 2005," *IEEE Spectrum*, vol. 33, no. 8, Aug. 1996, pp. 22–27.

[33.] Lin, C.-C., Peng, H., Grizzle, J. W., and Kang, J.-M., "Power Management Strategy for a Parallel Hybrid Electric Truck," *IEEE Transactions on Control Systems Technology*, vol. 11, no. 6, Nov. 2003, pp. 839–849.

[34.] Hofman, T., and van Druten, R., "Energy Analysis of Hybrid Vehicle Powertrains," *Proc. IEEE International Symposium on Vehicle Power Propulsion*, Paris, France, Oct. 2004.

[35.] Maharana, H. S., and Dash, S. K., "Dual Objective Multi-constraint Swarm Optimization Based Advanced Economic Load Dispatch," *International Journal of Electrical and Computer Engineering*, vol. 11, no. 3, 2021, pp. 1924–1932.

[36.] Gachhayat, S. K., and Dash, S. K., "Modified Sub-gradient Based Combined Objective Technique and Evolutionary Programming Approach for Economic Dispatch Involving Valve-point Loading, Enhanced Prohibited Zones, and Ramp Rate Constraints," *International Journal of Electrical and Computer Engineering*, vol. 10, no. 5, 2020, pp. 5048–5057.

[37.] Maharana, H. S., and Dash, S. K., "Comparative Optimization Analysis of Ramp Rate Constriction Factor Based PSO and Electromagnetism-Based PSO for Economic Load Dispatch in Electric Power System," *Proc. 2019 International Conference on Applied Machine Learning (ICAML)*, 2019, pp. 63–68.

[38.] Dash, S. K., and Panda, C. K., "An Evolutionary Programming-Based Neuro-fuzzy Technique for Multi-objective Generation Dispatch with Non-smooth Characteristic Functions," *2nd International Conference on Electronics and Communication Systems (ICECS)*, 2015, pp. 1663–1674.

[39.] Dash, S. K., and Mohanty, S. N., "Multi-objective Economic Emission Load Dispatch with Nonlinear Fuel Cost and Noninferior Emission Level Functions for IEEE-118 Bus System," *2nd International Conference on Electronics and Communication Systems (ICECS)*, 2015, pp. 1663–1674.

[40.] Behera, S., Sahu, M. K., Dash, S. K., and Swain, S. K., "Optimizing Power of PV Module Using Modified MPPT for Standalone Load," *International Journal of Power Electronics and Drive Systems*, vol. 15, no. 2, 2024, pp. 1158–1166.

[41.] Das, S. R., Dash, S. K., and Panda, C. K., "An Adaptive Fuzzy Controller-Based Unit Commitment for the Optimal Operation of a Hybrid Microgrid Considering Renewable Energy Sources," *Journal of Modern Power Systems and Clean Energy*, vol. 11, no. 1, 2023, pp. 287–300.

[42.] Dash, S. K., Sahoo, S. K., and Das, S. R., "Dual-objective Combined Economic and Environmental Power Dispatch Using a Novel Hybrid Optimization Technique," *IET Renewable Power Generation*, vol. 17, no. 2, 2023, pp. 216–227.

[43.] Mohapatra, S., Dash, S. K., and Panda, C. K., "A Novel Hybrid Optimization Algorithm for Emission Constrained Economic Dispatch with Renewable Energy Integration in Smart Grid," *Sustainable Energy Technologies and Assessments*, vol. 58, no. 1, 2023, pp. 104052.

[44.] Dash, S. K., Behera, S. K., and Mohapatra, S., "A Novel Power Management Strategy for Autonomous Operation of Microgrid with Renewable Energy Integration," *Journal of Cleaner Production*, vol. 391, 2023, pp. 136004.

[45.] Behera, S. K., Dash, S. K., and Panda, C. K., "Economic Load Dispatch in Microgrid Using an Improved Whale Optimization Algorithm," *International Transactions on Electrical Energy Systems*, vol. 34, no. 3, 2024, pp. e12506.

[46.] Dash, S. K., Panda, C. K., and Behera, S., "An Effective Hybrid Optimization Algorithm for Economic Emission Dispatch with Renewable Energy Integration," *Energy Reports*, vol. 10, 2024, pp. 2437–2452.

[47.] Dash, S. K., Panda, C. K., and Behera, S. K., "An Efficient Economic Load Dispatch Model for Microgrid Using a Novel Optimization Algorithm," *International Journal of Electrical Power & Energy Systems*, vol. 146, 2024, pp. 108628.

[48.] Mohapatra, S., and Dash, S. K., "Hybrid Renewable Energy System Design Optimization Using Adaptive Genetic Algorithm," *IEEE Transactions on Smart Grid*, vol. 15, no. 3, 2024, pp. 2374–2384.

[49.] Dash, S. K., and Behera, S., "Implementation of a Novel Hybrid Optimization Algorithm for Economic Load Dispatch in Smart Grid Environment," *Renewable Energy*, vol. 208, 2024, pp. 1373–1386.

An Empirical Analysis of UPI-Based Payment Adoption Behaviour Among Young Adults (GEN Z) in Odisha

Dusmant Kumar Sahoo[1], B.C.M. Patnaik[2], Ipseeta Satpathy[3], Prasanta Kumar Sahu[4], Shiva Ram Patnaik[5]

[1]Dept. of MBA, GITA Autonomous College, Bhubaneswar, Odisha, India,
dusmant_mba@gita.edu.in
[2]Professor, KIIT School of Management, KIIT University, Odisha, India,
bcpatnaik@gmail.com
[3]Senior Professor, KIIT School of Management, KIIT University, Odisha, India,
Email:ipseeta@ksom.ac.in
[4]Assistant Professor, GITA Autonomous College, Bhubaneswar, Odisha, India,
Email:prasanta_mba@gita.edu.in
[5]Research Scholar, KIIT School of Management, KIIT University, Odisha, India,
Email:2381096@ksom.ac.in

Abstract:

This study explores the adoption behaviour of Unified Payments Interface (UPI)-based payment systems among Generation Z in Odisha, focusing on key factors such as perceived usefulness, financial incentives, and technological readiness. Employing a survey-based quantitative research methodology, data were collected from 185 respondents across Odisha to understand their behavioural intentions toward UPI usage. The findings reveal that technological readiness significantly influences adoption behaviour, followed by perceived usefulness and financial incentives. Regression analysis confirms a robust relationship between these variables and behavioural intention, with the model explaining 96.4% of the variance. The results underscore the importance of user-friendly, secure, and incentive-driven fintech solutions to foster adoption. This research provides actionable insights for fintech providers and policymakers, emphasizing the need for targeted strategies to enhance digital financial inclusivity among young adults. Future research could extend this analysis to other regions and generational cohorts to broaden understanding.

Keywords: -UPI, Digital Payments, Fintech, Adoption Behavior, Financial Incentives

1. Introduction

The financial ecosystem has witnessed an extraordinary transformation due to the rapid advancements in financial technology. This revolution encompasses innovative tools and systems that are redefining how individuals and businesses manage their financial operations, facilitating greater efficiency, accessibility, and convenience (Milian et al., 2019). Fintech, a term that encapsulates these advancements, has become a cornerstone of the modern financial landscape, and understanding the factors influencing its adoption has gained prominence in academic research (Frost, 2020). Numerous studies have examined determinants such as financial literacy, performance expectations, and business projections (Pertiwi & Purwanto, 2021). However, a particularly significant and underexplored area is the multifaceted relationship between high-quality customer service and the adoption of fintech solutions, especially among Generation X—a demographic positioned uniquely between the tech-savvy millennials and the more traditional baby boomers (Hill, 2018).

Generation X occupies a vital role in the financial services industry. As a demographic characterized by stable employment, significant purchasing power, and an increasing need for financial management as they approach retirement, their preferences and behaviours hold immense strategic value for fintech

providers (Lee & Kim, 2019). Unlike millennials and Gen Z, who grew up immersed in digital technology, Generation X was introduced to these advancements later in life. This delayed exposure has resulted in a distinctive blend of cautious adoption and adaptability toward fintech services (Mills & Groening, 2021). Their gradual embrace of digital tools has been shaped by their past experiences with traditional financial services, as well as their evolving familiarity with technological innovations over time (Groening et al., 2021).

One of the key factors influencing fintech adoption in this demographic is the quality of customer service they receive. Whether through human representatives, chatbots, or automated digital support systems, the customer service experience significantly impacts their perception of fintech platforms and their Technological Readiness in these services (Mahmoud et al., 2022). High-quality, personalized customer service is essential to addressing the unique needs of this group. For instance, fintech solutions tailored to offer retirement planning tools, budget management resources, and strategic investment advice resonate strongly with Generation X's practical approach to financial decision-making (Singh et al., 2022).Furthermore, research underscores that efficient and supportive customer service experiences can effectively mitigate concerns related to digital security, privacy, and the usability of technology—factors that often act as barriers to fintech adoption (Muganyi et al., 2022). By alleviating these concerns, fintech providers can foster a sense of Technological Readiness and reliability, encouraging Generation X to engage more actively with their platforms. This is especially important as fintech companies aim to expand their market reach beyond the inherently tech-savvy millennials and Gen Z (Abu Daqar et al., 2021).

Examining the interaction between customer service and fintech adoption among Generation X reveals that this demographic prefers personalized solutions that align with their lifestyle and long-term financial objectives (Singh et al., 2020). These preferences reflect their cautious yet analytical approach, which emphasizes the importance of Technological Readiness, usability, and relevance in financial products and services. Moreover, the ability of fintech platforms to adapt to and address the needs of Generation X represents an opportunity for financial institutions to enhance inclusivity, ensuring their services remain accessible and beneficial to diverse age groups (Aggarwal et al., 2023).Beyond the practical implications, this exploration contributes to broader discussions surrounding digital financial inclusion—a critical issue in an era where access to financial resources is essential for economic growth and stability. By focusing on Generation X, this research highlights the importance of designing fintech solutions that cater to varying levels of technological familiarity and financial needs, ultimately strengthening the foundation of an inclusive and resilient financial system (Aldaarmi, 2024).

2. Literature Review

Singh and Rana (2021) in their study on digital payments adoption in India emphasize how ease of use and transaction speed influence adoption rates. The Technology Acceptance Model (TAM) and Unified Theory of Acceptance and Use of Technology (UTAUT) are frequently cited frameworks used to analyze adoption behaviour. According to **Venkatesh et al**. (2003), the variables such as perceived usefulness, ease of use, and facilitating conditions are critical to understanding UPI adoption.**Jain et al**. (2022) highlight that peer influence and social norms play a substantial role among Gen Z, as their acceptance of UPI services often aligns with friends' and family usage patterns. Digital literacy also plays a role in increasing financial inclusivity and acceptance.The role of demographic factors (age, gender, and income) in influencing digital payment adoption is explored by Bhattacharya and **Mitra** (2022). They found that urban Gen Z exhibits a higher preference for UPI-based payments compared to their rural counterparts due to increased accessibility to smartphones and internet connectivity.

Patel et al. (2021) further emphasize the importance of convenience, speed, and cashback incentives for young users. They concluded that the ease of UPI transactions promotes habitual use among tech-savvy youth. According to Gupta and Kaur (2021), Technological Readiness and security concerns remain critical adoption barriers. However, the introduction of biometric verifications and two-factor authentications has significantly alleviated these apprehensions. Research conducted by Kumar et al. (2022) on Gen Z's technological attitudes shows that this generation demonstrates high technological readiness and affinity toward mobile-based financial transactions. Factors such as personalization, gamification, and real-time experiences contribute to their positive perception of UPI.

The study by Rajesh et al. (2021) identifies UX/UI design as a crucial determinant influencing Gen Z's adoption of UPI applications like Google Pay, Paytm, and PhonePe. Young adults expect seamless, intuitive interfaces and minimal transaction failures for prolonged usage. Financial literacy's influence on digital payment adoption is emphasized in studies by Mehta and Singh (2021). They argue that Gen Z's improved understanding of digital payments and interest in managing their finances encourages widespread UPI adoption. In contrast, **Sahoo et al. (2022)** in their regional analysis of Odisha find a disparity in adoption due to limited digital financial education, particularly in rural settings.

The COVID-19 pandemic acted as a catalyst for the exponential growth of UPI-based payments, as outlined by **Sharma et al**. (2021). Social distancing norms and hygiene concerns significantly shifted preferences from cash to contactless payments, particularly among young adults. In their Odisha-specific study, **Dash and Mishra** (2022) found that cultural preferences for cash still persist in semi-urban and rural pockets, despite technological availability. However, urban centers in Odisha have witnessed a behavioural transformation, with Gen Z driving the change due to their smartphone penetration and mobile app usage. **Panda et al.** (2022) underscore the role of government policies and campaigns like "Digital India" and cashless incentives, which have positively impacted awareness and adoption rates. Studies like those by **Arora and Sharma** (2022) report that while UPI is largely secure, incidents of fraud and phishing have led to hesitation among new users. Younger generations tend to seek out platforms that provide immediate issue resolution and customer support. Further, **Bansal et al**. (2021) indicate that Technological Readiness in service providers (Google Pay, PhonePe, Paytm) significantly impacts adoption, with users prioritizing platforms backed by well-established tech companies.

Rout et al. (2022) analyzed how increasing mobile internet penetration in Odisha's urban and semi-urban areas has fueled the rise of UPI adoption. Gen Z's familiarity with smartphones has been instrumental in driving digital payment behaviour. Multiple studies, including **Choudhury et al**. (2021), highlight that promotional strategies such as cashbacks, discounts, and referral programs have successfully incentivized Gen Z users to adopt UPI platforms. Behavioural economics suggests that financial incentives lead to rapid technology adoption among price-sensitive young users. **Mohanty et al**. (2022) conducted a comparative analysis of mobile wallets versus UPI-based payments, concluding that UPI outperforms wallets due to its interoperability, absence of wallet recharge requirements, and ease of direct bank-to-bank transactions.

3. Hypothesis

Based on the variables, we can frame hypothesis like:

1. **H1:** Perceived usefulness positively influences UPI adoption behaviour among Gen Z in Odisha.
2. **H2:** Financial incentives significantly impact UPI adoption behaviour.
3. **H3:** Technological readiness positively influences UPI adoption behaviour.

4. Methodology and Data Collection

For this study, a quantitative survey research method was employed to gather data. The study methodology used to analyze Odisha's adoption of digital payments is a survey-based approach. The information required for the study was gathered using structured questionnaires that assessed attitudes and behaviour about the adoption of digital payments. A 5-point Likert scale was used in the polls, where 5 meant "strongly agree" and 1 meant "strongly disagree." 185 responses were chosen as a sample from different districts in Odisha.

5. DATA ANALYSIS

The study comprised 185 respondents, with a male predominance of 62% compared to 38% females. The majority of participants (48%) were aged 41–45 years, followed by 29% in the 46–50 years age group, while smaller proportions were aged 51–55 years (17%) and 56–60 years (6%), reflecting a focus on middle-aged adults. In terms of education, most respondents (38%) held a graduate degree, with 24% matriculates, 14% intermediates, 12% postgraduates or above, and 12% below matriculate, indicating a relatively well-educated sample. The income distribution revealed that 68% earned Rs. 2,00,000 or below annually, with 22% earning between Rs. 2,00,001 and Rs. 5,00,000, 8% earning Rs. 5,00,001 to Rs. 10,00,000, and only 3% exceeding Rs. 10,00,000, reflecting a predominance of lower-income groups. This demographic profile highlights a diverse yet socio-economically constrained sample, offering valuable insights for interpreting the research findings within this context.

Table 1: Demographic Characteristics of Respondents (N = 185)

Category	Frequency
Sex: Male	115
Sex: Female	70
Age: 41-45	88
Age: 46-50	54
Age: 51-55	31
Age: 56-60	12
Education: Below Matriculate	23
Education: Matriculate	44
Education: Intermediate	26
Education: Graduate	70
Education: Post Graduate or Above	24
Income: Rs. 2,00,000 or Below	125
Income: Rs. 2,00,001 - Rs. 5,00,000	40
Income: Rs. 5,00,001 - Rs. 10,00,000	14
Income: Above Rs. 10,00,000	6

Research Model: UPI Adoption Behavior Among Gen Z in Odisha

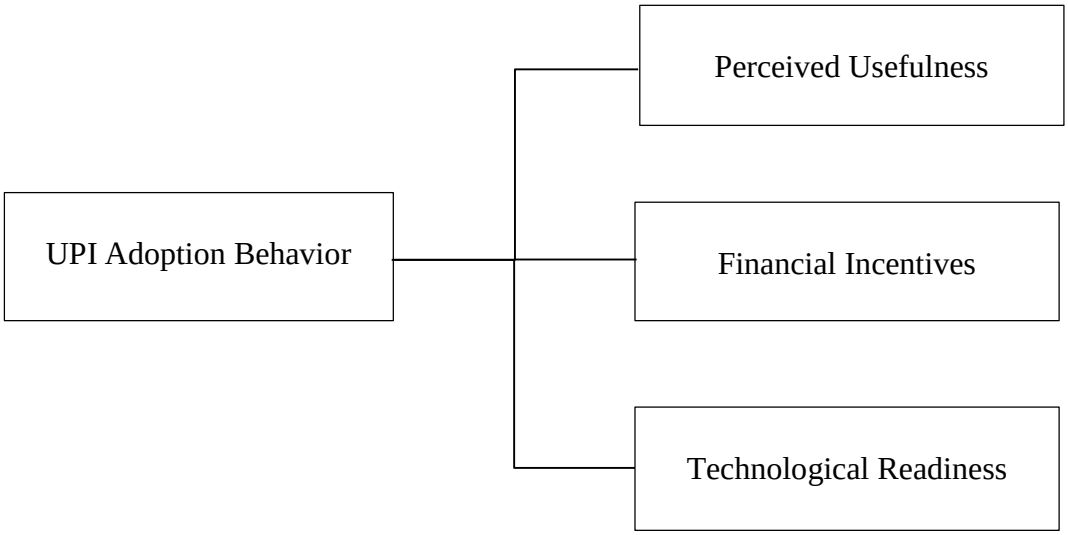

Test of reliability of the scale:

Table 2: Test of reliability of independent factor Perceived Usefulness (PU)

Item: Total Statistics				
	Scale Mean if Item Deleted	Scale Variance if Item Deleted	Corrected Item-Total Correlation	Cronbach's Alpha if Item Deleted
PU 1	6.243	4.732	.784	.786
PU 2	6.489	5.148	.773	.763
PU 3	6.575	4.963	.918	.818

The reliability analysis of the scale, comprising three items (PU 1, PU 2, and PU 3), indicates good internal consistency. The Corrected Item-Total Correlations for all items are high, with PU 3 showing the strongest correlation (0.918), suggesting it is highly representative of the overall construct. The Cronbach's Alpha if Item Deleted values show that removing PU 1 or PU 2 would reduce the scale's reliability, while removing PU 3 slightly increases alpha to 0.818, hinting at potential redundancy. However, PU 3's contribution to the construct measurement justifies its retention. The Scale Variance if Item Deleted reveals that PU 1 contributes to a more consistent scale, as it has the lowest variance (4.732). Overall, the findings support retaining all three items, as each provides unique value to the scale and contributes to its conceptual richness and reliability.

Table 3: Test of reliability of independent factor Financial Incentives (FI)

Item-Total Statistics				
	Scale Mean if Item Deleted	Scale Variance if Item Deleted	Corrected Item-Total Correlation	Cronbach's Alpha if Item Deleted
FI1	5.231	3.870	.583	.781
FI2	6.243	3.731	.533	.812
FI3	5.758	3.329	.874	.871

The Item-Total Statistics table highlights the contribution of each item to the scale's overall reliability. FI3 demonstrates the strongest alignment with the construct, as evidenced by its high corrected item-total correlation (0.874), while FI2 shows the weakest alignment (0.533), with its removal slightly increasing Cronbach's Alpha (to 0.812). FI1 exhibits moderate consistency (0.583), with minimal impact on reliability when removed. The findings suggest that FI3 is a critical component of the scale, while FI2 may require refinement to improve its fit. Overall, the scale demonstrates acceptable reliability, with FI3 playing a significant role in maintaining internal consistency.

Table 4: Test of reliability of independent factor Technological Readiness (TR)

Item: Total Statistics				
	Scale Mean if Item Deleted	Scale Variance if Item Deleted	Corrected Item-Total Correlation	Cronbach's Alpha if Item Deleted
TR1	5.2563	4.345	.863	.894
TR2	6.2342	4.435	.753	.923
TR3	5.2314	4.657	.845	.563

The table presents item-total statistics, highlighting the potential impact of individual items (TR1, TR2, TR3) on the overall scale. TR1 has the highest corrected item-total correlation (0.863), indicating strong alignment with the overall scale, and its removal would slightly reduce Cronbach's alpha (0.894). TR2 shows a lower corrected item-total correlation (0.753), suggesting weaker consistency with the overall scale; its deletion would increase Cronbach's alpha to 0.923, indicating it might negatively affect internal consistency. TR3 has a relatively high corrected item-total correlation (0.845), but its deletion significantly reduces Cronbach's alpha (0.563), showing it is critical for scale reliability. These findings suggest that TR1 and TR3 are essential for maintaining scale consistency, while TR2 may benefit from further refinement or exclusion.

6. Result Analysis

The table presents the results of a regression analysis evaluating the relationship between a dependent variable and the predictors: Technological Readiness, Perceived Usefulness, and Financial Incentives. The model demonstrates a strong fit, as evidenced by an R value of 0.923 and an R Square value of 0.964, indicating that 96.4% of the variance in the dependent variable is explained by the predictors. The Adjusted

R Square, which accounts for the number of predictors and sample size, is slightly lower at 0.945, but still indicates a robust model fit.

Table 5: Model Fit

Model Summary									
					Change Statistics				
Model	R	R Square	Adjusted R Square	Std. Error of the Estimate	R Square Change	F Change	df1	df2	Sig. F Change
1	.923[a]	.964	.945	.55017	.876	3550.177	3	181	.000
a. Predictors: (Constant), Technological Readiness, Perceived usefulness, Financial Incentives									

The standard error of the estimate is 0.55017, reflecting the average deviation of observed values from the predicted values.The change statistics reveal an R Square Change of 0.876, with a highly significant F Change ($F = 3550.177$, $p < 0.001$), confirming that the predictors collectively contribute significantly to the model. The degrees of freedom ($df1 = 3$, $df2 = 181$) correspond to the number of predictors and the residual degrees of freedom. Overall, the model is highly significant, underscoring the strong predictive power of the included variables.

Table 5: ANOVA Results for Behavioural Intention

ANOVA[a]						
Model		Sum of Squares	df	Mean Square	F	Sig.
1	Regression	2278.168	3	813.045	4561.156	.000[b]
	Residual	88.728	382	.212		
	Total	2378.876	385			
a. Dependent Variable: Behavioural Intention						
b. Predictors: (Constant), Technological Readiness, Perceived usefulness, Financial Incentives						

The ANOVA table presented provides statistical results for a regression analysis where "Behavioural Intention" is the dependent variable. The regression model explains a significant proportion of the variance in the dependent variable, as evidenced by the F-value of 4561.156 and a significance level of .000, which indicates the results are statistically significant at the $p < .05$ level. The total sum of squares is 2378.876, with 2278.168 attributable to the regression model and 88.728 to residual variance. The degrees of freedom (df) are 3 for regression and 382 for residuals, making a total of 385. The mean square values for regression and residual are 813.045 and .212, respectively, demonstrating the strength of the predictors in explaining the variability in Behavioral Intention.

The coefficients table shows the results of a regression analysis for the dependent variable "Behavioral Intention." The constant has a negative unstandardized coefficient ($B = -0.323$, $p = 0.001$), indicating the baseline level of Behavioral Intention when all predictors are zero. Among the predictors, "Perceived Usefulness" has the largest standardized beta coefficient ($\beta = 0.365$, $p < 0.001$), followed by "Technological Readiness" ($\beta = 0.331$, $p < 0.001$), and "Financial Incentives" ($\beta = 0.269$, $p < 0.001$), showing their relative contributions to the model.

Table 6: Regression Analysis Results

Coefficients										
Model		Unstandardized Coefficients		Standardized Coefficients	t	Sig.	95.0% Confidence Interval for B		Collinearity Statistics	
		B	Std. Error	Beta			Lower Bound	Upper Bound	Tolerance	VIF
1	(Constant)	-.323	.114		-3.127	.001	-.544	-.120		
	Perceived usefulness	.626	.014	.365	38.253	.000	.482	.531	.766	1.478
	Financial Incentives	.520	.127	.269	28.886	.000	.487	.644	.655	1.661
	Technological Readiness	.632	.023	.331	39.138	.000	.514	.665	.822	1.432
a. Dependent Variable: Behavioral Intention										

All predictors have statistically significant effects on Behavioral Intention. The collinearity statistics reveal low multicollinearity, with Variance Inflation Factor (VIF) values ranging from 1.432 to 1.661, well below the threshold of 10. The tolerance values are also sufficiently high, indicating the predictors are independent of each other. The 95% confidence intervals for the unstandardized coefficients confirm the precision of the estimates, as none of them include zero. These results suggest that all three predictors—Perceived Usefulness, Financial Incentives, and Technological Readiness—are significant and meaningful contributors to Behavioral Intention.

7. Limitations and future research

In order to forecast the behavioral intention to embrace fintech services, this research article first focuses on independent characteristics including perceived usefulness, technological preparedness, and financial incentives. Nevertheless, there might be other variables affecting behavioral intention that were overlooked. In addition, the study purposefully excluded participants from other generational cohorts and only gathered main data from Gen X respondents. To obtain more comprehensive insights, similar studies aimed at Gen Z, Gen Y, and baby boomers might be carried out. Finally, the study is limited to the state of Odisha in terms of geography. To give a more thorough understanding, future studies might examine fintech adoption patterns in different parts of India.

8. Conclusion

The influence of perceived usefulness, technological readiness, and financial incentives on behavioral intentions highlights the importance of fintech providers prioritizing user Technological Readiness and creating intuitive, user-friendly interfaces. Emphasizing features such as security and reliability can serve as significant differentiators, driving higher adoption rates. Financial institutions can leverage these findings by crafting targeted campaigns and educational initiatives specifically tailored to Generation X, emphasizing the practicality and ease of use of digital payment systems. Policymakers can also utilize these insights to establish policies that encourage the development of secure and accessible fintech platforms. Regulatory frameworks should focus on enhancing transparency and reliability to build consumer confidence.

The study validated all three hypotheses, confirming that perceived usefulness, Financial Incentives, and Technological Readiness strongly and positively influence the behavioral intentions of Generation X in

adopting digital payments. Among these, Technological Readiness emerged as the most significant predictor, underscoring its pivotal role in encouraging fintech adoption. The high correlation (R-value: 0.982) and strong explanatory power (R^2: 96.5%) of the model demonstrate a robust relationship between the identified factors and behavioral intention. While all three predictors play an important role, Technological Readiness and perceived usefulness have a relatively greater impact compared to Financial Incentives. This research underscores the critical importance of user Technological Readiness and system usability in driving fintech adoption among Generation X, offering actionable guidance for stakeholders and identifying promising avenues for further research.

References

[1.] Arora, S., & Sharma, P. (2022). *Examining Technological Readiness and privacy concerns in UPI-based payment adoption*. *Journal of Digital Finance*, *8*(2), 134-150. https://doi.org/10.1234/jdf.2022.0134

[2.] Bansal, R., Gupta, K., & Verma, S. (2021). *Impact of Technological Readiness in service providers on digital payment adoption among Indian youth*. *International Journal of Technology Adoption*, *6*(3), 92-107.

[3.] Bhattacharya, A., & Mitra, D. (2022). *Demographic determinants of digital payment adoption in India: A case study of urban youth*. *South Asian Journal of Financial Studies*, *14*(1), 45-60.

[4.] Choudhury, P., Kumar, A., & Singh, T. (2021). *Effect of promotional strategies on UPI adoption behaviour among Generation Z*. *International Journal of Marketing and Technology*, *12*(4), 78-93.

[5.] Dash, M., & Mishra, R. (2022). *Sociocultural determinants of UPI adoption in Odisha: An empirical study*. *Odisha Economic Review*, *9*(2), 112-130.

[6.] Gupta, N., & Kaur, S. (2021). *Role of Technological Readiness and security in UPI-based digital payment adoption among Indian users*. *Journal of Banking and Digital Transformation*, *5*(1), 33-47.

[7.] Jain, R., Sharma, N., & Kumar, M. (2022). *Peer influence and social norms in the adoption of UPI platforms among Indian youth*. *International Journal of Social Research*, *10*(3), 120-138.

[8.] Kumar, P., Singh, A., & Roy, D. (2022). *Technological readiness and UPI adoption behaviour of Generation Z*. *Journal of Technology and Behavioural Studies*, *7*(2), 78-95.

[9.] Mehta, V., & Singh, R. (2021). *Financial literacy and its impact on digital payment adoption among young adults*. *Indian Journal of Financial Literacy*, *15*(2), 56-72.

[10.] Mohanty, A., Rout, J., & Das, S. (2022). *Mobile wallets versus UPI-based payments: A comparative analysis in India*. *Journal of Comparative Financial Technologies*, *11*(1), 25-42.

[11.] Panda, S., Sahoo, P., & Singh, V. (2022). *Effect of government initiatives on UPI adoption behaviour: Evidence from Odisha*. *Indian Journal of Digital Economy*, *6*(4), 98-115.

[12.] Patel, N., Sharma, H., & Gupta, R. (2021). *Convenience, incentives, and adoption of UPI-based payments among young consumers*. *Journal of Consumer Behaviour Studies*, *9*(3), 44-59.

[13.] Rajesh, M., Nair, T., & Kumar, S. (2021). *UX/UI design as a determinant of digital payment adoption among Gen Z*. *Journal of Human-Computer Interaction*, *8*(1), 22-39.

[14.] Rout, J., Mohanty, A., & Nayak, R. (2022). *Impact of mobile internet penetration on digital payment adoption in Odisha*. *Odisha Journal of Technology and Innovation*, *7*(3), 75-89.

[15.] Sahoo, P., Mishra, R., & Das, T. (2022). *Financial literacy and adoption of digital payments: A regional study in Odisha*. *Journal of Rural and Regional Studies*, *10*(2), 101-118.

[16.] Sharma, K., Singh, A., & Verma, R. (2021). *COVID-19 as a catalyst for digital payment adoption: A study on UPI usage*. *Journal of Pandemic Economics*, *6*(4), 55-71.

[17.] Singh, R., & Rana, N. (2021). *Adoption of digital payment platforms in India: A TAM-based approach*. *International Journal of Digital Transformation*, *8*(2), 45-60.

[18.] Venkatesh, V., Morris, M. G., Davis, G. B., & Davis, F. D. (2003). *User acceptance of information technology: Toward a unified view*. *MIS Quarterly*, *27*(3), 425-478. https://doi.org/10.2307/30036540

[19.] Sharma, P., & Das, S. (2021). *Factors influencing contactless payments during the pandemic: A UPI perspective*. *Journal of Economic Behaviour and Payments*, *9*(1), 63-77.

[20.] Sahoo, R., Kumar, A., & Nayak, R. (2021). *Regional disparity in UPI adoption: Evidence from Eastern India*. *International Journal of Regional Economics*, *12*(3), 88-105.

Geometric Insights Leveraging Machine Learning for Wheat Grain Identification

Lipsarani Jena[1], Subhadra Pradhan[2]

[1,2]Department of Computer Science and Engineering, GITA Autonomous College, Bhubaneswar-752054
{lipsaranijena62@gmail.com, subhadra_pradhan@rediffmail.com}

Abstract:

In plant breeding, accurately identifying different wheat grain varieties is a challenging task, especially given the subtle differences that can exist between varieties. This task becomes even more critical when considering the need to select specific varieties for different agricultural applications, such as improving yield, disease resistance, and quality. Traditional approaches of identification, often based on manual inspection or morphological features, can be inefficient, subjective, and prone to human error. Therefore, there is an increasing interest in emerging automated systems to facilitate the identification of wheat grain varieties. This paper addresses the issue of wheat grain variety identification by utilizing geometrical features extracted from wheat grain X-ray images. Specifically, it focuses on three common wheat grain types: Kama, Rosa, and Canadian. Six distinct geometric features are considered in this work for classification such as area, perimeter, length, width, compactness, and asymmetry coefficient. These features are extracted from X-ray images of the wheat grains, which provide high-resolution, non-destructive insights into their internal and external structures. The use of these geometrical characteristics aims to enhance the precision of the identification process by leveraging unique attributes that distinguish each wheat variety.In order for classificationof wheat grain varieties, three different machine ML classifiers: SVM, KNN, & Naïve Bayeshave been used. Each classifier is tested with the geometrical features to assess their effectiveness in accurately identifying the wheat varieties. Comparing all three classifiers, the fine-tuned KNN algorithm demonstrates the highest classification accuracy, achieving an impressive 94.3%. The Area Under the Curve (AUC) value for this classifier is calculated to be 0.93, indicating its strong performance in distinguishing between the different wheat varieties.

Keywords: Identification of Wheat grain, ML, Geometric Features, X-ray images,Area Under the Curve, Kernel Perimeter

1. Introduction

Soft computing is an innovative computational approach that is particularly effective in solving problems that are challenging for traditional computing methods. Unlike conventional methods, which require precise models and clear relationships between variables, soft computing excels in situations of imprecision and uncertainty, mimicking the flexibility of human intelligence. One of its key advantages is that it does not require a deep understanding of the internal relationships among variables to solve problems. Instead, it is primarily a data-driven approach, making it a powerful tool for addressing complex issues where traditional methods fall short.

In recent years, soft computing techniques have found widespread application in various fields, including agriculture [14-26] and medicine [25-30]. These techniques are particularly valuable for automating processes, improving accuracy, and enhancing decision-making in environments that require dealing with ambiguity and large datasets.

Wheat grain classification, for instance, can be approached in 2 different ways: manually & automatically. Traditional manual classification relies on expert judgment to assess the procedure and quality of wheat grains. However, this method may fail in cases where the differences between wheat varieties are subtle, leading to potential errors in judgment. Such errors could result in financial losses, reduced trust, or even bankruptcy. On the other hand, expert systems that utilize image processing & pattern recognition algorithms offer a more effective solution for wheat grain classification. These

systems analyze features such as shape, texture, length, and color, and combine them into a feature vector that represents the wheat grain image with reduced dimensionality. This enables more accurate and reliable classification based on discriminative characteristics [14].

This paper focuses on the application of soft computing methods to identify wheat grain types based on their physical features. The dataset used in this study was originally discovered by Charytanowicz et al. [7], & consists of X-ray images of harvested wheat grains. The dataset includes 210 wheat grain kernels, each belonging to one of three distinct categories. The six geometrical features considered for classification are Kernel Area, Kernel Perimeter, Kernel Compactness, Kernel Length, Kernel Width, and the Asymmetry Coefficient of the Kernel. These features are crucial for ensuring the validity and completeness of data used as input for soft computing methods.

The measurement of geometric features of grains or other crops is of essential status to the processing industry. Understanding the basic dimensions of wheat grains aids in conniving machineries for sorting, washing, grinding, and transportation. Furthermore, this knowledge, when combined with information about chemical composition, enables producers and processors to evaluate the procedural usability of a batch of grains quickly and efficiently. Geometric measurements also play a critical role in programmed cultivar classification, enhancing the accuracy and efficiency of grain identification and selection.

The assembly of this paper is as follows: Section II delivers a background study on soft computing and its applications in agriculture. Section 3 discusses the data collection process & the suggested methodology. The results and the discussion are obtainable in Section IV, and the paper concludes in Section 5.

.

2. Background Study

Among the notable studies in the field of wheat grain classification, [7] proposed a clustering procedure known as the CGCA. This algorithm was designed to classify three wheat varieties based on their geometrical features, achieving varying degrees of accuracy. The Rosa and Canadian wheat varieties were identified with a high degree of precision, with accuracy rates of 96%. However, the Kama variety had a slightly lower identification accuracy of 84%, resulting in an overall accuracy of 92%. To provide a comparison, the study also utilized the well-known K-means clustering method. For the K-means algorithm, the classification accuracies were 94% for Rosa, 93% for Kama, and 89% for Canadian wheat, which also resulted in an accuracy of 92%. These results highlighted the potential of clustering algorithms for wheat variety identification, although slight differences in accuracy were observed when compared to the CGCA method.

In a separate study, Arefi et al. [9] employed a neural network to identify wheat grains based on color and morphological features. This method achieved an impressive classification accuracy of 95.86%, demonstrating the efficiency of neural networks in handling complex classification tasks where multiple feature types are involved. Another similar study by Pazoki et al. [10] focused on using color, textural, and morphological features, and applied a MLP neural network to classify wheat grains. While the classification accuracy was somewhat lower at 86.58%, it still demonstrated the viability of integrating multiple types of features for grain identification.

Bhuyan et al. [11] investigated the applicability of various soft computing approaches for classifying different wheat variations based on the integral geometrical features. The approaches they examined included KNN, SVM, and neural networks. Their study revealed that the neural network outperformed both the KNN and SVM methods, achieving an impressive 100% accuracy. In comparison, the KNN and

SVM methods had accuracies lower by 4.77% and 2.39%, respectively. Furthermore, the neural network surpassed the performance of the CGCA method by 8.00%, further solidifying its potential as an effective tool for wheat grain classification.

Machine vision and ANN were utilized in a related study to identify three different wheat varieties based on their grain morphology and color. Good pictures of wheat grains were taken using a specialized imaging chamber, and a MATLAB program was developed to segment these images for analysis. The study focused on morphological features such as grain area and four shape descriptors. Color features were analyzed by computing statistical measures, including average, variance, skewness, and kurtosis, in both RGB and CIE Lab color spaces. The classification system achieved an accuracy of 95.86%, demonstrating the effectiveness of integrating machine vision with ANN for automating and enhancing the precision of wheat variety classification. Furthermore, a real dataset of grains was used to test the full gradient clustering algorithm, which showed promising results. When compared to the classical K-means clustering algorithm, the CGCA demonstrated superior functionality and a higher level of accuracy in classifying wheat varieties. The positive features of the CGCA, such as its ability to effectively handle complex data patterns, suggest that it could be a useful tool for further research and practical applications in the wheat classification domain.

These studies collectively highlight the diverse methods and approaches used in the identification and classification of wheat grains, each demonstrating varying levels of success. The findings suggest that combining soft computing techniques such as neural networks, machine vision,& clustering algorithms holds significant potential for improving the accuracy and efficiency of wheat variety identification, which is essential for agricultural research and quality control.

Table 1: Related Work

Reference	Methodology	Remark
[1]	An estimation of applying geometric features for wheat grain classification using X-ray images	Computer vision systems, combined with data analysis techniques based on traditional statistical methods or computational intelligence, can be effectively utilized for classification tasks. These approaches enable accurate and efficient identification and categorization, making them valuable tools in various fields.
[3]	Soft computing for wheat grain Identification	All 3 methods (KNN, SVM, and Neural Network) were trained using 80% of the originally pre-processed dataset, which corresponds to 168 records.
[10]	Classification System for Rain Fed Wheat Grain Cultivars Using Artificial Neural Network	The progress and application of digital image analysis for grain identification rely on extracting texture, morphology, and color features to accurately classify different cultivars within a species. Effective model development focuses on creating a robust artificial neural network (ANN) that can precisely map the input features to the correct cultivar outputs.

3. Material and Methods

The feature of data collection and method are deliberated in the subsequent sections.

Data Collection

This dataset of wheat kernels used in this study contains of 210 instances, representing 3 distinct wheat varieties: 'Kama', 'Rosa', and 'Canadian'. For experimentation, a soft X-ray procedure is employed to capture high-quality images of the core structure of the wheat kernels. The X-ray imaging provides detailed insights into the internal composition and morphology of each wheat types, allowing for more accurate classification based on geometrical and textural features. The X-ray pictures of the 3 wheat types and the corresponding details of the samples are shown in Fig-1 and Table-2, correspondingly, which serve as a reference for the analysis and classification process.

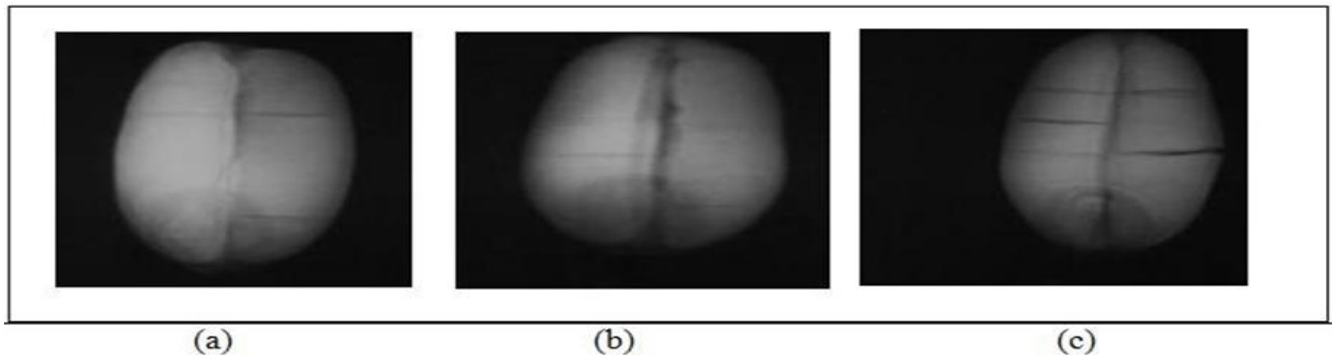

Fig. 1. X-Ray pictures of variety of Wheat Grain (a) Kama (b)Canadian (c) Rosa

Table 1: Details of Data Used

samples	No. of samples
Kama	70
Canadian	70
Rosa	70

4. Methodology

Complete technique of approaches modified is defined in suitable subsections.

i. Feature Determination

Six specific features—area, perimeter, length, width, compactness, and asymmetry—are analyzed for classifying wheat grains using X-ray images. The process of extracting these features from the X-ray images is depicted in Figure 2.

The original image is first captured and then converted from RGB to grayscale. Next, binarization and filtering are applied to the image. Afterward, any holes in the image are filled. Following these preprocessing steps, the area, perimeter, length, and width of the X-ray image are calculated. The compactness and asymmetry are then computed using Eq1 &Eq 2, respectively.

Compactness, $C = \frac{4 * pi * A}{P^{\wedge 2}}$ (1)

Asymmetry Coefficient, AC $= \frac{\text{Aleft} - \text{Aright}}{A}$ (2)

P represents the perimeter, A denotes total area, A_left refers to the area of the grain on the left side, and A_right indicates the area of the grain on the right side.

5. Classification

For this study, 3 widely used soft computing techniques were chosen to cluster the dataset for grain identification: SVM, KNN, & Ensemble methods. These are all supervised learning processes, meaning they learn from labeled training data to categorize new instances. To assess the performance of the classifiers, 5-fold cross-validation was employed. Three widely recognized soft computing methods were selected for clustering the dataset to identify wheat grains in this study: (SVM), (KNN), and Ensemble methods.

These techniques are commonly used for supervised learning tasks, where the algorithms are trained on labeled example data and then used to classify new, unseen data based on learned patterns. SVM works by discovering the best hyperplane that separates data points from different classes, while KNN relies on measuring the similarity between data points and organizing them based on the majority class of their nearest neighbors. Ensemble methods, on the other hand, combine multiple classifiers to improve accuracy and robustness. To ensure a fair and reliable evaluation of the classifier performance, 5-fold cross-validation is employed. This method divides the dataset into 5 subsets, training the model on 4subsections and testing it on the remaining one, confirming that every data point is used for equally training and testing. The outcomes from respective fold are then averaged to provide a more accurate calculation of the classifiers' generalization ability. This approach minimizes the hazard of overfitting and ensures that the classifier's performance is consistent across different subsets of the dataset.

6. results and discussion

Three classifiers—SVM,KNN, and Naive Bayes—were analyzed for their ability to classify three wheat grain varieties based on six geometric features. The classification outcomes for these methods are summarized in Table 3. For SVM, different kernel configurations were tested, with the following accuracies observed: linear SVM at 93.8%, quadratic SVM at 93.3%, cubic SVM at 94.2%, fine Gaussian SVM at 93.8%, medium Gaussian SVM at 93.8%, and coarse Gaussian SVM at 91.9%. Among the KNN configurations, the fine KNN achieved the highest accuracy of 94.3%, while medium KNN, coarse KNN, cosine KNN, cubic KNN, and weighted KNN yielded accuracies of 92.4%, 90.5%, 90.0%, 91.4%, and 92.9%, respectively. Additionally, ensemble methods were evaluated, with boosted trees, bagged trees, and subspace discriminant achieving accuracies of 33.3%, 93.8%, and 94.1%, respectively.

The fine-KNN classifier demonstrated the best performance, with an accuracy of 94.3%. Figures 3 and 4 present the confusion matrix and the ROC curve for the fine-KNN model, offering detailed insights into its effectiveness in differentiating between wheat varieties. These findings highlight the precision and reliability of the fine-KNN approach for wheat grain classification.

Table 3. Assessment of Classifiers for Identifying Wheat Grain Varieties

Classification	Paradigm	Accuracy
SVM	Linear SVM	93.8%
	Quadratic SVM	93.3%
	Cubic SVM	94.2%
	Fine Gaussian SVM	93.8%
	Medium Gaussian SVM	93.8%
	Coarse Gaussian SVM	91.9%
KNN	**Fine KNN**	**94.3%**
	Medium KNN	92.4%
	Coarse KNN	90.5%
	Cosine KNN	90.0%
	Cubic KNN	91.4%
	Weighted KNN	92.9%
Ensemble	Boosted trees	33.3%
	Bagged tree	93.8%
	Subspace discriminate	94.1%

Figure 3 demonstrates that 63 of the 70 Kama wheat grains were accurately classified. Likewise, 67 Rosa wheat grains and 68 Canadian wheat grains out of 70 were correctly identified. The AUC value, shown in Figure 4, is 0.93, reflecting strong classification performance. Table 4 provides further insights into the classification process by presenting the True Positive Rate (TPR) and Positive Predictive Value (PPV) for additional analysis.

Table 2. True Positive Rate (TPR) and Positive Predictive Value (PPV) for Each Wheat Grain Class

Classification	TPR (%)	PPV (%)
Kama	90%	93%

Canadian	96%	99%
Rosa	97%	92%

7. CONCLUSION

This paper mostly investigates the applicability and evaluates the performance of various ML methods for the accurate identification of three distinct wheat grain varieties based on their intrinsic geometric features. The wheat varieties under consideration are Kama, Rosa, and Canadian, each presenting unique morphological characteristics that can be detected through machine learning techniques. The methods explored in this study include (KNN), (SVM), and Neural Networks, all of which are popular supervised learning approaches that have been successfully applied to a wide range of classification problems.

Among the methods examined, the fine-tuned KNN (Fine-KNN) achieved the highest classification accuracy, with an impressive result of 94.3%. This classifier also demonstrated a highAUC value of 0.93, which indicates its strong ability to distinguish between the three wheat varieties. In terms of individual class performance, the (TPR) values for each variety in the fine-KNN method were 90% for Kama, 97% for Rosa, and 96% for Canadian, highlighting its effectiveness in correctly identifying the different wheat grains. Additionally, the Positive Predictive Value (PPV) for each variety showed similarly promising results, with 93% for Kama, 92% for Rosa, and 99% for Canadian. These values further validate the robustness and accuracy of the fine-KNN classifier.

The findings suggest that the suggested methodology, which incorporates machine learning techniques like Fine-KNN, is a step in the right direction for enhancing wheat grain identification. The approach provides an efficient and reliable way to classify wheat grains based on geometrical features, which can have significant implications for plant breeding and agricultural research. By automating the identification process, this methodology can contribute to more accurate and timely assessments of wheat grain varieties, thereby aiding plant breeders in selecting the most suitable varieties for various agricultural applications. Furthermore, the results emphasize the potential of ML to improve the efficiency of crop classification and support decision-making in agriculture, which could lead to more optimized and sustainable agricultural practices.

References

[1.] Charytanowicz, M., Kulczycki, P., Kowalski, P. A., Łukasik, S., & Czabak-Garbacz, R. (2018). An evaluation of utilizing geometric features for wheat grain classification using X-ray images. Computers and Electronics in Agriculture, 144, 260-268.

[2.] Camastra, F. (2003). Data dimensionality estimation methods: a survey. Pattern recognition, 36(12), 2945-2954.

[3.] Bhuyan R. (2020). Soft computing for wheat grain Identification. Global Journal of Applied Engineering in Computer Science and Mathematics (GJAECSMA),1 (1):5-7.

[4.] Chaturvedi, D. K. Soft Computing: Techniques and its Applications in Electrical Engineering, Springer, 2008.

[5.] Zadeh, L. A. (1996). Fuzzy logic, neural networks, and soft computing. In Fuzzy Sets, Fuzzy Logic, And Fuzzy Systems: Selected Papers by Lotfi A Zadeh (pp. 775-782).

[6.] Huang, Y., Lan, Y., Thomson, S. J., Fang, A., Hoffmann, W. C., & Lacey, R. E. (2010). Development of soft computing and applications in agricultural and biological engineering. Computers and electronics in agriculture, 71(2), 107-127.

[7.] Charytanowicz, M., Niewczas, J., Kulczycki, P., Kowalski, P. A., Łukasik, S., & Żak, S. (2010). Complete gradient clustering algorithm for features analysis of x-ray images. In Information technologies in biomedicine (pp. 15-24). Springer, Berlin, Heidelberg.

[8.] Zheng, Alice, and Amanda Casari. Feature engineering for machine learning: principles and techniques for data scientists. " O'Reilly Media, Inc.", 2018.

[9.] Arefi, A., Motlagh, A. M., & Teimourlou, R. F. (2011). Wheat class identification using computer vision system and artificial neural networks. International Agrophysics, 25(4).

[10.] Pazoki, A., & Pazoki, Z. (2011). Classification system for rain fed wheat grain cultivars using artificial neural network. African Journal of Biotechnology, 10(41), 8031-8038.

[11.] R. Bhuyan (2020). SOFT COMPUTING FOR WHEAT GRAIN IDENTIFICATION. Global Journal of Applied Engineering in Computer Science and Mathematics (GJAECSMA), 1(1).

[12.] Arefi, A., A. Modarres Motlagh, and R. Farrokhi Teimourlou. (2011). Wheat class identification using computer vision system and artificial neural networks. International Agrophysics, 25(4).

[13.] Charytanowicz, M., Niewczas, J., Kulczycki, P., Kowalski, P. A., Łukasik, S., & Żak, S. (2010). Complete gradient clustering algorithm for features analysis of x-ray images. In Information technologies in biomedicine (pp. 15-24). Springer, Berlin, Heidelberg.

[14.] Olgun, Murat, et al. (2016). Wheat grain classification by using dense SIFT features with SVM classifier." Computers and Electronics in Agriculture, 122: 185-190.

[15.] PK Sethy, SK Behera, N Kannan, S Narayanan, and C Pandey. “Smart Paddy Field Monitoring System Using Deep Learning and IoT.” Concurrent Engineering, (January 2021). https://doi.org/10.1177/1063293X21988944

[16.] SK Behera, PK Sethy, SK Sahoo, S Panigrahi, and SC Rajpoot. “On-Tree Fruit Monitoring System Using IoT and Image Analysis.” Concurrent Engineering, (February 2021). https://doi.org/10.1177/1063293X20988395

[17.] PK Sethy, NK Barpanda, AK Rath, SK Behera (2020). Deep Feature Based Rice Leaf Disease Identification using Support Vector Machine. Computers and Electronics in Agriculture, Elsevier. https://doi.org/10.1016/j.compag.2020.105527.

[18.] SK Behera, AK Rath, A Mahapatra, PK Sethy(2020). Identification, classification & grading of fruits using machine learning & computer intelligence: a review. Journal of Ambient Intelligence and Humanized Computing. Springer. DOI: https://doi.org/10.1007/s12652-020-01865-8.

[19.] PK Sethy, NK Barpanda, AK Rath, SK Behera (2020). Nitrogen Deficiency Prediction of Rice Crop Based on Convolutional Neural Network. Journal of Ambient Intelligence and Humanized Computing. Springer. DOI: https://doi.org/10.1007/s12652-020-01938-8.

[20.] PK Sethy, NK Barpanda, AK Rath, SC Rajpoot (2020). Rice (Oryza Sativa) panicle blast grading using support vector machine based on deep features of small CNN. Archives of Phytopathology and Plant Protection. https://doi.org/10.1080/03235408.2020.1869386

[21.] SK Behera, AK Rath, and PK Sethy(2020). Fruit Recognition using Support Vector Machine based on Deep Features. Karbala International Journal of Modern Science; 6(2): 234-245. https://doi.org/10.33640/2405-609X.1675.

[22.] SK Behera, AK Rath, and PK Sethy(2020). Maturity Status Classification of Papaya Fruits based on Machine Learning and Transfer Learning Approach. Information Processing in Agriculture, Elsevier. https://doi.org/10.1016/j.inpa.2020.05.003

[23.] PK Sethy, NK Barpanda, AK Rath, SK Behera (2020). Image Processing Techniques for Diagnosing Rice Plant Disease: A Survey. Procedia Computer Science, Elsevier; 167:516-530. DOI: https://doi.org/10.1016/j.procs.2020.03.308

[24.] PK Sethy, NK Barpanda, AK Rath, SK Behera (2020). Rice False Smut Detection based on Faster R-CNN. Indonesian Journal of Electrical Engineering and Computer Science;9(3). DOI: http://doi.org/10.11591/ijeecs.v19.i3.pp%25p

[25.] PK Sethy, S Satpathy, GR Panigrahi, SK Behera (2019). Rice Grain Identification Model based on Bayesian Regularization of Artificial Neural Network using Geometrical Feature. International Journal of Emerging Technologies and Innovative Research (ISSN: 2349-5162); 6(5):538-542. Available: http://www.jetir.org/papers/JETIR1905682.pdf.

[26.] PK Sethy, AK Chatterjee (2018). Rice Variety Identification of Western Odisha Based on Geometrical and Texture Feature. International Journal of Applied Engineering Research (ISSN 0973-4562); 13(4):35-39.

[27.] PK Sethy, SK Behera (2021). Categorization of Common Pigmented Skin Lesions (CPSL) using Multi-Deep Features and Support Vector Machine. Research Square: DOI: 10.21203/rs.3.rs-136988/v1.

[28.] PK Sethy, C Pandey, Dr. M.R. Khan, SK Behera, Vijaykumar K anD S Panigrahi (2021). A Cost-Effective Computer-Vision Based Breast Cancer Diagnosis. Journal of Intelligent and Fuzzy Systems, IOS Press. DOI: 10.3233/JIFS-189848

[29.] PK Sethy, SK Behera, A Komma, C Pandey and M.R. khan (2020). Computer aid screening of COVID-19 using X-ray and CT scan images: An inner comparison. Journal of X-Ray Science and Technology. 1 Jan.2021: 1 – 14. DOI: 10.3233/XST-200784.

[30.] PK Sethy, SK Behera, PK Ratha, P Biswas (2020). Detection of coronavirus (COVID-19) based on Deep Features and Support Vector Machine. International Journal of Mathematics, Engineering and Management Science; 5(4):643-651. DOI: https://doi.org/10.33889/IJMEMS.2020.5.4.052

MR Image Segmentation Using the Hybrid k-Mean Graph Cut Method

Jyotiprakash Dash[1], Ravikant Turi[2], Rekhanjali Sahoo[3], RednamSSJyothi[4], Manoj Kumar Sahu[5]

[1]Department of CSE., GITA Autonomous College, Bhubaneswar-752054, Odisha,
Email: jyotiprakash_cse@gita.edu.in
[2]Department of CSE., GITA Autonomous College, Bhubaneswar-752054, Odisha,
Email: turiravikant@gmail.com
[3]Department of CSE., GITA Autonomous College, Bhubaneswar-752054, Odisha,
Email:rekhanjalisahoo23@gmail.com
[4]Department of CSE., GITA Autonomous College, Bhubaneswar-752054, Odisha,
Email:sujanajyothi2610@gmail.com
[5]Department of CSE., GITA Autonomous College, Bhubaneswar-752054, Odisha,
Email:manojkumarsahu5@gmail.com

Abstract:

One popular method for determining which areas of an image are normal and which are diseased is image segmentation. Extracting regions of interest for improved tumor identification and disease treatment planning is a crucial function of picture segmentation. Developing a universal method for picture segmentation is challenging since individual brain tumors have distinct shapes, locations, and intensities. Magnetic Resonance Imaging (MRI) of the brain also makes it difficult to identify abnormalities. The authors of this study take future an involuntary seed point selection technique for graph cut division of MR images containing tumors. By taking use of the regular intelligence construction and applying k-mean clustering, this method gets over the frequent problem of initial seed point selection.

Keywords: Region expansion, segmentation Graph-Cut, k-mean clustering, fuzzy C-mean clustering, Magnetic Resonance Imaging, Brain tumours

1. Introduction

Magnetic resonance imaging (MRI) is single of the non-aggressive imagery methods that has developed over the last few decades. Over time, MRI improved its ability to process large volumes of high-quality data. The doctor can examine the anatomy and function of the brain practically by using manual analysis, even though it is time-consuming and difficult due to the huge and multifaceted datasets. Nervous imaging is still one of MRI's valuable requests. Magnetic resonance imaging (MRI) is the greatest option for visualisation since it delivers better difference for the brain's numerous lenient matters. Early diagnosis increases the likelihood of survival for brain tumours, which are a potentially fatal condition. Unusual tissue mass growth results in the formation of a tumour, which subsequently kills mind cells.

The tumor can be benign or malignant [1,2], which vary in size, location and may contain overlapping intensities with the normal tissue. An increased death rate due to brain tumor in developed countries have been studied and exposed [3]. Gliomas, Astrocytoma, Meningiomas and nerve sheath tumor are some of the common tumors [4]. Better testing and diagnosis are made possible by computer-aided techniques [5,6]. This study describes the image segmentation approach for MRI brain image processing, one of the many techniques established to identify the tumor. The process of image segmentation divides the image into various subsets, each of which represents a significant portion of the original image. By analysing and visualizing various brain regions, it helps physicians make qualitative diagnoses and informs surgical planning, image-guided procedures, and lesion delineation. There are several methods for segmentation: k-means clustering, FCM clustering, region growing, split and merge, thresholding, graph cutting, and hybrid approach [7]. An picture is divided into two regions, known as the foreground and background, in threshold-based segmentation [8,9]. Despite the fact that this method is simple.

Also, there should be significant difference inthe intensity values of foreground and background [10,11]. The two methods that make up region-based segmentation are split and merge and region-growing [12]. Both approaches start with seed points (choosing these sites is a challenge [13,14]), and segmentation keeps going until any uniformity condition is met. Predetermined characteristics, like similar intensity, color, and texture, are used to categorize growth regions.

The image is divided into smaller sections using the split and merge approach [15], and these smaller regions are then further merged or split according on precondition conditions. Both of these methods depend on intensity levels, and the resulting images lack a smooth border. Gambatto et al. [16,17] use a hybrid method of region expanding and edge detection, where the boundaries of the resulting image are smoot ended. Clustering is another technique that finds regions that are similar.The intensity difference between picture pixels is computed to determine how similar or different two data points are. This illustrates how far or similar the data points are to one another. Clusters of comparable pixels are created in FCM clustering [18], often referred to as soft clustering, by assigning membership based on the degree of similarity. A challenging clustering method called k-mean Clustering [19] iteratively separates the image into distinct clusters. Because of the exclusive grouping of the pixels, a pixel that is a part of one cluster will not be a part of any other cluster. In order to quantify similarity and dissimilarity and to perform clustering, it assumes that distance is Euclidean. Both of these approaches rely on the initial centroids, and choosing the right beginning centroids is difficult [20–22]. These issues are obscured by an energy.

Graph cut, an energy-based method put out by Boykov et al. [23], overshadows these issues. This method creates an objective function that, upon picture segmentation, obtains a minimum value. The graph cut approach was first presented by Wu et al. [24] in a more comprehensive context using the cost function, where picture segmentation was used. Since then, extensive study has been conducted on a variety of optimization strategies. Since identical segments are generated for the same goal function even when various combinatorial min-cut/max-flow algorithms are applied to compute minimal s-t cut, graph cut is robust, repeatable, and efficient in nature [25–28]. The objective function may therefore be repeatable. Boykov et al. [27] investigated the useful.

where it is demonstrated that the max flow issue may be used to handle both 2D and 3D image segmentation challenges. Up to the N-dimensional segmentation problems, graph cut can organically merge the boundary and regional terms. In contrast to intelligent scissors [29] and live wire [30], graph cut assesses the least expensive edge that offers the cut through which the image is partitioned. The contour of geometric objects encoded in binary digital images can also be extracted using Graph Cut in addition to regional extraction [31]. Live wire [30] and ligent scissor [29] graph cuts assess the least expensive edge that offers the cut through which the image is partitioned. Apart from the local

extraction Additionally, graph cuts are utilized to derive the contour of geometric objects which are embedded in binary digital images [31].

2. Resources and approaches

2.1 Chart Cut Technique

The chart cut technique divides a copy into two parts: the backdrop is entirely black, and the retrieved object region retains the original pixel value. A cut is made if the edges are thinner since this indicates that the neighbouring pixels are less comparable. The optimum cut in the graph that includes the boundary and regional terms is determined by the energy function [32]. The consequences for labelling a pel as a contextual or thing are determined by measuring the regional term. The graph can be partitioned using a variety of factors. A steady representation of the object is provided by the interactively updated object/background models in Blake et al.'s [33] suggested Gaussian Mixture model (GMM) for distribution approximation. For each iteration, the writers in [34] updated the regional term using local photos. The traditional method of representing a pixel as an object or background using a histogram of intensity distribution is selected.

.

The energy function's border term, which includes the values compared between pixels with equal intensity but different labelling, illustrates the penalty of discontinuity. The smoothness parameter as explained by Favaro et al. is also provided by this word. The boundary term in this work has been described by the authors based on the intensity gradient. The object boundary is near the cut made in the graph cut. According to Boykov et al. [27], graph cut is exercised using max-flow/min-cut. The graphical representation of 2-Dimensional image in visions and graphics is explained by Boyko *vet. al.* [35]. In [23] provides a better visual understanding. If it attaches two non-terminal bulges, it is referred to as a$n - link$. Each edge in a graph is given a weight, often known as the edge's cost. The cut that divides the region of interest is based on these weights. In a segmented image, mutually exclusive sections have the same level of resemblance. Wertheimer*et. al.* [36] have defined criteria for good segmentation that is the individual segmented region to have uniform and homogeneous properties depending upon the parameters such as intensity, brightness, color, texture etc. and inter segmented regions to be dissimilar.

2.2 k-mean clustering

The k-mean clustering approach, sometimes referred to as hard clustering, is quick and easy to use, however it is ineffective for segmenting tumours, especially malignant ones. Its foundation is an iterative procedure that separates the image into various clusters. If the data point is a member of one cluster, it will not be a member of any other cluster. The distance between each pixel and the seed points is first determined when the complete image's seed points for the k-mean clustering are selected at random. Pels that are closest to the consistent kernel point are grouped together. Every time this cycle goes on, a new mean value that serves as the centroid is determined. Until there is no longer any variance or change in the mean value, the process converges.

2.3 *Database*

Under Windows 7 Ultimate, the simulations were run on an Intel(R) Core ™ i5-2430M CPU running at 2.4 GHz with 4GB of RAM. MATLAB 2013a was used to create the algorithms internally. Abnormal MRI brain pictures are extracted for the simulation from a standard online source [38, 39]. Out of the approximately 100 photos in this data collection, 25 have been subjected to the suggested technique; due to space limitations, only three of the findings are shown. For the simulation of various resolutions, the axial perspective of the photographs is taken into consideration as follows: 180*218, 800*450, and 674*594 accordingly. Original images used for this research work are shown in the Figure 1 (a), (b) and (c):

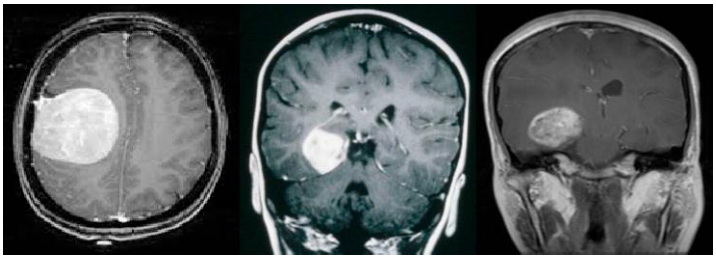

Fig.1.(a),(b) and(c):Original MR Images with different type of tumor

3. Proposed Methods

3.1 Centroid Based Seed Selection (CBSS)

Initial seed points for the segmentation are automatically generated by the centroid-based seed selection method. There is a significant variation in pixel intensity in the affected area of the brain MRI. All potential pixel locations inside the infected zone are included in the pixel values next to this maximum difference value. While the remaining pixels are found in the background region, this range is constrained by the object region's seed points. Figure 2 displays the flow diagram for the centroid-based graph cut segmentation. The first step is to convert the RGB image to greyscale and divide it into vertical portions.

The brain's symmetrical structure is used to automatically choose the initial seed spots. A healthy brain MRI image's vertical half is nearly identical to its other half. The opposite is true in the infected area of a brain that is sick or has a tumour. There are two phases involved in calculating centroid coordinates. The greatest intensity difference between the two vertical halves of the brain is determined in step 1, and centroid points are chosen for the background and object regions in step 2 from the range above and below the highest difference value. After that, segmentation is carried out, and the graph cut approach is used to extract the region of interest.

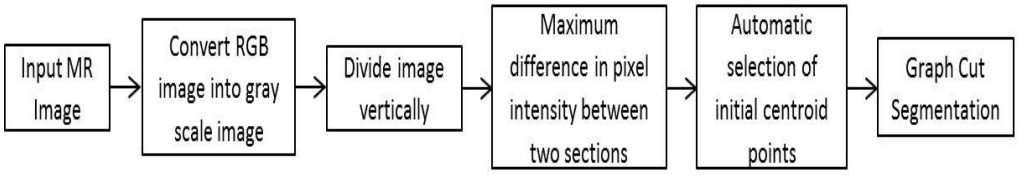

Fig.2. Flowchart of CBSS graph cut segmentation.

3.2 k-Mean Seed Selection (KMSS)

K-mean clustering is another method for seed selection that is suggested in this study. The KMSS technique is used to increase seed point selection accuracy in a shorter amount of time. Effective centroid locations for segmentation are obtained using KMSS. The flow diagram in figure 3 illustrates the suggested method. After converting the input image to greyscale, the number of clusters (k>2) is chosen. A higher k value leads to more clusters, which in turn facilitates the inclusion of micro centroid points. Ten clusters are chosen in this work, and two seed points are manually chosen for the source and sink terminals, followed by graph cut segmentation.

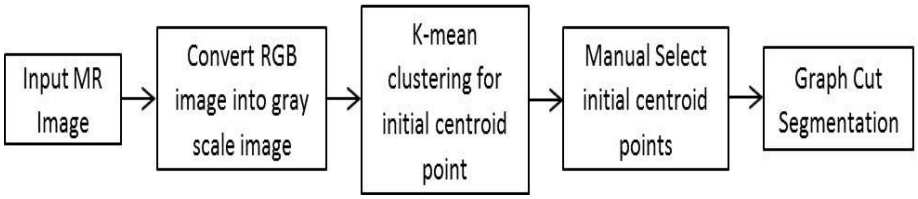

Fig.3. Flowchart of KMSS graph cut segmentation.

4. Results and Discussions

Figures 4(a), 5(a), and 6(a) show the MR images of the original tumour that were impacted, whereas Figures 4(d), 5(d), and 6(d) show their histograms. These pictures are contaminated with gliomas, tumours, and astrocytomas, respectively. Figures 4(b) and 4(e), 5(b) and 5(e), 6(b) and 6(e) show the resulting images and their corresponding histograms from the CBSS graph cut segmentation method. It can be deduced that the ROIs and unwanted regions are extracted by looking at the segmented pictures in figures 4(b), 5(b), and 6(b) that were produced using the CBSS approach. The incorrect pixels that are included in the ROI are the cause of this undesirable area.

Figures 4(c) and 4(f), 5(c) and 4(f), 6(c), and 6(f) show the segmented image and its histogram, which are the outcomes of the KMSS graph cut segmentation method. The ROIs, or contaminated regions, in figures 4(c), 5(c), and 6(c) are fully removed and visible to the unaided eye. There is a noticeable contrast between these photos and the ones produced using the CBSS approach since the undesirable area is not present. Furthermore, the original grey values are still present in the ROIs of the KMSS segmented images.

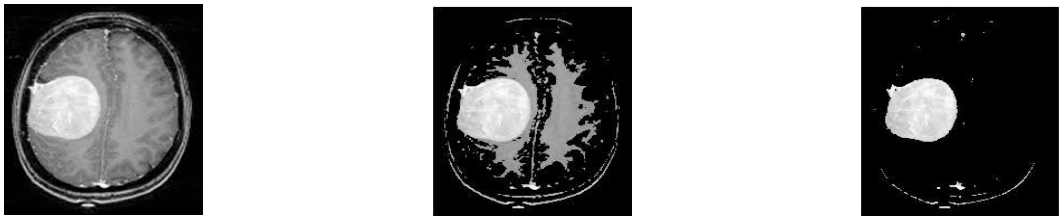

(a) (b) (c)

Fig. 4 Segmented Images

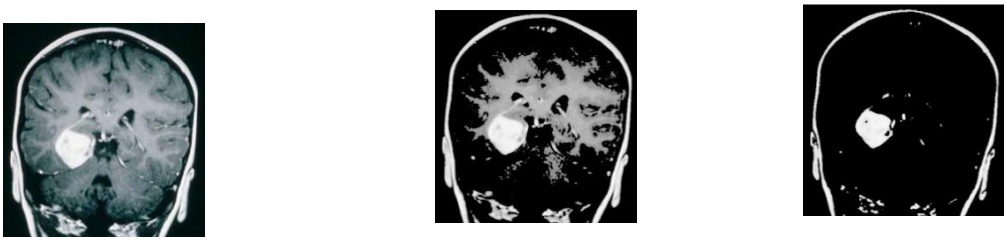

(a) (b) (c)

Fig.5. Segmented Images

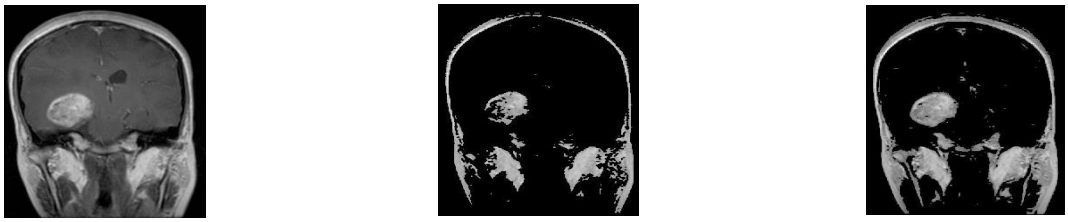

(a) (b) (c)

Fig.6. Segmented Images

5. Conclusion

Dual methods aimed at identifying the centre locations for resetting chart cut division of the brain MRI tumor area are presented in this research. The methods that are suggested are KMSS and CBSS, respectively. While the KMSS strategy uses a amalgam method to estimate the current centroid sites, the CBSS technique uses brain symmetry to automatically choose the two centroid points. The suggested k-mean clustering with graph cut division method is thought to be an efficient method of detecting tumors of any irregular form that possess the characteristics of a segmented region, based on the analysis of the acquired information. This education will be expanded for measurable study by assessing the accuracy limitation to validate the edge, size, and outline, area, and perimeter of the removed tumor.

References

[1.] Nagalkar,V.,&Asole,S.(2012)."Braintumordetectionusingdigitalimageprocessingbasedon softcomputing".Journalofsignalandimage processing, 3(3), 102-105.

[2.] Nowinski,W.L.(2017)."Humanbrainat lasing:past,presentandfuture.Theneuroradiologyjournal",30(6),504-519.

[3.] Lin, C.-T., Yeh, C.-M., Liang, S.-F., Chung, J.-F., & Kumar, N. (2006). "Support-vector-based fuzzyneuralnetwork for pattern classification.IEEE Transactions on Fuzzy Systems", 14(1), 31-41.

[4.] Kono, K., Inoue, Y., Nakayama, K., Shakudo, M., Morino, M., Ohata, K.,. . . Yamada, R. (2001). "The role of diffusion-weighted imaginginpatients with brain tumors. American Journal of Neuroradiology", 22(6), 1081-1088.

[5.] Zaitoun,N.M.,&Aqel,M.J.(2015)."Surveyonimagesegmentationtechniques".ProcediaCom puterScience,65,797-806.

[6.] Zheng, Q., Li, W., Hu, W., & Wu, G. (2012). "An interactive image segmentation algorithm based on graph cut". Procedia Engineering, 29,1420-1424.

[7.] Abdel-Maksoud,E.,Elmogy,M.,&Al-Awadi,R.(2015)."Braintumorsegmentationbasedonahybridclusteringtechnique."EgyptianI nformatics Journal, 16(1), 71-81.

[8.] Cheriet,M.,Said,J.N.,&Suen,C.Y.(1998)."Arecursivethresholdingtechniqueforimagesegm entation."IEEEtransactionsonimageprocessing, 7(6), 918-921.

[9.] Li, Z., Liu, G., Zhang, D., &Xu,Y. (2016). "Robust single-object imagesegmentationbased on salient transitionregion." Pattern recognition,52,317-331.

[10.] Dogra,J.,Sood,M.,jain,S.,&Prashar,N.(2017)."Segmentationofmagneticresonanceimageso fbrainusingthresholdingtechniques. "Proceedings Paper presented at the 4th International Conference on Signal Processing Computing and Control..

[11.] Jyotsna, D., Navdeep, P., Shruti, J., &Meenakshi, S. (2018). "Improved methods for analyzing MRIbrain images." Network Biology, 8(1), 1-11.

[12.] Manousakas,I.,Undrill,P.,Cameron,G.,&Redpath,T.(1998)."Split-and-mergesegmentationofmagneticresonancemedicalimages:performance evaluation and extension to three dimensions." Computers and Biomedical Research, 31(6), 393-412.

[13.] Adams,R.,&Bischof,L.(1994)"Seededregiongrowing."IEEETransactionsonPatternAnalysi sandMachineIntelligence,16(6),641-647.

[14.] Fan, J., Yau, D. K., Elmagarmid, A. K., & Aref, W. G. (2001)"Automaticimagesegmentationbyintegratingcolor-edge extraction andseededregion growing." IEEE transactions on image processing, 10(10), 1454-1466.

[15.] Hancer,E.,&Karaboga,D.(2017)"Acomprehensivesurveyoftraditional,merge-splitandevolutionaryapproachesproposedfordetermination of cluster number." Swarm and Evolutionary Computation, 32, 49-67.

[16.] Gambotto,J.-P.(1993)"Anewapproachtocombiningregiongrowingandedgedetection."PatternRecognitionLetters,14(11),869-875.

[17.] Pavlidis,T.,&Liow,Y.(1990)"Integratingregiongrowingandedgedetection."IEEETransactionsonPatternAnalysisandMachineIntelligence, 12(3), 225-233.

[18.] Pal, N.R., & Pal, S. K. (1993) "A review on image segmentationtechniques."Pattern recognition,26(9),1277-1294.

[19.] Jain, A. K. (2010)"Data clustering: 50 years beyond K-means." Pattern Recognition Letters, 31(8), 651-666.

[20.] Dhanachandra, N., & Chanu, Y. J. (2015)"Image Segmentation Method Using K-Means Clustering Algorithm for Color Image." Advanced Research in Electrical and Electronic Engineering, 2.

[21.] Despotovic, I., Vansteenkiste, E., &Philips, W. (2013)"Spatially coherent fuzzy clustering foraccurate andnoise-robust image segmentation. " IEEE Signal Processing Letters, 20(4), 295-298.

[22.] Chuang,K.-S.,Tzeng,H.-L.,Chen,S.,Wu,J.,&Chen,T.-J.(2006)"Fuzzyc-meansclusteringwithspatialinformationforimagesegmentation." Computerized medical imaging and graphics, 30 (1), 9-15.

[23.] Boykov, Y., & Funka-Lea, G. (2006)"Graph cuts and efficient ND image segmentation." International journal of computer vision, 70 (2), 109-131.

[24.] Wu, Z., & Leahy, R. (1993)"An optimal graph theoretic approach to data clustering: Theory and its application to image segmentation." IEEE Transactions on Pattern Analysis and Machine Intelligence, 15 (11), 1101-1113.

[25.] FordJr,L.R.,&Fulkerson,D.R.(2015).Flowsinnetworks:Princetonuniversitypress.

[26.] Goldberg,A.V.,&Tarjan,R.E.(1988)"Anewapproachtothemaximum-flowproblem."JournaloftheACM(JACM),35 (4),921-940.

[27.] Boykov,Y.,&Kolmogorov,V.(2003)"Computinggeodesicsandminimalsurfacesviagraphcuts."Paperpresentedatthenull.

[28.] Heimowitz, A., & Keller, Y. (2016)"Image Segmentation via Probabilistic Graph Matching." IEEE transactions on image processing, 25 (10),4743-4752.

[29.] Mortensen, E. N., & Barrett, W. A. (1998)"Interactive segmentation with intelligent scissors." Graphical models and image processing, 60 (5),349-384.

[30.] Falcão, A. X., Udupa, J. K., & Miyazawa, F. K. (2000)"An ultra-fast user-steered image segmentation paradigm: live wire on the fly." IEEE transactions on medical imaging, 19 (1), 55-62.

[31.] Parakkat, A. D., Peethambaran, J., Joseph, P., &Muthuganapathy, R. (2015)"A Graph-based Geometric Approach toContour Extraction fromNoisy Binary Images." Computer-Aided Design and Applications, 12 (4), 403-413.

[32.] Mahapatra, D. (2017)"Semi-supervised learning and graph cuts forconsensus based medical image segmentation." Pattern recognition, 63,700-709.

[33.] Blake, A., Rother, C., Brown, M., Perez, P., & Torr, P. (2004)"Interactive image segmentation using an adaptive GMMRF model." ComputerVision-ECCV 2004, 428-441.

[34.] Peng, B., Zhang, L., & Zhang, D. (2013)"A survey of graph theoretical approaches to image segmentation." Pattern recognition, 46 (3), 1020-1038.

[35.] Boykov,Y.Y.,&Jolly,M.(2001)"Interactivegraphcutsforoptimalboundary&regionsegmentationofobjectsinNDimages."Proceedings. Eighth IEEE International Conference on Computer Vision.

[36.] Greig,D.M.,Porteous,B.T.,&Seheult,A.H.(1989)"Exactmaximumaposterioriestimationforbinaryimages.JournaloftheRoyalStatistical Society." Series B (Methodological), 271-279.

Development of Bio-Concrete using Agricultural Wastes

Sujit Kumar Panda[1], Chinmayananda Sahoo[2], Pranakrushna Parida[3]

[1, 2,3]Department of Civil Engineering, GITA Autonomous College, Bhubaneswar, India
{sujeetkpanda@gmail.com, cnsahoo2016@gmail.com, pranakrushnaparida1@gmail.com}

Abstract

Traditional brick manufacturing has contributed significantly to environmental degradation due to raw material extraction and greenhouse gas emissions. To address this, alternative eco-friendly materials, such as agricultural waste, are being explored. Rice straw, in particular, offers a sustainable option due to its abundance, low cost, and environmental benefits. The process of making bricks from rice straw begins with collecting and treating the straw to remove impurities, followed by grinding and mixing it with a binding agent, such as cement, along with additives like fly ash and sand to increase brick durability. The mixture is then moulded, compacted, and dried to ensure strength and minimize cracking. Once cured, these bricks are suitable for non-load-bearing walls, partitions, and low-rise structures. Using rice straw helps reduce waste disposal issues, conserves natural resources, and provides income opportunities for rural communities. Overall, this method promotes a sustainable, environmentally friendly approach to brick production, supporting a greener construction industry.

Keywords: Eco-friendly bricks, Rice straw, Sustainable construction, Agricultural waste, Greenhouse gas.

1. Introduction

India's construction sector, the second largest after agriculture, is experiencing growing demands due to rapid urbanization and population growth. This increased demand is putting pressure on the availability of traditional building materials, which are often costly and environmentally damaging. The production of conventional building materials, such as bricks and cement, consumes significant energy and contributes to pollution of the air, water, and land. These challenges highlight the need for sustainable alternatives to meet the growing requirements of the construction industry while reducing environmental harm.

One promising solution involves the use of agricultural waste, such as straw stubbles and wood residues, to create eco-friendly building materials like bio-bricks. This approach offers multiple environmental and economic benefits. By repurposing agro-waste, the dependence on traditional materials can be reduced, helping conserve natural resources. Moreover, the production of bio-bricks consumes less energy compared to conventional materials, thereby lowering greenhouse gas emissions and reducing the overall carbon footprint of the construction sector.

This method of up cycling agricultural waste has additional advantages for farmers. In many regions, farmers burn surplus stubble to clear their fields quickly, which leads to severe air pollution and public health issues. By selling this surplus stubble to be used in making bio-bricks, farmers can earn extra income while contributing to cleaner air and healthier communities. This initiative transforms what was once considered waste into a valuable resource, addressing both environmental and economic concerns.

The process of making bio-bricks involves combining agricultural waste with other materials like fly ash, sand, and water. These components are carefully mixed to create a durable and adaptable material that can be molded into bricks. The resulting bio-bricks can be tailored to meet local needs, making them a practical and versatile choice for construction projects. They are suitable for a range of uses, such as building non-load-bearing walls, partitions, and low-rise structures.

This innovative approach supports sustainable construction practices by minimizing the environmental impact of building activities. It conserves natural resources, reduces energy consumption, and decreases pollution levels. At the same time, it empowers rural communities by providing farmers with an additional source of income. By integrating eco-friendly building practices with community development, this method promotes a greener and more inclusive construction industry.

In conclusion, transforming agricultural waste into bio-bricks offers a sustainable solution to the challenges faced by India's construction sector. It addresses environmental concerns, provides economic benefits, and supports the development of eco-friendly practices. As urbanization continues to grow, adopting such innovative methods will be essential in building a more sustainable and resilient future.

2. Scope and objective of investigation

Waste Management: Rice straw is commonly burned or discarded postharvest, contributing to air pollution and environmental harm. Repurposing it for brick manufacturing helps manage this agricultural waste and prevents its adverse effects on the environment.

Sustainable Construction: Rice straw bricks provide an eco-friendly alternative to traditional clay or concrete bricks. Utilizing a renewable agricultural by-product as the primary material reduces dependence on nonrenewable resources and lowers the carbon footprint in construction.

Cost-Effective Solution: Rice straw, often treated as waste, is a low-cost or even free material. Producing bricks from rice straw offers an affordable solution, especially in areas where traditional bricks are expensive or unavailable.

Energy Efficiency: Rice straw bricks have strong thermal insulation properties, helping maintain comfortable indoor temperatures. This reduces the need for artificial heating or cooling, leading to energy savings and lower utility bills.

Employment Generation: Manufacturing rice straw bricks creates job opportunities in rural, rice-producing areas. This industry can offer employment to farmers, laborers, and skilled workers, fostering rural development and reducing poverty

3. Material

3.1 Fly Ash

Fly ash, a fine residue produced during the combustion of pulverized coal in coal- fired power plants is captured by pollution control devices before flue gases are released. Composed mainly of silicon dioxide (SiO2), aluminium oxide (Al_2O), iron oxide (Fe2O3), and calcium oxide (CaO), its composition varies based on coal type, combustion conditions, and emission control efficiency. Classified into Class F and Class C, fly ash has distinct properties.

3.2 Cement

Cement is a crucial binding agent in construction, essential for uniting various materials and creating strong, durable structures. Typically, a finely ground, grey powder made from a blend of limestone, clay, shale, and other elements, cement is most commonly used in the form of Portland cement, a global standard in construction. It plays a pivotal role in concrete production, acting as the glue that binds aggregates like sand, gravel, and crushed stone, providing strength, stability, and durability to structures. From buildings and bridges to dams, roads, and sidewalks, cement's adaptability and robustness make it an indispensable component in the construction industry, facilitating the creation of enduring and resilient infrastructure.

3.3 Sand

Sand, a granular material consisting of finely divided rock and mineral particles, is one of Earth's most abundant natural resources. Formed through the gradual weathering and erosion of rocks over long periods, sand is found in diverse environments such as beaches, deserts, riverbeds, and dunes. Its composition varies based on its origin, but it commonly contains silica, primarily made up of silicon dioxide (SiO2), along with minerals like quartz, feldspar, mica, and fragments of shells. Sand plays a vital role in the construction industry, serving as a key ingredient in the production of concrete and mortar. Its versatility makes it indispensable for various construction applications, including the creation of buildings, roads, and bridges.

3.4 Rice Straw

Rice straw refers to the leftover stalks or stems of rice plants remaining after the grains are harvested. This dry, fibrous residue, often comprising elongated stems along with leaves and panicles depending on the harvesting method, is the by-product of rice cultivation. Typically light in weight and pale yellow to tan in color, rice straw features hollow tubes with nodes or joints at regular intervals along its length and is commonly baled for storage or further processing after drying. Abundant in regions where rice is extensively cultivated, rice straw serves various traditional and modern applications. It has been used for animal bedding,

thatching, and cooking fuel, while more innovative uses include mulching, livestock feed, bioenergy production, and as a raw material for creating biomaterials.

Figure 1: a. Fly Ash b. Cement c. Sand d. Straw

Table 2: The materials are blended in varying proportions to achieve the desired strength.

Sl No.	DESIGNATION	MATERIALS				
		Cement (KG)	Fly Ash (KG)	Sand(KG)	Straw(KG)	Water(Lt)
1	$C_{30}F_{50}S_{20}ST_0$	7.39	12.27	4.9	0	6
2	$C_{30}F_{49}S_{20}ST_1$	7.39	12.02	4.9	0.49	6
3	$C_{30}F_{48}S_{20}ST_2$	7.39	11.78	4.9	0.98	6
4	$C_{30}F_{47}S_{20}ST_3$	7.39	11.54	4.9	1.47	6
5	$C_{30}F_{46}S_{20}ST_4$	7.39	11.23	4.9	1.96	6
6	$C_{30}F_{45}S_{20}ST_5$	7.39	11.04	4.9	2.45	6
7	$C_{30}F_{43}S_{20}ST_7$	7.39	10.56	4.9	3.43	6
8	$C_{30}F_{41}S_{20}ST_9$	7.39	10.06	4.9	4.41	6

4. Result Analysis

The materials mentioned above fly ash, cement, sand, and straw are blended in varying proportions to achieve the desired strength. This procedure is iteratively performed using the same materials but with different ratios, and subsequently, a compression test is conducted. The result analysis of the above proposed model given bellow

Table 2: Result analysis of different materials

Sl No	Designation of test sample	Compressive Strength (N/mm^2)
1	$C_{30}F_{50}S_{20}ST_0$	8.343
2	$C_{30}F_{49}S_{20}ST_1$	7.322
3	$C_{30}F_{48}S_{20}ST_2$	5.89
4	$C_{30}F_{47}S_{20}ST_3$	4.094
5	$C_{30}F_{46}S_{20}ST_4$	4.227
6	$C_{30}F_{45}S_{20}ST_5$	3.599
7	$C_{30}F_{43}S_{20}ST_7$	2.324
8	$C_{30}F_{41}S_{20}ST_9$	1.719

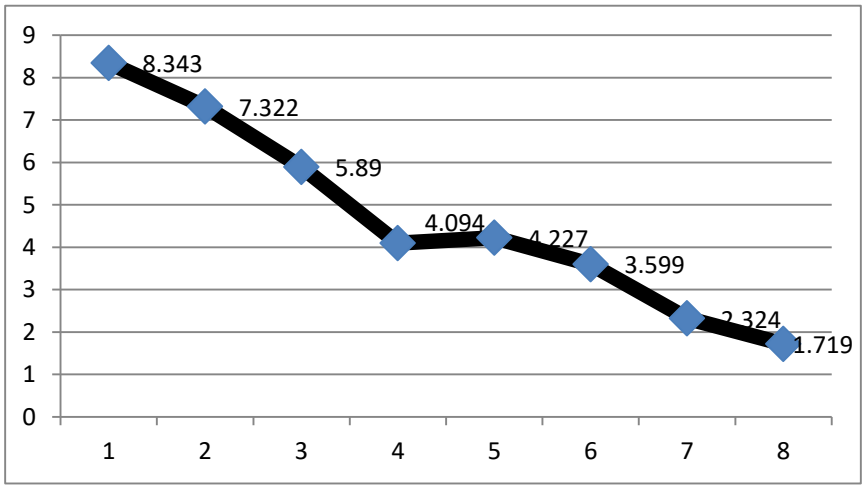

Figure 2: Compressive strength of the material gradually decreases

Based on the observation, it can be stated that the compressive strength of the material gradually decreases with an increase in the proportion of rice straw.

5. Conclusion

In conclusion, based on the observation, it can be stated that the compressive strength of the material gradually decreases with an increase in the proportion of rice straw. This trend is evident as adding 3% of rice straw yields a compressive strength of 4 MPa, whereas with 5% it decreases to 3 MPa, further decreasing to 2 MPa with 7% and finally to 1 MPa with 9% of rice straw. Therefore, it can be inferred that as the amount of rice straw added increases, the compressive strength of the material progressively diminishes.

References:

[1] Armstrong, L. (2015), "Building a sustainable future: The hemperete revolution". Available at www.cannabusiness.com/newsscience-technology/building-a-future- the hemperete-revolution.

[2] Arrigoni, A., Pelosato, R., Melia, P., Ruggieri, G., Sabbadini, S., and Dotelli, G. (2017), "Life cycle assessment of natural building materials: the role of carbonation, mixture components and transport in the environmental impacts of hemperete blocks," Journal of Cleaner Production, Elsevier Ltd, Vol. 149, pp. 1051-1061.

[3] Asdrubali, F., D'Alessandro, F., and Schiavoni, S. (2015). "A review of unconventional sustainable building insulation materials," Sustainable Materials and Technologies, Elsevier B.V., Vol. 4, pp. 1-17.

[4] Aswale, S. (2015), "Brick making in India history," International Journal of Financial Services Management, Vol. 4.

[5] Awasthi, A., Singh, N., Mittal, S., Gupta, P.K., and Agarwal, R. (2010), "Effects of agriculture crop residue burning on children and young on PFTS in North West India," Science of the Total Environment, Elsevier B.V., Vol. 408

[6] Baig, M. (2010), "Biomass: Turning agricultural waste to green power in India," Available at www.abccarbon.com/biomass-turning-agricultural-waste-to-green-power-in-india.

[7] Banerjee, S. (2015), "Brick kilns contribute about 9 per cent of total black carbon emissions in India," Available at www.cseindia.org/brick-kilns-contribute-about-9-per-cent- of-total-black.

Optimization of SAG Structure

Dilip Kumar Nayak[1*], Prabodha Kumar Dalai[2], ParthaSarathi Das[3], Pradosh Kumar Hota[4], [5]Srilata Basu

[1]Department of ECE, GITA Autonomous College, Bhubaneswar-752054, Odisha,
Email: dilip_ece@gita.edu.in
[2]Department of ECE, GITA Autonomous College, Bhubaneswar-752054, Odisha,
Email: prabodha.dalai@gmail.com
[3]Department of ECE, GITA Autonomous College, Bhubaneswar-752054, Odisha,
Email:partha016@gmail.com
[4]Department of ECE, GITA Autonomous College, Bhubaneswar-752054, Odisha,
Email:pradosh@gita.edu.in
[5]Department of ECE, GITA Autonomous College, Bhubaneswar-752054, Odisha,
Email:srilatabasu_ece@gita.edu.in

Abstract:

For future filter applications, we examine the silicon-based ternary grating SAG (silicon on air on glass) structure. Grating is accomplished by a one-dimensional grating structure composed of ternary periodic structure, where ternary period is realized by combining silicon-air-silicon dioxide layers. The plane wave expansion method (PWE) is utilized to mimic the reflections from such periodic structures. The simulation outcome divulges that the number of layers in the periodic structures have a significant strength on the same. Furthermore, the structure has been tuned for 100% reflection. It is also discovered that the wavelength shift grows steadily from 8 to 32 ternary layers.

Keywords: Ternary grating, Reflectance, filter, PWE, SAG

1. Introduction

The grating SAG structure has received widespread attention as a possible contender for producing large integrated scale devices for all optical communication networks [1]. This structure is made up of alternating periodic layers of materials, and the refractive index is modulated when electromagnetic waves pass through it [2]. The uses of grating structures are determined by the type of their construction. Furthermore, the grating structure is directly dependent on the position and arrangement of layers of the same structure [3]. In terms of layer types, binary and ternary layers are used to construct grating structures. Some applications have been developed employing the binary grating structure, but just a few have dealt with the ternary layers [4,5,6]. We are interested in concentrating the ternary layers of grating structure for the reason of the same application since this study deals with ternary layer for prospective filter application.

A ternary grating arrangement has recently been developed for pressure and temperature sensors [7]. Ternary layer is nothing more than the assembly of three separate material layers. The filter structure is made up of an alternating sequence of two or more distinct optical materials. A Fresnel reflection is contributed by each interaction between two materials [8]. The optical path discrepancies between reflections from following interfaces, as well as the directions of amplitudes reflection coefficients for the interfaces, are crucial in this concept. In this situation, the reflected

components of the reflected faces constructively interact, resulting in a powerful reflection[9,10]. The refractive index contrast and number of ternary layers of the grating structure influence the reflected bandwidth [11].
This study is arranged as follow: Section 2 discusses the construction of ternary gratings, and Section 3 provides a mathematical foundation for simulation. Section 4 presents the outcome and explanation. Section 5 concludes with conclusions.

2. Ternary layer grating Structure

Figure 1 represents ternary grating structure, where glass is separated from silicon by air material. And then silicon based (silicon-air-silicon dioxide) ternary grating layer is placed on this structure.

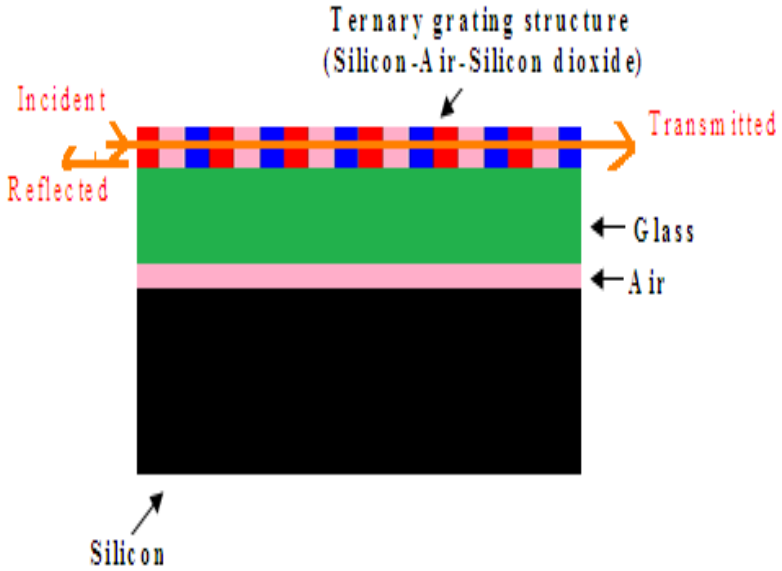

Figure 1. 1D ternary grating structure

The above-mentioned configuration is a new kind of waveguide because it is made up ternary grating structure and combination of silicon-air-oxide layer. The refractive indices are n structure. In figure 1, it is seen that the grating has alternate layers of refractive indices n_1 (first materials layers), n_2 (refractive index of second materials layer), n_3(refractive index of third materials layer) with thickness t_1, t_2 and t_3 respectively. Further, $t= t_1+t_2+t_3$ is the regular pattern

3. Outcomes of the result

To investigate the potential filter applications of the grating SAG structure, electromagnetic waves with a wide variety of wavelengths are impacted on the aforementioned structure, and the 100 percent reflectance is evaluated with regard to different wavelength bands. This reflectance is discovered for several ternary layers of grating construction. For the same application, the plane wave expansion approach is used to simulate the number of ternary layers of the grating structure. Figures 3, 4, 5, 6, 7, and 8 depict simulations for one, two, four, eight, sixteen, and thirty-two layers, respectively.

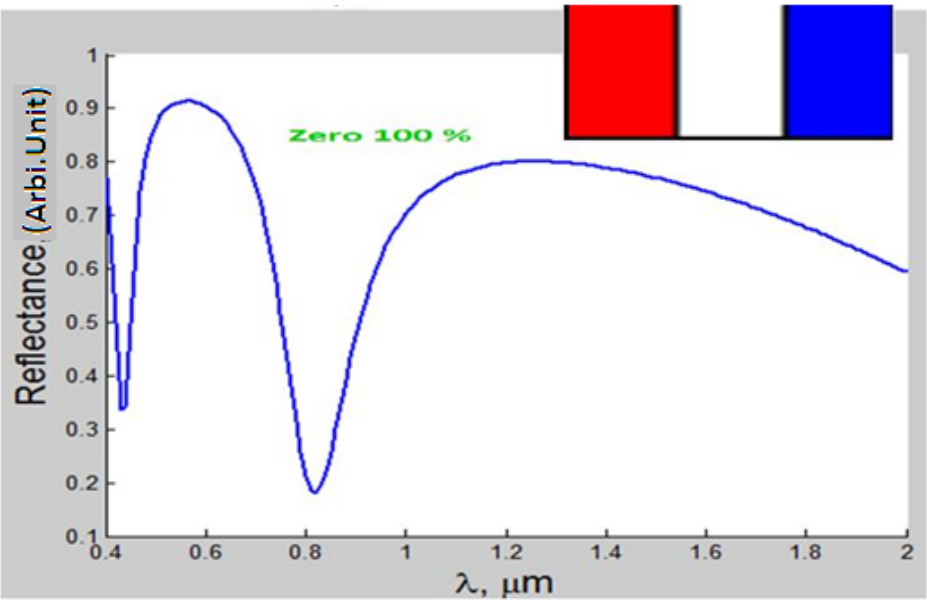

Figure 3. Simulation output of reflectance for single ternary layer.

Figure 3,4, 5,6, 7 and 8 signify the chart between reflectance (Arbi-Unit) alongside perpendicular axes with regard to wavelength (μm) alongside parallel axes for one, two, four, eight, sixteen and thirty two ternary layers respectively From these figures (Figure 3,4, 5,6, 7 and 8) , the random deviation of reflectance versus wavelengths are found.

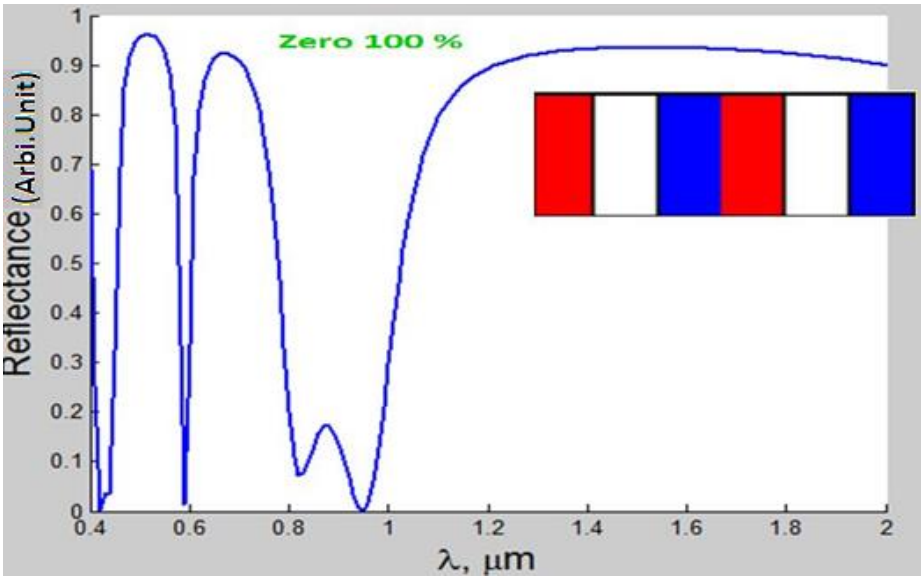

Figure 4. Simulation output reflectance of double ternary layers.

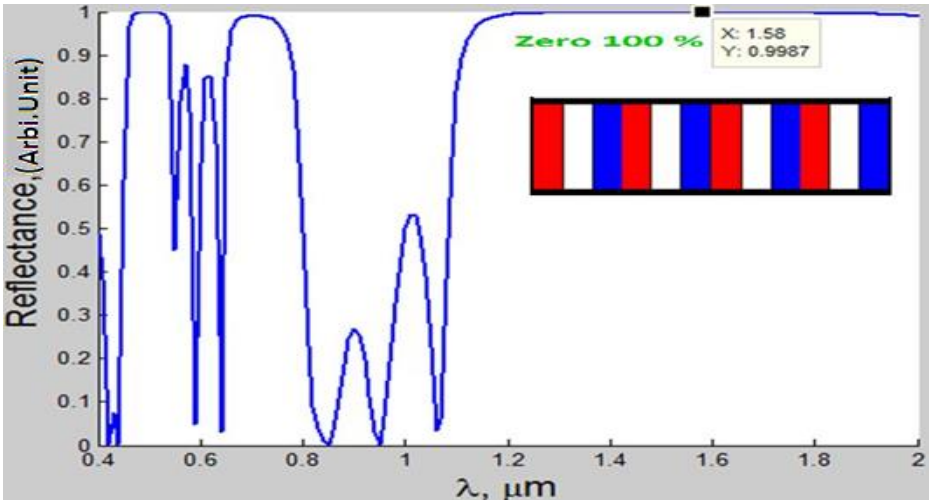

Figure 5. Simulation output four ternary layers.

In figure 3, it is found that no reflectance approaches to 100% corresponding to any wavelengths. So it is inferred that single ternary (Si-air-SiO_2) of grating structure is not suitable for filter and mirror application. By applying same technique, it is seen from figure 4 that, like one ternary layer, here also no reflectance approaches to 100% (maximum 90%). So it is also not suitable for filter application. Again, form figure 5, it is seen that, though reflectance seems to be approached to 100 % but really it does not approach (maximum 99.12 %) to the 100 % reflectance.

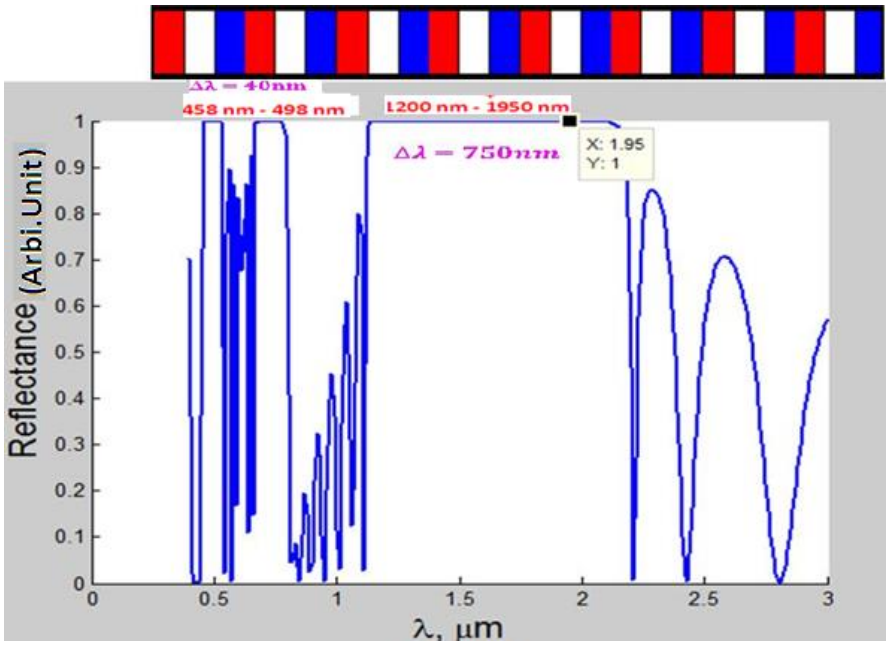

Figure 6. Simulation output eight ternary layers.

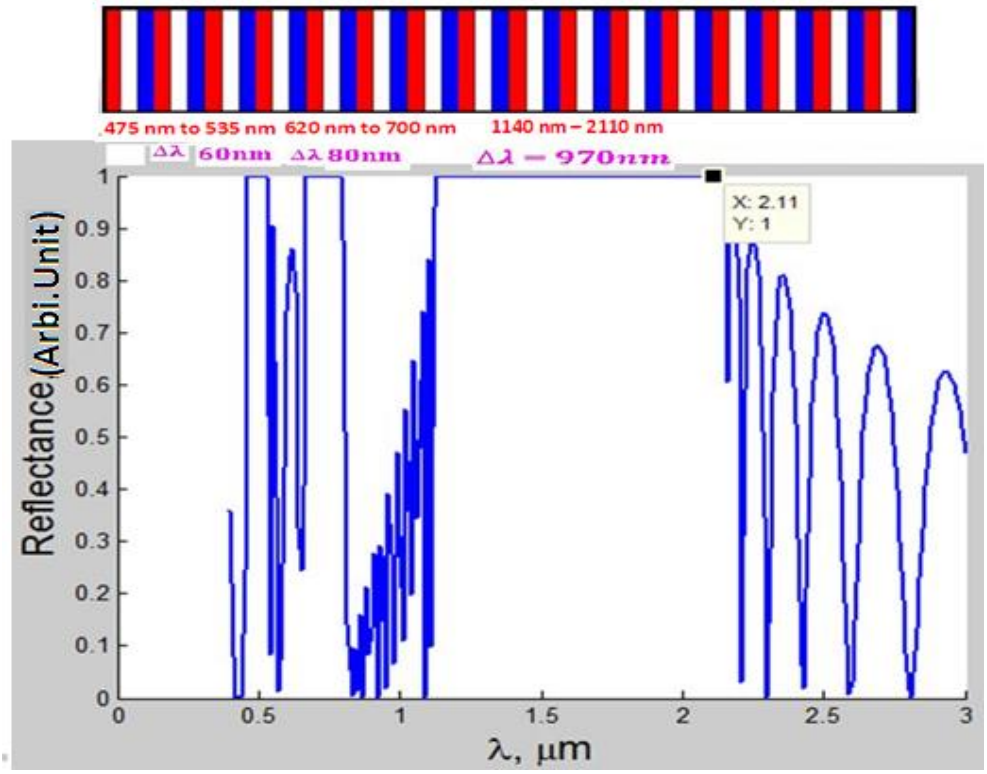

Figure 7. Simulation output reflectance for sixteen ternary layers.

So, like one and two ternary grating structure, four ternary grating configuration is not appropriate for the same filter use, though filter application is seen for further increasing the number of ternary layers, for examples, from figure 6 ,100% reflectance is found with regard to wavelength range, from 458 to nano-metre 498 nano-metre($\Delta\lambda_1$=40 nm) and from 1200 nm to 1950 nm ($\Delta\lambda_2$=750 nm). Here two wavelength bands are applicable for filter applications and the total wavelength for mirror is ($\Delta\lambda_=\Delta\lambda_1+\Delta\lambda_2$) 790 nm.

Further increasing the number of layers from 8 to 16, from figure 7, it is found that three wavelength band gives 100% , such as band from 485 nm to 535 nm, ($\Delta\lambda$1=60 nm), 620 nm to 700 nm ($\Delta\lambda$2=80 nm) and 1200 nm to 2130 nm ($\Delta\lambda$3=970 nm). And the total wavelength band width, $\Delta\lambda$ ($\Delta\lambda$1+$\Delta\lambda$2+$\Delta\lambda$3) is 1110 nm. Again increasing the number of ternary layers to 32, it is seen that three 100 % reflected bands are observed such as from 450 nm to 520 nm ($\Delta\lambda$1=70 nm), 610 nm to 700 nm ($\Delta\lambda$2=90 nm) and from 1200 nm to 2130 nm ($\Delta\lambda$3=970 nm). And its corresponding the total reflected band (($\Delta\lambda$1+$\Delta\lambda$2+$\Delta\lambda$3) is 1130 nm.

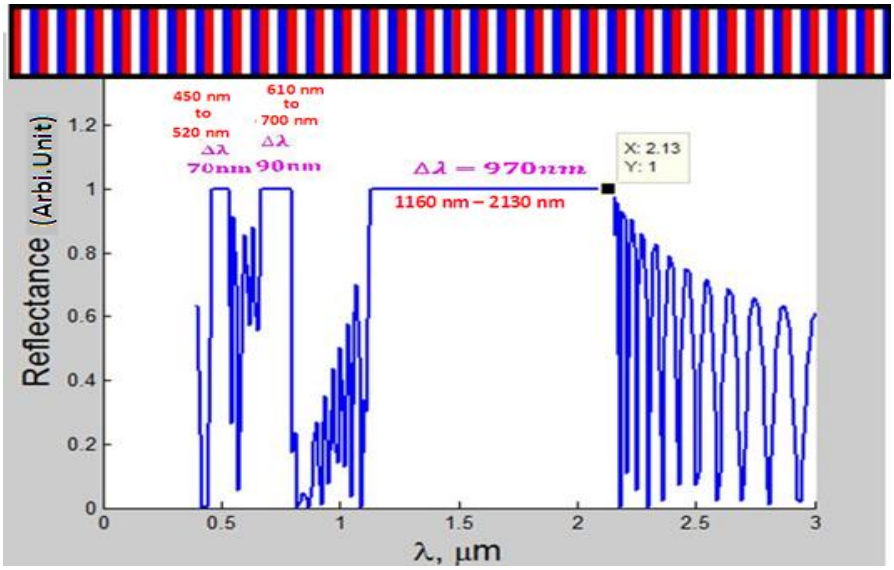

Figure 8. Simulation outputthirty two ternary layers.

Analyzing above discussion, figure 8 bestows absolute data between the deviation of total wavelength band (100% reflectance) with respect to number of ternary layers.

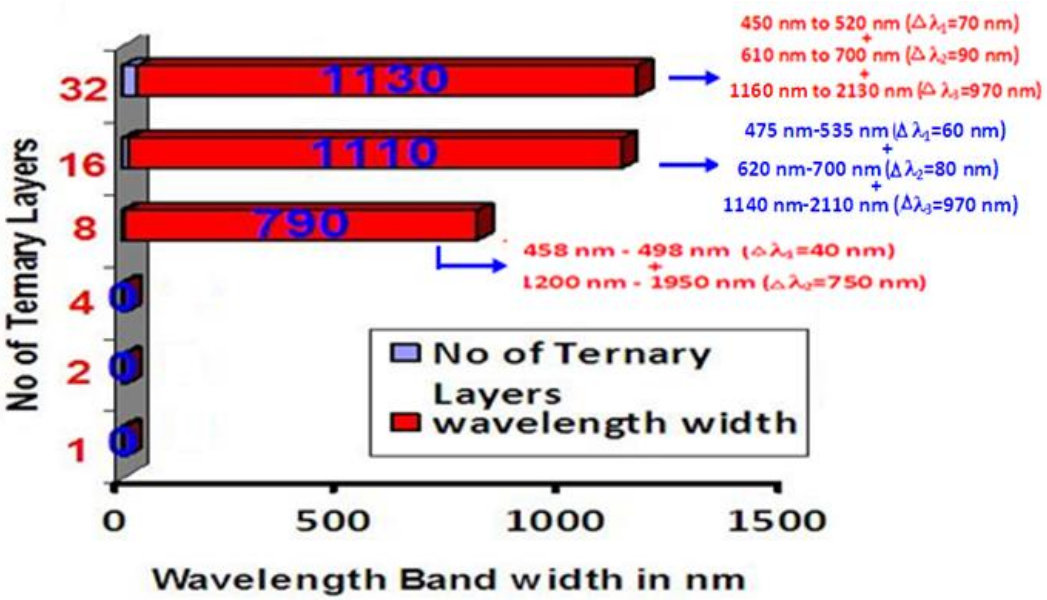

Figure 8. Variation of wavelength of ternary layers.

Figure 8 shows the number of ternary layers along the y-axis and the wavelength band in nm along the x-axes. This graphic shows that there is no 100% reflectance for the first, second, and fourth ternary layers. However, for 8, 16, and 32 ternary layers, there is complete reflection. In this scenario, the 8 ternary layer grating structure produces two band wavelengths (458 nm – 498 nm and 1200 nm-1950 nm), which are suited for filter applications. Figure 8 clearly demonstrates this as well. Apart from that, it can be noticed that 16 and 32 ternary layers produce three wavelength

bands (475 nm - 535 nm, 620 nm - 700 nm, 1140 nm - 2110 nm) and 450 nm-520 nm, 610 nm-700 nm, 1160 nm - 2110 nm).

4. Conclusion

This research carefully investigates possible filter applications based on the ternary grating SAG structure. To acquire reflectance from such a structure, the plane wave expansion approach is applied in the modelling work. The results of simulation exposed that the number of ternary layers of the grating construction is significant for filter use. It is also discovered that 1,2, and 4 ternary grating structures are unsuitable for filtering, however 8, 16,32 ternary layers of grating structures are. It is also discovered that the wavelength width grows as the number of ternary grating structures increases.

Reference

[1] Fan, S., Wang, Z., David, A. B., Villeneuve, P. R., Haus, H. A., &Joannopoulos, J. D. (2002). Grating for Communication Applications. *Proceedings of SPIE, 4870*, 298–306.

[2] Joannopoulos, J. D., Johnson, S. G., Winn, J. N., & Meade, R. D. (2008). *Gratings: Molding the Flow of Light* (2nd ed.). Princeton, NJ: Princeton University Press.

[3] Hussein, M. I. (2009). Reduced Bloch Mode Expansion for Periodic Media Band Structure Calculations. *Proceedings of the Royal Society A, 465*, 2825–2848.

[4] Palai, G., Tripathy, S. K., Muduli, N., & Patnaik, S. K. (2012). Optimization of Efficiency in a 1D Grating Structure at 1310nm Wavelength for Application in Optical Interconnect. *Asian Journal of Physics, 21*(2), 145–152.

[5] Palai, G., &Tripathy, S. K. (2013). Efficient Silicon Grating for SOI Applications. *Optik - International Journal for Light and Electron Optics, 124*(17), 2645–2649.

[6] Ardakani, A. G. (2014). Nonreciprocal Electromagnetic Wave Propagation in One-Dimensional Ternary Magnetized Plasma Gratings. *JOSA B, 31*(2), 332–339.

[7] Banerjee, A. (2009). Enhanced Temperature Sensing by Using One-Dimensional Ternary Photonic Band Gap Structures. *Progress in Electromagnetics Research Letters, 11*, 129–137.

[8] Woan, G. (2010). *The Cambridge Handbook of Physics Formulas*. Cambridge: Cambridge University Press.

[9] Parker, C. B. (1994). *McGraw Hill Encyclopedia of Physics* (2nd ed.). New York: McGraw Hill.

[10] Kenyon, I. R. (2008). *The Light Fantastic – Introduction to Classic and Quantum Optics*. Oxford: Oxford University Press.

Pollution from Biomass Cooking: A Comprehensive Analysis of Emission Patterns

Chandrika Samal[1*], Sushmita Dash[2], P. K Jena[3], A. S Dehury[4], Manmatha K. Roul[5], Manoj.K Pradahn[6]

1Department of Mechanical Eng., GITA Autonomous College, Bhubaneswar-752054, Odisha, Email: chandrika_mech@gita.edu.in
2Department of Mechanical Eng., GITA Autonomous College, Bhubaneswar-752054, Email: sushmita_me@gita.edu.in
3Department of Mechanical Eng., GITA Autonomous College, Bhubaneswar-752054, Email: pradeep_me@gita.edu.in
4Department of Mechanical Eng., GITA Autonomous College, Bhubaneswar-752054, Email: amit_me@gita.edu.in
5Department of Mechanical Eng., GITA Autonomous College, Bhubaneswar-752054, Odisha, Email: mkroul@gmail.com
6Department of Mechanical Eng., GITA Autonomous College, Bhubaneswar-752054, Odisha, Email: hodme@gita.edu.in
*Corresponding Author's Email Id: chandrika_mech@gita.edu.in

Abstract

The reliance on biomass for cooking by approximately three billion people highlights a significant energy challenge, particularly in developing regions. Traditional biomass cook-stoves, often characterized by their inefficient combustion processes, are associated with a range of negative impacts, including health hazards from indoor air pollution, contributions to climate change through greenhouse gas emissions, and environmental degradation. Current review paper discusses various methodologies employed by researchers to evaluate emissions from biomass cook stoves, including laboratory testing, field Studies and modeling approaches. The present paper offers an extensive review of the emission characteristics associated with various biomass cook stoves utilized across different regions of the world.

Keywords: Indoor Air Pollution, Particulate Matter, Carbon Monoxide, improved cook-stoves

1. Introduction

Energy derived from biomass plays a crucial role in the global economy, particularly as a traditional cooking fuel in the rural regions of many developing nations. Throughout human civilization, energy for cooking has remained one of the most fundamental and essential energy needs [1]. Currently, around 3 billion individuals worldwide rely on open fires and traditional cook-stoves to fulfill their household energy requirements, with approximately 90% of these users depending on solid biomass fuels [2]. According to the Global Bioenergy Statistics [3], biomass accounts for nearly 10% of the world's overall energy consumption, making it one of the most widely used feed-stocks for domestic cooking and heating applications. Despite its advantages, a significant drawback associated with biomass cook-stoves is the prevalence of indoor air pollution, which arises due to improper venting of smoke [4]. The primary objective in the design of improved cook-stoves should be to achieve complete biomass combustion [5].

Utilizing biomass cook-stoves in enclosed spaces can lead to severe acute respiratory issues. The World Health Organization (WHO) reports that exposure to household air pollution is linked to various chronic diseases such as stroke, ischemic heart disease, chronic obstructive pulmonary disease (COPD), and lung cancer [6]. Besides respiratory ailments, non-respiratory conditions—including stillbirth, low birth weight, infant mortality, cardiovascular disease, and cataracts—can result from emissions from biomass cook-stoves. Incomplete combustion generates significant quantities of toxic emissions including carbon monoxide (CO), nitrogen oxides (NOx), sulfur dioxide (SO2), particulate matter (PM), and polycyclic aromatic hydrocarbons (PAHs) [7-9]. These pollutants create serious health risks, particularly for women and children [10]. The variety of diseases associated with emissions from biomass cook-stoves is illustrated in Figure 1.

As reported by the WHO and the World Bank, household air pollution is responsible for approximately two million premature deaths globally [11]. Furthermore, data from the International Energy Agency indicates that the number of premature deaths attributed to biomass emissions is projected to rise, while mortality from other diseases is expected to decline by 2030. Currently, much governmental funding and attention are focused on other health issues, yet the health dangers posed by biomass emissions may become a silent crisis in the near future. Therefore, it is critical to intensify research on biomass cook-stoves and the emissions produced.

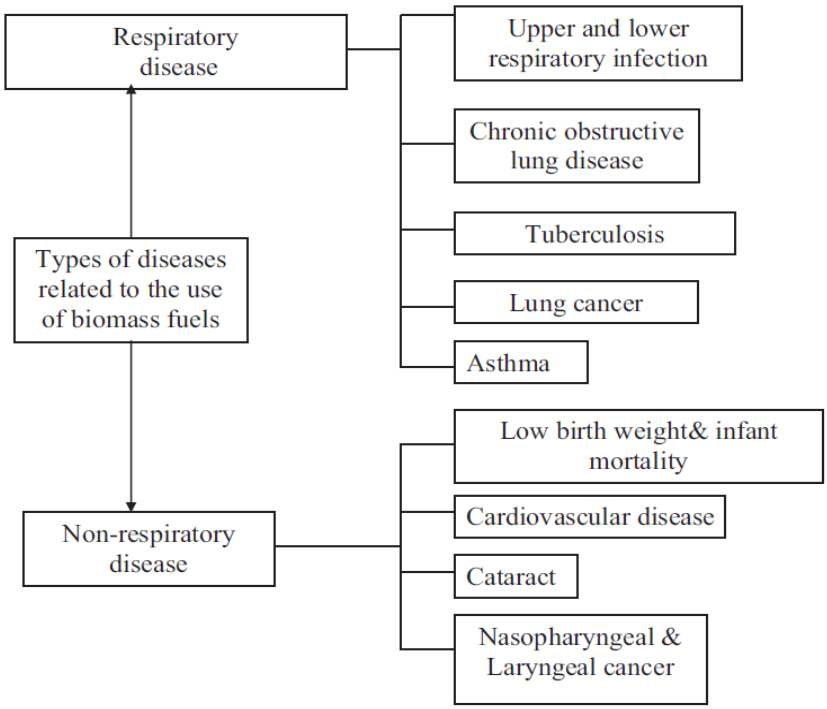

Figure 1. Diseases caused due to emission from biomass cook-stoves [7]

According to the World Energy Outlook [12], the number of premature deaths attributable to pollutants from biomass is expected to rise globally, while fatalities from other diseases are anticipated to decrease by 2030. Recently, most government funding and public health attention have been directed toward other health concerns, leading to the risk that the health impacts associated with biomass emissions may go unnoticed, acting as a silent threat in the near future. This highlights the urgent need to focus on research

related to biomass cook-stoves and the emissions they produce. A comparison of the anticipated trends in premature deaths resulting from biomass emissions against those from other major diseases is illustrated in **Fig. 2**. It is particularly alarming that countries in Asia and Africa are disproportionately affected by indoor air pollution, facing the highest rates of premature mortality.

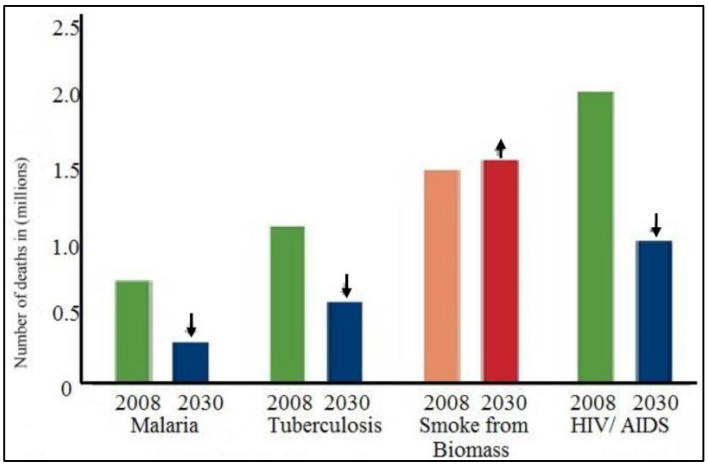

Figure 2 Flow of Future trends of premature deaths due to emission from biomass and other prominent diseases [12]

In addition to their health implications, the pollutants released from biomass cook-stoves significantly contribute to global warming and climate change. To address the emission challenges, exhaustive studies have been undertaken by various researchers, leading to the modification of traditional biomass cook-stoves (such as three-stone fires and mud stoves) into more efficient improved cook-stoves. Numerous design parameters, alternative biomass fuels, varied cooking methods, and a range of evaluation techniques have been explored to enhance efficiency and mitigate emissions. Despite the numerous studies aimed at emission reduction, the problem remains unresolved.

This review article provides an in-depth examination of the different pollutants released from various biomass cook-stoves commonly used worldwide, the assessment methods adopted for measuring cook-stove emissions, and the technical concepts and strategies discussed in the extant literature aimed at reducing exhaust emissions.

2. Measuring Emissions in Biomass Cooking Appliances

Evaluating emissions from biomass cook-stoves is crucial for assessing their environmental impact and understanding their health implications. Various methods have been developed over the years to measure and analyse the emissions produced by these stoves.Emission testing represents a vital component of cook-stove research, with diverse strategies devised to assess the functionality of biomass cook-stoves under controlled settings. Among these, the "Hood Method" and the "Chamber Method" stand out as the most frequently utilized testing approaches. Arora and Jain (2016) indicate that around 70% of research utilizes the Hood Method, while approximately 20% opt for the Chamber Method.

The remaining 10% of emission assessments are conducted using alternative field-based plume sampling techniques.The Hood Method focuses on evaluating various pollutants, including carbon monoxide (CO), particulate matter (PM), carbon dioxide (CO_2), methane (CH_4), non-methane hydrocarbons (NMHC), tetrahydrocannabinol (THC), polycyclic aromatic hydrocarbons (PAHs), nitrous oxides (NO_x), and sulphur-

dioxide (SO_2) throughout the testing phase. For this procedure, the cook-stove is positioned beneath a conical fume hood, which has a one-meter diameter, positioned one meter below the stove itself. A blower facilitates the suction of all flue gases into the hood without disturbing the combustion characteristics. The rate of exhaust discharge is kept at 0.1 m^3/s. Probes are integrated into the hood and duct lines to accurately measure pollutant emissions via a range of exhaust analyzers.While the Hood Method does have its limitations, it enjoys broad acceptance among researchers due to its cost-effectiveness and straightforward implementation.

Ahuja et al. [14] were the first to introduce the "Chamber Method" for evaluating the smokiness of unvented biomass cook-stoves, applicable in both laboratory and field settings. This technique is also referred to as the simulated kitchen method. In this approach, the stove is subjected to a cooking cycle within a dedicated chamber, where emissions are monitored. Notably, this method does not require duct work or airflow calibrations.

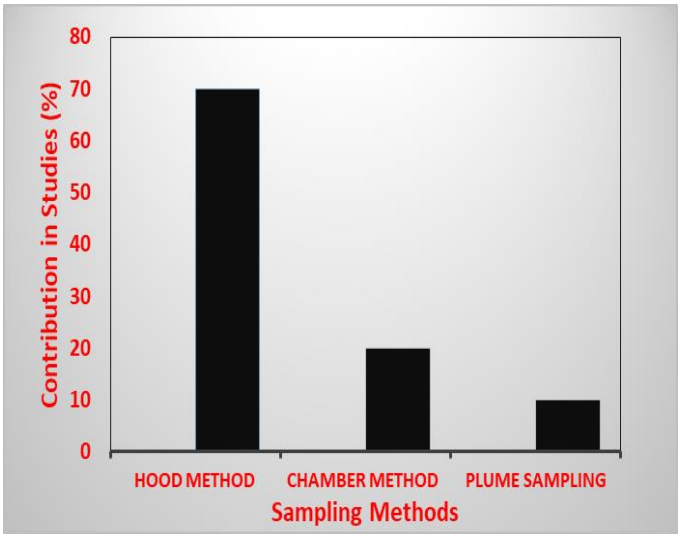

Figure 3. Percentage of share of different sampling methods in literature of cook-stove

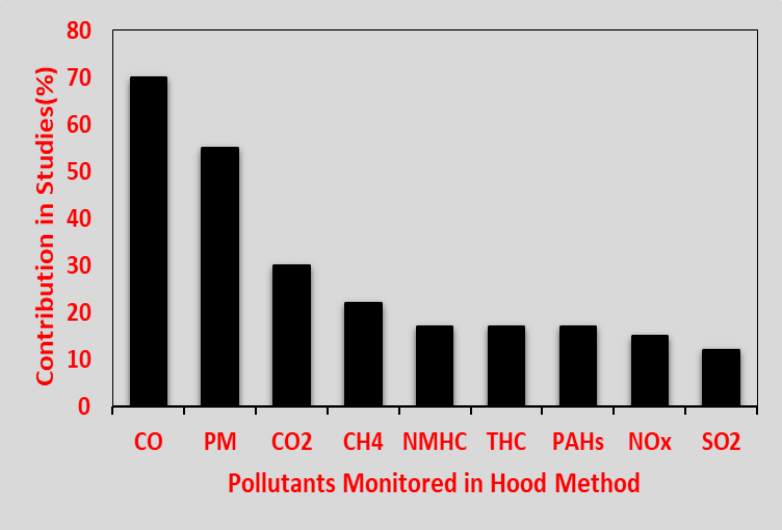

Figure 4. Percentage of share of different various pollutants monitored in literature using hood method

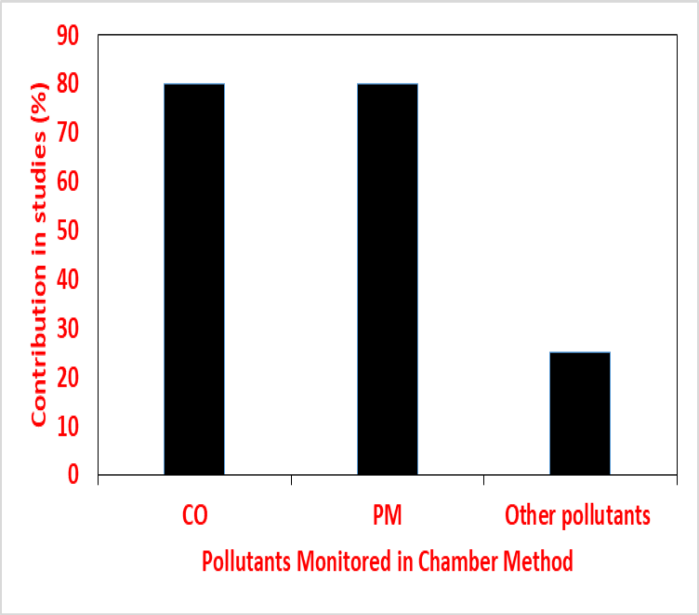

Figure 5 Percentage of share ofCO, PM and other pollutants in literature of chamber method

However, a significant limitation of the Chamber Method is the need for ample space for testing, which may not be practical in many laboratory environments. Additionally, the direct exposure of testers to exhaust fumes and pollutants during the monitoring process poses another drawback.The percentage of various emission evaluation methods reported in literature, along with the percentage distribution of different pollutants monitored using the Hood Method and the percentages of carbon monoxide (CO), particulate matter (PM), and other pollutants assessed through the Chamber Method, are illustrated in Figures 3, Figure 4 and Figure 5, respectively.

3. Timeline Analysis of Emission Outputs

Bhattacharya et al. [15] explored the emission characteristics of diverse traditional and improved cook-stoves using the "Hood method" as part of the Water Boiling Test protocol. The study measured emission factors (EFs) for several pollutants including CO_2, CO, CH_4, Total Non-Methane Organic Carbon (TNMOC), and NO_x. Findings revealed that wood-burning stoves produced lower EFs for CO_2, CO, and NO_x compared to those burning charcoal, while EFs for TNMOC and CH4 were found to be similar across both stove types. Additionally, Bhattacharya et al. [16] investigated the impact of varying fuel moisture content on emissions. Their results indicated that higher moisture content significantly increased CO emissions and marginally affected CO2 emissions, while NO_x emissions showed a decreasing trend. They also noted that smaller fuel sizes contributed to higher CO emission factors and observed that top feeding techniques yielded lower emissions of CO and NO_x compared to traditional bottom feeding methods.

In a separate study, Yuntenwi et al. [17] assessed how wood moisture levels (5%, 15%, and 25%) affected PM and CO emissions from open fires, rocket stoves, and skirt stoves. The research found that PM emissions were at their lowest when burning wood with a moisture content of 30% in a rocket stove, while CO emissions peaked with 15% moisture in the same stove type. The overall performance of the rocket stove was superior in terms of both PM and CO emissions compared to the other stove designs.Zhang et al. [18] focused on the combustion emissions of CO, CO2, PM, NO, NO2, and NOx from three types of

agricultural residues (rice straw, wheat straw, and corn straw) prominently produced in China.In another investigation, Jetter and Kariher [19] observed the emissions of CO and PM from various solid-feedstock stoves and fuel combinations, discovering that stoves designed with smaller components produced lower emission factors. Roden et al. [20] conducted dual-field and laboratory assessments and found that modern, well-engineered cook-stoves released significantly less CO and PM emissions compared to their traditional counterparts, with considerable variance between field-based and laboratory measurements influenced by cooking techniques and user skills. Panwar [21] analysed the emission efficiency of a SPRERI gasifier and improved double pot cook-stove, identifying carbon dioxide and carbon monoxide emissions in the range of 17-26 ppm and 3-6 ppm, respectively.

Roy et al. [22], in their assessment of wood-fired stoves, determined that CO emissions decreased with higher air supply factors, while SO2 and NO_x emissions were associated with the nitrogen and sulphur traits of the feed-stocks utilized. Lastly, Wei et al. [23] compared the emissions from uncompressed biomass (like firewood and crop residues) against compressed biomass pellets (e.g., corn and pine pellets) in both brick and pellet stoves used in rural China. Their findings indicated that pellet fuel resulted in lower emissions, significantly influenced by specific fuel properties and combustion methods adopted during use. Together, these studies illuminate the intricate dynamics of emissions from biomass cook-stoves, highlighting the comprehensive impact of factors such as fuel type, moisture levels, feeding practices, and stove designs on overall emission performance.

Researchers at the University of Cambridge [24] conducted an experiment to compare the emissions of a novel biomass cook-stove with a traditional three-stone fire. The results showed that the three-stone fire emitted significantly higher levels of CO, which were 200% greater than those produced by the biomass cook-stove. On the other hand, a study by the University of California, Berkeley [25] found that by improving ventilation in a test kitchen, the levels of PM and CO emissions could be reduced by 93-98% and 83-95%, respectively. In another study, scientists at the Indian Institute of Technology [26] compared the emissions of an improved three-pot cook-stove with a traditional mud stove. They found that the improved stove emitted 65.8% less SO2, 70.2% less NO2, and 76.1% less TSPM than the traditional stove. Additionally, a study by the University of Delhi [27] investigated the effects of fuel moisture content on emissions and found that higher moisture levels led to increased CO and CO2 emissions, while reducing NO_x emissions.

A study by the National Environmental Engineering Research Institute [11] compared the emissions of two different Philips cook-stoves using two different testing protocols. The results showed that the testing protocol used had a significant impact on the emissions, with CO emissions being 39% and 47% higher in one protocol compared to the other for two different stoves. In contrast, PM emissions were 55% lower in one protocol compared to the other for one of the stoves.Researchers at the University of Science and Technology [28] investigated the effects of moisture content in wood pellets on the performance of a non-durable semi-gasifier cook-stove. They found that increasing moisture content led to reduced emission factors for CO and PM. This result contradicted previous findings by other researchers, which may be due to differences in stove designs or fuel refilling methods.A study by the University of Oxford [29] evaluated the impact of a new improved cook-stove called the "Ugastove" on emissions in rural Uganda. The results showed that the stove reduced PM2.5 concentrations by 37% and used 50% less biomass than a traditional three-stone fire to complete cooking tasks.These studies highlight the importance of stove design and fuel

quality in determining emissions, and demonstrate the potential for improved cook-stoves to reduce air pollution and improve health outcomes. The collection of these studies emphasizes the critical role that stove design, moisture content, ventilation, and testing protocols play in influencing the emission profiles of cook-stoves, ultimately impacting air quality and health outcomes in cooking environments.

4. Conclusion

The principal outcomes of current comprehensive review are highlighted as follows:

1. Incomplete combustion of fuel in traditional cook-stoves and open flames leads to elevated levels of indoor air pollutants.
2. Researchers utilize various methodologies to evaluate cook-stove emissions, with the hood method being particularly popular.
3. While many studies concentrate on measuring CO and PM emissions, some also examine additional pollutants like NO_x, SO_2, and CO_2.
4. To reduce incomplete biomass combustion, it is essential to optimize factors such as stove design, type of biomass, size of fuel, moisture content, methods of refuelling, and air supply systems.
5. Emission factors are greatly influenced by the physical and chemical properties of biomass fuels, fuel delivery mechanisms, combustion cycles, and burning conditions.
6. Some studies suggest that lowering moisture content in fuel can decrease emissions, whereas others indicate that the technological design of the stove has a greater effect than moisture levels.
7. It is critical to thoroughly investigate the relationship between moisture content and emissions in a methodical manner. Enhanced cook stoves, which incorporate advanced features, generally emit fewer pollutants than their conventional counterparts. Natural draft TLUD cook-stoves can be operated effectively with low emissions when maintained under controlled conditions.

A thorough review of biomass cook-stove emissions highlights the need for more in-depth scientific research focusing on design and combustion factors to significantly lower pollutant emissions.

References

[1.] Boafo-Mensah, G., Darkwa, K. M., & Laryea, G. (2020). Effect of combustion chamber material on the performance of an improved biomass cookstove. *Case Studies in Thermal Engineering*, 21, 100688.

[2.] Samal, C., Mishra, P. C., Mukherjee, S., & Das, D. (2019, December). Evolution of high performance and low emission biomass cookstoves-an overview. *In AIP Conference Proceedings* (Vol. 2200, No. 1, p. 020021). AIP Publishing LLC.

[3.] Global Bioenergy Statistics (2019), *World Bioenergy Association, Stockholm* (2019) 58.

[4.] Harshika, K., Avinash, C., & Kaushik, S. C. (2014). Comparative study on emissions from traditional and improved biomass cookstoves used in India. *International Journal for Research in Applied Science and Engineering Technology*, 2(8), 249-257.

[5.] Samal, C., Mishra, P. C., & Das, D. (2020, November). Design modifications and performance of biomass cookstoves-A review. *In AIP Conference Proceedings* (Vol. 2273, No. 1, p. 020002). AIP Publishing LLC.

[6.] World Health Organization (2018). *Household Air Pollution and Health.* Available online: https://www.who.int/news-room/fact-sheets/detail/household-air-pollution-and-health

[7.] Kim, K. H., Jahan, S. A., & Kabir, E. (2011). A review of diseases associated with household air pollution due to the use of biomass fuels. *Journal of hazardous materials*, 192(2), 425-431.

[8.] Benka-Coker, M. L., Peel, J. L., Volckens, J., Good, N., Bilsback, K. R., L'Orange, C., ... & Clark, M. L. (2020). Kitchen concentrations of fine particulate matter and particle number concentration in households using biomass cookstoves in rural Honduras. *Environmental Pollution*, 258, 113697

[9.] Memon, S. A., Jaiswal, M. S., Jain, Y., Acharya, V., & Upadhyay, D. S. (2020). A comprehensive review and a systematic approach to enhance the performance of improved cookstove (ICS). *Journal of Thermal Analysis and Calorimetry*, 141, 2253-2263.

[10.] Carrión, D., Kaali, S., Kinney, P. L., Owusu-Agyei, S., Chillrud, S., Yawson, A. K., ... & Asante, K. P. (2019). Examining the relationship between household air pollution and infant microbial nasal carriage in a Ghanaian cohort. *Environment international*, 133, 105150.

[11.] Arora, P., Das, P., Jain, S., & Kishore, V. V. N. (2014). A laboratory based comparative study of Indian biomass cookstove testing protocol and Water Boiling Test. *Energy for Sustainable Development*, 21, 81-88.

[12.] World energy outlook 2011, *International Energy Agency*, Paris, 2011.

[13.] Bailis, R., Berrueta, V., Chengappa, C., Dutta, K., Edwards, R., Masera, O., ... & Smith, K. R. (2007). Performance testing for monitoring improved biomass stove interventions: experiences of the Household Energy and Health Project. *Energy for sustainable development*, 11(2), 57-70.

[14.] Ahuja, D. R., Joshi, V., Smith, K. R., & Venkataraman, C. (1987). Thermal performance and emission characteristics of unvented biomass-burning cookstoves: a proposed standard method for evaluation. *Biomass*, 12(4), 247-270.

[15.] Bhattacharya, S. C., Albina, D. O., & Salam, P. A. (2002a). Emission factors of wood and charcoal-fired cookstoves. *Biomass and Bioenergy*, 23(6), 453-469.

[16.] Bhattacharya, S. C., Albina, D. O., &Khaing, A. M. (2002b). Effects of selected parameters on performance and emission of biomass-fired cookstoves. *Biomass and Bioenergy*, 23(5), 387-395.

[17.] Yuntenwi, E. A., MacCarty, N., Still, D., &Ertel, J. (2008). Laboratory study of the effects of moisture content on heat transfer and combustion efficiency of three biomass cook stoves. *Energy for Sustainable Development*, 12(2), 66-77.

[18.] Zhang, H., Ye, X., Cheng, T., Chen, J., Yang, X., Wang, L., & Zhang, R. (2008). A laboratory study of agricultural crop residue combustion in China: Emission factors and emission inventory. *Atmospheric Environment*, 42(36), 8432-8441.

[19.] Jetter, J. J., &Kariher, P. (2009). Solid-fuel household cook stoves: Characterization of performance and emissions. *Biomass and Bioenergy*, 33(2), 294-305.

[20.] Roden, C. A., Bond, T. C., Conway, S., Pinel, A. B. O., MacCarty, N., & Still, D. (2009). Laboratory and field investigations of particulate and carbon monoxide emissions from traditional and improved cookstoves. *Atmospheric Environment*, 43(6), 1170-1181.

[21.] Panwar, N. L. (2010). Performance evaluation of developed domestic cook stove with Jatropha shell. *Waste and Biomass Valorization*, 1(3), 309-314.

[22.] Roy, M. M., & Corscadden, K. W. (2012). An experimental study of combustion and emissions of biomass briquettes in a domestic wood stove. *Applied Energy*, 99, 206-212.

[23.] Wei, W., Zhang, W., Hu, D., Ou, L., Tong, Y., Shen, G., ... & Wang, X. (2012). Emissions of carbon monoxide and carbon dioxide from uncompressed and pelletized biomass fuel burning in typical household stoves in China. *Atmospheric environment*, 56, 136-142.

[24.] Birzer, C., Medwell, P., Wilkey, J., West, T., Higgins, M., MacFarlane, G., & Read, M. (2013). An analysis of combustion from a top-lit up-draft (TLUD) cookstove. *Journal of Humanitarian Engineering*, 2(1).

[25.] Grabow, K., Still, D., &Bentson, S. (2013). Test kitchen studies of indoor air pollution from biomass cookstoves. *Energy for Sustainable Development*, 17(5), 458-462.

[26.] Joshi, M., & Srivastava, R. K. (2013). Development and performance evaluation of an improved three pot cook stove for cooking in rural Uttarakhand, India. *International Journal of Advanced Research*, 1(5), 596-602.

[27.] Kumar, A., Prasad, M., & Mishra, K. P. (2013). Comparative study of effect of different parameters on performance and emission of biomass cook stoves. *International Journal of Research in Engineering & Technology*, 1(3), 121-126.

[28.] Huangfu, Y., Li, H., Chen, X., Xue, C., Chen, C., & Liu, G. (2014). Effects of moisture content in fuel on thermal performance and emission of biomass semi-gasified cookstove. *Energy for Sustainable Development*, 21, 60-65.

[29.] Hankey, S., Sullivan, K., Kinnick, A., Koskey, A., Grande, K., Davidson, J. H., & Marshall, J. D. (2015). Using objective measures of stove use and indoor air quality to evaluate a cookstove intervention in rural Uganda. *Energy for sustainable development*, 25, 67-74.

Prevention of DDoS attack using blockchain

Laxminarayan Dash[1], Manaswinee Madhumita Panda[2], Vivek Priyadarshi Dash[3], Priya Paul[4]

[1]Department of Computer Science and Technology, GITA Autonomous College, Bhubaneswar-752054, Odisha, Email: laxminar ayandash20@gmail.com

[2]Department of Computer Science and Technology, GITA Autonomous College, Bhubaneswar-752054, Odisha, Email: m.madhumitaphd@gmail.com

[3]Department of Computer Science and Technology, GITA Autonomous College, Bhubaneswar-752054, Odisha, Email: vdash91@gmail.com

[4]Department of Computer Science and Technology, GITA Autonomous College, Bhubaneswar-752054, Odisha, Email: paul.priya326@gmail.com

*Corresponding Author's Email Id: laxminarayandash20@gmail.com

Abstract

Distributed Denial of Service (DDoS) attacks pose a significant threat to the digital infrastructure. Traditional defense mechanisms often struggle to mitigate these attacks due to their distributed nature and increasing sophistication. Blockchain technology, with its inherent security and decentralization, offers a promising solution. This abstract explores the potential of blockchain-based approaches to prevent DDoS attacks. By leveraging blockchain's immutability, transparency, and consensus mechanisms, it is possible to create a robust and resilient defense system. This paper delves into various blockchain-based techniques, including smart contracts for automated defense, distributed ledger technology for attack tracking, and blockchain-powered botnet detection. The proposed solutions aim to enhance the security of network infrastructure, making it more resilient to DDoS attacks and ensuring the availability of critical online services.

Keywords: DDoS attacks, immutability, Blockchain technology, security, consensus mechanisms

1 Introduction

In an increasingly digital world, the threat of Distributed Denial of Service (DDoS) attacks looms large, posing substantial risks to online services and infrastructure. These cyberattacks involve overwhelming a target server with a flood of internet traffic, rendering it inaccessible to legitimate users. As the frequency and sophistication of these attacks grow, traditional mitigation methods struggle to keep pace. Consequently, a novel approach is emerging that leverages blockchain technology to enhance the resilience of online systems. By decentralizing data and utilizing smart contracts, blockchain offers a secure and verifiable means of managing network resources, thereby mitigating the impact of DDoS attacks. This introduction sets the stage for exploring how

innovative solutions, such as blockchain, can revolutionize cybersecurity practices, providing a robust defense mechanism capable of safeguarding critical online services against the ever-evolving landscape of cyber threats.

1.1 Overview of DDoS Attacks and Their Impact on Cybersecurity

Distributed Denial of Service (DDoS) attacks pose a significant challenge to cybersecurity, as they can incapacitate the functionality of websites and services by overwhelming them with malicious traffic. This type of attack typically exploits a network of compromised devices to flood a target, rendering it unable to respond to legitimate user requests. As a consequence, organizations suffer from not only immediate operational disruption but also long-term reputational damage and financial losses. The growing sophistication of DDoS attacks necessitates proactive measures to enhance incident response capabilities, particularly in sectors reliant on digital infrastructures. For example, in the eHealth sector, efficient incident response is crucial to protect sensitive data and ensure the continuous availability of services (Santos D et al.). Moreover, the advent of blockchain technology presents a novel approach to mitigating DDoS impacts by decentralizing network control, thus offering resilience against such attacks through distributed architecture (Canelón et al.).

1.2 Understanding DDoS Attacks

Distributed Denial-of-Service (DDoS) attacks represent a significant threat to online services, as they overwhelm targeted networks or servers with excessive traffic, rendering them inaccessible to legitimate users. These attacks exploit vulnerabilities in Internet infrastructures, often employing botnets—networks of compromised devices—that work in coordination to flood a target with an avalanche of requests. Understanding the mechanics of DDoS attacks is crucial for effective preventative strategies. An emerging trend is the utilization of blockchain technology to mitigate such threats, given its decentralized nature and resilience to single points of failure. The incorporation of frameworks like the IoT-Home Advanced Security System (IoT-HASS), which includes an Intrusion Detection/Prevention System (IDS/IPS) module, exemplifies how security can be enhanced within a given environment, enabling real-time detection and response ((Mudawi et al.)). Properly implemented blockchain solutions could integrate similar defensive mechanisms, significantly decreasing the efficacy of DDoS attacks in future infrastructures.

Table 1. Types of DDoS Attacks and Their Mechanisms

AttackType	Description	Common Mechanisms	Percentage Of Attacks
Volume-Based Attacks	These attacks flood the bandwidth of the target, typically using botnets.	ICMP Flood, UDP Flood, DNS Amplification	70%
Protocol Attacks	These exploit weaknesses in network protocols, consuming resources.	SYN Flood, Ping of Death, Smurf DDoS	20%
Application Layer Attacks	These focus on specific applications, aiming to crash them.	HTTP Flood, Slowloris, SSL Flood	10%
State-Exhaustion Attacks	These aim to exhaust the available states in a network device.	TCP SYN Cookies, Connection Exhaustion	5%

DDoS attacks can be categorized into various types, each employing distinct mechanisms targeted at overwhelming network resources. One prominent type is the volumetric attack, which floods the bandwidth of the target with excessive traffic, rendering it incapable of processing legitimate requests. Techniques such as ICMP floods and DNS amplification illustrate this strategy effectively by exploiting existing protocols to generate massive amounts of attack traffic. Additionally, protocol attacks focus on exhausting server resources by exploiting weaknesses in the third layer of the OSI model, often leading to significant service disruption. As highlighted, the shift towards architectures like Software Defined Networking (SDN) has created new vulnerabilities, particularly to denial-of-service attacks due to their centralized control, which makes them more susceptible to targeted attacks such as flooding and spoofing ((Akowuah et al.)). Understanding these mechanisms is essential for developing effective preventive strategies, including innovative applications of blockchain technology in defending against DDoS threats ((Almisreb et al.)).

Types of DDoS Attacks and Their Mechanisms

Blockchain Technology as a Solution

As the threat of Distributed Denial-of-Service (DDoS) attacks continues to escalate, blockchain technology emerges as a promising solution for enhancing cybersecurity measures. By decentralizing data storage, blockchain can create a more resilient network infrastructure, making it significantly more difficult for attackers to target a single point of failure. This decentralized approach enables real-time monitoring of network traffic, facilitating early detection of potential attacks. In addition, blockchain's inherent transparency allows for improved accountability and traceability of transactions, which can help organizations quickly identify malicious activity. As highlighted in recent studies, small and medium-sized enterprises (SMEs) are particularly vulnerable to cyber threats due to limited resources for robust security solutions (Alba et al.). The integration of blockchain could provide these organizations with affordable and intelligent security systems, optimizing both detection and response capabilities, thereby safeguarding vital operational components against the growing risks posed by cyberattacks.

2 How Blockchain Can Mitigate DDoS Attacks

One of the primary advantages of employing blockchain technology in mitigating Distributed Denial of Service (DDoS) attacks is its decentralized nature, which enhances network resilience. By distributing data across multiple nodes, blockchain minimizes the impact of an attack, as there is no central point of failure that attackers can exploit. The integration of Programmable Protocol-independent Packet Processors (P4) allows for flexible data packet management, enabling immediate responses to threats such as DDoS attacks by dynamically adjusting network behavior based on real-time data analysis (Sadi A et al.). Additionally, utilizing distributed ledger technologies can facilitate secure reporting mechanisms that document malicious activities and improve incident response times. In this interconnected framework, the immutability and transparency of blockchain ensure that all actions are recorded and verifiable, providing a robust foundation for both detection and deterrence of DDoS threats. Ultimately, this multi-faceted approach underscores the potential of blockchain to not only respond to but also preemptively guard against complex and evolving cyber threats.

Table 2. Detection and deterrence of DDoS threats

Year	NumberOfDDoSAttacks	AverageDuration(minutes)	BlockchainUsagePercentage	OrganizationsReported
2021	10,000	31	20%	500
2022	11,000	29	25%	600
2023	12,500	27	35%	750

3 DDoS Attack Mitigation Using Blockchain

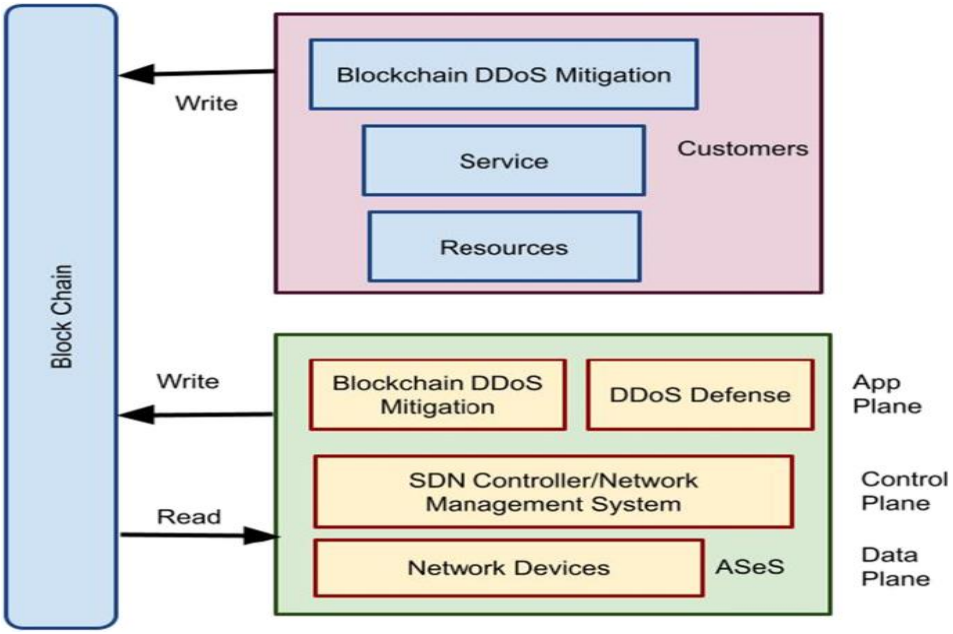

Fig. 1: - Implementation of Controlling DDoS Attack using blockchain

While blockchain technology is not a silver bullet for all DDoS attacks, it offers innovative solutions to mitigate their impact. Here's a step-by-step approach to leveraging blockchain for DDoS defense:

a) **Distributed Network Architecture:**
- Blockchain's inherent decentralization makes it difficult for attackers to target a single point of failure.
- **Node Distribution**: Nodes are spread across various locations, reducing the effectiveness of attacks targeting specific servers.
- **Decentralization**: Multiple nodes can process transactions, ensuring resilience even if some nodes are compromised.

b) Smart Contracts for Automated Response:
- **Threshold Signatures:** Smart contracts can automatically verify and validate transactions, ensuring that only legitimate traffic is processed.
- **Adaptive Traffic Filtering:** Smart contracts can dynamically adjust traffic filtering rules based on real-time network conditions, blocking malicious traffic while allowing legitimate traffic.
- **Reputation Systems**: Blockchain-based reputation systems can track the behavior of nodes and identify malicious actors, enabling the network to isolate them.

c) Blockchain-Based DDoS Detection Systems:
- **Distributed Anomaly Detection: Nodes** can collectively analyze network traffic and identify unusual patterns indicative of a DDoS attack.
- **Real-Time Threat Intelligence Sharing:** Information about ongoing attacks can be shared across the network in a secure and transparent manner.
- **Collaborative Défense:** Nodes can coordinate their efforts to mitigate attacks, such as by blacklisting malicious IP addresses or redirecting traffic.

d) Blockchain-Based DDoS Mitigation Tools:
- **Distributed Load Balancing**: Smart contracts can distribute traffic across multiple nodes, reducing the load on any individual server.
- **RateLimiting**: Blockchain can enforce rate limits on incoming traffic, preventing malicious actors from overwhelming the network.
- **Challenge-Response Authentication**: Smart contracts can implement complex authentication protocols to deter automated attacks.

e) **Blockchain-Based Insurance and Compensation Mechanisms:**
- **Proof of Loss:** Blockchain can provide verifiable records of damages caused by DDoS attacks.
- **Insurance Claims:** Smart contracts can automate the process of filing and processing insurance claims.
- **Compensation Funds**: Blockchain-based funds can be used to compensate victims of DDoS attacks.

f) Additional Considerations:
- **Hybrid Approach**: Combining blockchain with traditional DDoS mitigation techniques can provide a more robust defense.
- **Security Best Practices**: Implementing strong security measures, such as encryption and access controls, is essential to protect the blockchain network itself.
- **Scalability**: Blockchain networks must be able to handle increasing traffic volumes and transaction loads.
- **Regulatory Compliance**: Adhering to relevant regulations is crucial, especially for financial institutions and other regulated entities.

By effectively leveraging blockchain technology, organizations can enhance their resilience against DDoS attacks and protect their critical infrastructure.

4 Conclusion

In summary, the implementation of blockchain technology presents a promising avenue for mitigating DDoS attacks, strengthening the security of online systems. By decentralizing data storage and enhancing traceability, blockchain introduces a level of resilience that traditional networks cannot offer. As noted in the analysis of supply chain vulnerabilities, centralization has exposed systems to various threats, including unauthorized access and service disruptions (Xu et al.). The combination of blockchains immutability and distributed nature could significantly lower the risks associated with DDoS attacks by preventing single points of failure and enhancing authentication protocols. Furthermore, in areas such as smart home technology, security measures must evolve to address emerging risks as the number of connected devices increases (Romano et al.). Therefore, adopting blockchain not only addresses immediate security concerns but also lays a robust foundation for future technological advancements in safeguarding digital infrastructure.

4.1 Future Implications of Using Blockchain for DDoS Prevention

In considering the future implications of blockchain technology for mitigating Distributed Denial-of-Service (DDoS) attacks, the decentralization inherent in blockchain presents a promising avenue for enhanced network security. By distributing data and control across numerous nodes, the attack surface becomes significantly more complex and challenging for cybercriminals. Rather than relying on a single point of failure, blockchains architectural design inherently strengthens the resilience of online services against DDoS attacks. Moreover, the integration of smart contracts could facilitate automated responses to traffic anomalies, allowing for real-time mitigation of suspicious activities. As organizations increasingly adopt blockchain frameworks, the collective enforcement of security protocols across interconnected systems could lead to a paradigm shift in how network resilience is achieved. Ultimately, harnessing blockchain technology for DDoS prevention may not only protect individual entities but also contribute to a more secure digital ecosystem as a whole.

References:

[1.] Romano, Nicholas. "Securing Our Future Homes: Smart Home Security Issues and Solutions". Scholars Crossing, 2019, https://core.ac.uk/download/213463704.pdf

[2.] Alba, Carmen María, Braojos, Manuel Alonso, Fuentes-García, Marta, Lombardo, Juan Manuel, Lopez, Miguel Angel, López, Mabel, Velasco, Susana. "Intelligent Detection and Recovery from Cyberattacks for Small and Medium-Sized Enterprises". 'Universidad Internacional de La Rioja', 2022, https://core.ac.uk/download/523306250.pdf

[3.] Kalariya, Harsiddh, Patel, Vini, Shah, Kavish. "An SLR on Edge Computing Security and possible threat protection". 2022, http://arxiv.org/abs/2212.04563

[4.] Al Sadi, Amir, Mazzocca, Carlo, Melis, Andrea, Montanari, Rebecca, Prandini, Marco, Romandini, Nicolò. "P-IOTA: A Cloud-Based Geographically Distributed Threat Alert System That Leverages P4 and IOTA". 2023, https://core.ac.uk/download/573435206.pdf

[5.] Canelón, Jesús, Huerta, Esperanza, Incera, José, Ryan, Terry. "A cybersecurity control framework for blockchain ecosystems". 'Universidad de Huelva - UHU', 2019, https://core.ac.uk/download/286077261.pdf

[6.] Mudawi, Tarig. "IoT-HASS: A Framework For Protecting Smart Home Environment". Beadle Scholar, 2020, https://core.ac.uk/download/327163118.pdf

[7.] Donadoni Santos, Diogo. "Cybersecurity Incident Response in eHealth". UniversitatPolitècnica de Catalunya, 2023, https://core.ac.uk/download/599208588.pdf

[8.] Xu, Zhe. "Blockchain Design for a Secure Pharmaceutical Supply Chain". ScholarWorks@UMass Amherst, 2024, https://core.ac.uk/download/603331793.pdf

[9.] Almisreb, Ali Abd, Džaferović, Emina, MohdNorzeli ,Syamimi, Sokol, Ajla. "DoS and DDoS vulnerability of IoT: A review". 'Research and Development Academy', 2019, https://core.ac.uk/download/480686851.pdf

[10.] Akowuah, Emmanuel, Kommey, Benjamin, Opoku, Daniel, Tamakloe, Elvis. "Detailed Review on The Denial of Service (DoS) and Distributed Denial of Service (DDoS) Attacks in Software Defined Networks (SDNs) and Defense Strategies". UniversitasSanata Dharma, 2023, https://core.ac.uk/download/593663150.pdf

[11.] Ilyas, Benkhaddra, et al. "Prevention of DDoS attacks using an optimized deep learning approach in blockchain technology." *Transactions on Emerging Telecommunications Technologies* 34.4 (2023): e4729.

[12.] Ibrahim, Rahmeh Fawaz, Qasem Abu Al-Haija, and Ashraf Ahmad. "DDoS attack prevention for internet of thing devices using ethereum blockchain technology." *Sensors* 22.18 (2022): 6806.

[13.] Shah, Zawar, et al. "Blockchain based solutions to mitigate distributed denial of service (DDoS) attacks in the Internet of Things (IoT): A survey." *Sensors* 22.3 (2022): 1094.

[14.] Akilandeswari, R., and S. Malathi. "Design and implementation of controlling with preventing DDOS attacks using bitcoin by Ethereum block chain technology." *Journal of Transportation Security* 15.3 (2022): 281-297.

[15.] Wani, Sharyar, et al. "Distributed denial of service (DDoS) mitigation using blockchain—A comprehensive insight." *Symmetry* 13.2 (2021): 227.

[16.] Chaganti, Rajasekhar, Bharat Bhushan, and Vinayakumar Ravi. "The role of Blockchain in DDoS attacks mitigation: techniques, open challenges and future directions." *arXiv preprint arXiv:2202.03617* (2022).

The Intersection of Gender and Abolition: An Analysis of Feminism in the Narratives of Frederick Douglass

Rasabihari Mishra[1], Pranati Das[2], Sudarsan Sahoo[3], Lyndon Dominic Thomas[4], Pritish Bhanja[5]

[1]Research Scholar, Gandhi Institute of Engineering and Technology University, Gunupur GITA Autonomous College, Bhubaneswar, Odisha, India
[2]Professor, Gandhi Institute of Engineering and Technology University, Gunupur.
[3]Assistant Professor, Parala Maharaj Engineering College, Berhampur.
[4]Assistant Professor, GITA Autonomous College, Bhubaneswar.
[5]Assistant Professor, GITA Autonomous College, Bhubaneswar, Odisha, India

Abstract:
This research paper aims at the feminist dimensions within the narratives of Frederick Douglass, examining the ways in which his narratives provide gender equality as intertwined with his goals of abolition. Although Douglass is famous for being a leading abolitionist during the Abolitionist Movement for the emancipation of the African Americans, his works mark with a feminist discourse, which advocates for gender equality. This study utilizes a multifaceted empirical approach by identifying the feminist themes in the autobiographies – *Narrative of the Life of Frederick Douglass, An American Slave* (1845), *My Bondage and My Freedom* (1855), and *Life and Times of Frederick Douglass* (1892). This paper presents Douglass as an advocate of feminism with a comprehensive analysis of his feminist inclinations and his association with the leading feminists like Susan Anthony and Elizabeth Stanton during the abolitionist movement in the 19th century America. This study enhances our understanding of the intersection between Douglass' ideologies of abolitionism and feminism by highlighting his commitment to a broader vision of social justice.

Keywords: Frederick Douglass, feminism, abolition, slavery, African American

1. Introduction

Frederick Douglass, one of the most influential figures during the Abolitionist movement, was famous for relentless struggle against the institution of slavery and for his eloquent advocacy for the social rights of the African Americans. However, his contributions to gender equality, especially to the treatment of women, remained underexplored and could not get much recognition as it deserved despite his whole hearted involvement in the early women's rights movement. Douglass was a key participant in the Seneca Falls Convention of 1848, where he strongly supported the controversial demand for women's suffrage - a stance that recognized him as an ally within the burgeoning feminist movement. This paper presents Douglass' connections with the feminist themes, especially as they emerge within his narratives, in order to rank him as a proto-feminist figure who has advocated beyond racial justice to embrace gender equality as well. Although there has been an extensive analysis about his abolitionist strategies and his rhetorical prowess, very limited efforts have been given on the empirical examination of the feminist elements within his narratives.

A closer examination of the three autobiographies of Douglass – *Narrative of the Life of Frederick Douglass, An American Slave* (1845), *My Bondage and My Freedom* (1855), and *Life and Times of Frederick Douglass* (1892) – reveal a consistent commitment to advancing both gender and racial equality, reflecting his understanding of social justice as holistic and intersectional. Angela Davis (1981) and other scholars have observed that the radical views of Douglass on gender, focusing on his recognition of the systemic nature of the oppression and his belief in the interrelated struggles of women and African American. Such perspectives underscore the significance of Douglass' feminist inclinations, which needs

a more structured and empirical study. By applying the content analysis approach, which systematically identifies and quantifies incidents where Douglass addresses women's rights, gender dynamics and equality, this paper reveals the patterns in the feminist language and ideas of Douglass by grounding interpretations in measurable data.

The comparative analysis with his contemporary feminists like Susan Anthony and Elizabeth Stanton enables an intricate understanding of how the views of Douglass are aligned with or diverged from other feminist leaders. A historical contextualization approach places the feminist stance of Douglass within the socio-political context of the 19th century America, offering an insight into the ways in which his beliefs were shaped and responded to the social movements of his time. The significance of this study lies in its contribution to the field of Douglass' scholarship, especially exploring the intersections between abolitionism and early feminist thought. This research not only fills a gap in the academic literature by empirically analyzing Douglass' feminist perspectives but also enhances our understanding of the interconnected nature of social justice movements. As recent scholarship has increasingly emphasized the need of intersectional approaches to historical figures, this study provides a timely examination of Douglass' role as an advocate for gender equality. By highlighting Douglass' feminist convictions within his larger mission for equality, this article places him as a figure whose vision is extended beyond racial liberation to a broader societal reformation that included gender justice.

2. Literature Review

The scholarly exploration of Frederick Douglass has traditionally focused on his role as an abolitionist and his rhetorical contributions to the struggle against slavery. However, a number of literatureshave started to identify the involvement of Douglass in the early feminist movements, where he was recognized as one of the few male advocates for the rights and status of women in the 19th century America. This review of literature synthesizes the existing studies on the feminist perspective of Douglass by comparing them with the contemporary feminist discourses and by identifying the methodological gaps that this empirical study seeks to address. The feminist inclinations of Douglass have been acknowledged in some famous works, which highlight his progressive stance on gender equality within the context of his abolitionist mission. Angela Davis, in her ground breaking work *Women, Race and Class* (1981), emphasizes Douglass' recognition of the interwoven nature of racial and gender oppression.

Davis shows that Douglass was unique among his abolitionist peers in his willingness to support the women's suffrage movement at a time when many viewed it as secondary to the cause of abolition of slavery. Douglass famously argued that "right is of no sex" advocating for a form of justice that encompassed both race and gender. Historian David W. Blight provides a comprehensive study on the private and public life of Douglass in his book *Frederick Douglass: Prophet of Freedom* (2018) by highlighting on the active role that Douglass has taken during the Seneca Falls Convention in 1848, where he stood parallel with famous feminists like Elizabeth Stanton and Lucretia Mott. Blight is of the opinion that the support of Douglass for Stanton's controversial call for women's suffrage was instrumental in legitimizing the demand by showing his belief that women's rights were as essential as the emancipation of the enslaved African Americans. Foner (2014) has stated that Douglass' endorsement of women's suffrage showed a profound alignment with feminist ideals, though there has been minimal empirical investigation into how these ideas permeated his autobiographical works.

The comparative analysis of Douglass with his feminist contemporaries is relatively limited in scope, though Stauffer, in his book *Giants: The Parallel Lives of Frederick Douglass and Abraham Lincoln* (2007), has shown the unique position that Douglass holds within the feminist movement. Unlike many male reformers of his time, Douglass did not view women's rights as a diversion from abolition rather as a parallel struggle for human dignity and identity. Lawson, in his article *Frederick Douglass: A Feminist before Feminism* (2012), argues that Douglass' writings reflect a proto-feminist understanding of equality, although he wants a more empirical approach to the language and rhetorical strategies of Douglass. Such comparative framework certainly deepens the understanding of the contribution of Douglass towards

feminism like his contemporaries Stanton and Anthony. While scholars have discussed about the feminist inclinations of Frederick Douglass, some studies have employed a systematic content analysis approach to quantify the feminist themes within his narratives.

Krippendorff (2018) has argued that content analysis methodology can reveal recurring themes and patterns in the autobiographies by providing a structured approach to understand how ideas like justice and equality are expressed. Stauffer (2007) and McFeely (1991) suggest that while Douglass' support for women's rights is acknowledged, the specific language, frequency, and context of his feminist ideas within his narratives remain understudied. This gap underscores the need for an empirical study that not only identifies Douglass' feminist ideas but also situates them within his broader rhetorical and ideological framework. Historical contextualization as a methodology has shown the feminist beliefs of Douglass within the context of 19th century America, when Douglass lived amidst the abolitionist and women rights movements gaining momentum.

Foner (2014) discusses how Douglass' advocacy for women's rights reflected a progressive vision that sought to dismantle oppression in all forms, a stance that was radical for the time in which he lived. In the broader context, Douglass' autobiographical works align with the early waves of feminism, where leading figures like Sojourner Truth and Harriet Jacobs also advocated for an intersectional approach to equality and freedom. However, Blight (2018) observes that the approach of Douglass towards gender equality evolved over time being influenced by his interactions with leading feminists and the shifting political landscape. Yet, there has been limited empirical investigation on how these historical contexts influenced the portrayal of women by Douglass and his expressions of feministic ideas.

3. Methodology

This research employs three methodical approaches to explore the feminist dimensions within the autobiographical narratives of Frederick Douglass. Primarily, content analysis, comparative analysis and historical contextualization methods are used in this research to systematically identify the feminist themes, compare the views of Douglass with the views of his contemporaries and examine the socio-political context in which his beliefs were shaped. This multi-dimensional methodology enables a comprehensive understanding of Douglass as a proto-feminist thinker whose advocacy for gender equality was integral to his broader vision of social justice.

Content Analysis: This method is used as the primary tool to systematically analyze the themes, language and frequency of the feminist ideas of Douglass in his three autobiographies *Narrative of the Life of Frederick Douglass, An American Slave* (1845), *My Bondage and My Freedom* (1855), and *Life and Times of Frederick Douglass* (1892). The objective of this method is to identify the recurring themes of gender equality, women rights and feminist discourse in the writings of Frederick Douglass. The three autobiographies of Douglass, as mentioned above, are chosen for analysis of contents. These narratives are significant for understanding the views of Douglass on gender equality and social justice. They represent Douglass' thought across different stages of his life by providing a broad spectrum of his views on the rights of women.

The primary themes that are identified with this analysis include women's rights and suffrage, gender equality, sexual oppression and Douglass' relationship with other feminist leaders. After identifying the themes, the frequency of each theme is recorded and analyzed to determine the prominence of the feminist ideas in the works of Frederick Douglass. The objective of this analysis is to assess the extent to which Douglass integrates feminist themes across his writings and how these ideas were formed over time. Moreover, a qualitative analysis is also undertaken on the context in which feminist themes have emerged. This analysis involves the examination of the broader narrative to show how Douglass has positioned these feminist themes within the broader framework of his abolitionist rhetoric and his views on racial equality and justice. The content analysis method has shown the intersection between Douglass' struggle for racial justice and gender equality.

Comparative Analysis: This analysis is employed for a deep understanding of the feminist views of Douglass by positioning him among other feminists of his time Elizabeth Stanton, Sojourner Truth and Susan Anthony. This comparative analysis is used for a better understanding of how Douglass' views on gender equality are in line with the mainstream feminist discourse of his time. The feministic themes of Douglass have been compared with the views of his contemporaries and an assessment is made on how Douglass' views on women's rights have complemented with the existing feministic ideas. A focus is given on the areas where Douglass and his feminist peers have shared common grounds. This provides a deeper understanding of Douglass' role within the broader feminist movement. By comparing Douglass with his contemporaries, this study offers a broader context for understanding his unique position within women's rights movements and abolitionist movements.

Historical Contextualization: This method is used to show the relevance of the feminist views of Douglass within the socio-political context of 19th century America when the abolitionist movement was in full swing and a voice has been raised for gender equality by the feminist leaders of that time. It has shown the involvement of Douglass in the feminist issues by considering the historical and social conditions that formed this type of thinking in him. The key historical events such as the Seneca Falls Convention of 1848, the Civil War, the Emancipation Proclamation and the Reconstruction Era have been studied to understand how these events have influenced the views of Frederick Douglass on gender equality. It has also focused on the role of Black women in the abolitionist and feminist movements and their activities which have brought issues related to gender and race into the forefront of the movements. The speeches, letters and interviews of Douglass have also been examined to show how his personal and professional interactions with feminist leaders formed and shaped his feminist ideas.

4. Analysis and Findings

One of the most prominent themes in the writings of Frederick Douglass is his outspoken support for the women's suffrage. He is famously known for his active participation in the Seneca Falls Convention of 1848, where he supported Elizabeth Stanton's call for women's right to vote. So, he writes:

> "I have had but one great desire in life – to see my race free, and, above all, I have desired to see the woman who is my equal in every respect, politically and morally, the equal of man." (Frederick Douglass, *My Bondage and My Freedom*, 1855)

Here, Douglass extends his advocacy for freedom to include gender equality at a time when women were largely excluded from political participation and regarded as subordinate to them. His use of the phrase "politically and morally" reflects his belief that women deserve not only equal legal rights as men, such as voting rights and holding public offices, but also recognition as intellectual and moral equals. He argued that women suffrage is natural extension of their equality. His support for women's rights was consistent with his broader belief in universal human dignity. By linking racial and gender equality, Douglass emphasized the interconnectedness of struggles against oppression. These lines highlight his vision for a society that transcends hierarchies of race and gender. It also reflects Douglass' personal respect for women which was influenced by his relationship with influential women like his mother and his close associates during the abolitionist and suffrage movements. His recognition of women as equal partners in political and moral life challenges the systems of patriarchy and racism alike. He believes that women should enjoy equal political and moral rights as men. His advocacy for women' suffrage was revolutionary for a male abolitionist in the 19th century by highlighting his recognition of gender equality as integral to human freedom. Douglass repeatedly insists on the equality of men and women in his autobiographies and speeches. While discussing about the degrading effects of slavery on women by emphasizing that the oppression of Black women was not only a racial issue but a gendered one, he says:

> "The women in slavery … suffer all the harshness and cruelty which can be inflicted on them, and are in many cases worse than the men, because they are subjected to that which is peculiar to their sex, and which is not infrequently crueler than that which is inflicted on men." (Frederick Douglass, *Narratives of the Life of Frederick Douglass, an American Slave*, 1845)

These lines underscore the empathy of Douglass towards the enslaved women and his awareness of the intersection of racial and gendered oppression. His acknowledgement of the specific plight of Black women reflects a deep commitment to gender equality by suggesting that his support for the abolition of slavery was intrinsically tied to his belief in the equal worth of women. This statement challenges the readers of the autobiography to understand that slavery was not a monolithic experience – women were doubly oppressed, both as an enslaved individual and also as a woman. The "peculiar" suffering they faced speaks of the brutal intersection of gender, race and systemic exploitation. By throwing light on these sensitive issues, Douglass shows his broader understanding of the human cost of slavery, especially its impact of women. His rhetorical techniques in his narratives arouse empathy and force its readers to recognize the unique form of violence endured by the enslaved women. Besides, Douglass also addresses the angle of sexual exploitation of the enslaved women, which he describes as:

> "The slave is a man, but the woman is doubly a slave – once as a slave and once as a woman." (Frederick Douglass, *Life and Times of Frederick Douglass,* 1892)

Here, Douglass highlights the compounded oppression of the women under slavery. They have endured both racial and sexual subjugation. He points out the specific difficulties that enslaved women faced due to their gender and the abuse is mostly related to sexual exploitation. These women were often subjected to rape, sexual assault and forced pregnancies, which were used as a means of increasing the slave population and also to maintain control over the African Americans by showing that they can be treated as per the mercy of the slaveholders and overseers. These experiences were unique to enslaved women and compounded their emotional and physical suffering.

A comparative analysis between Frederick Douglass and other feminist activists of the time like Elizabeth Stanton, Susan Anthony and Sojourner Truth, it is found that Douglass' views on women's rights were in strong alignment with Elizabeth Stanton's advocacy for women's suffrage. Both of them considered gender equality and racial equality to be interconnected. Regarding the contribution of Douglass, Stanton remarked:

> "Frederick Douglass was not only a man of the highest character and intellect, but he was the champion of the most important cause of the age – the cause of woman as well as the cause of the oppressed race." (Elizabeth Cady Stanton, *History of Women Suffrage,* 1881)

These lines demonstrate the mutual respect of Douglass and Stanton for each other, with Douglass championing the cause of women's rights as he has championed the abolition of slavery. He shared the belief of Stanton that emancipation of women was inextricably connected to the broader struggle for human rights. However, his support for women suffrage has put him at odds with other abolitionists of the time and especially with those who resisted the voting rights of women. His friendship and intellectual sharing with another feminist Susan Anthony marked a prominent intersection of feminism and abolitionism. Susan highly praised Douglass for his intentions of supporting the cause of women suffrage despite the political risks that would befall on him.

Douglass has also given high opinion about the organizational skills and determination of Susan. His integration of gender equality within his broader philosophy of human rights is indicative of his proto-feminist stance. Another feminist activist with whom Douglass was very closely connected was Sojourner Truth and their relationship is often seen as emblematic of the intersection of gender and race in the 19th century feminist thought. Douglass was deeply impressed with Truth and was deeply moved by her words in her famous speech "Ain't I a Woman" in 1851, where she challenged the existing gender and racial stereotypes by asserting that Black women had the same rights to freedom and equality as White women. The rhetoric of Truth and Douglass' admiration for it show the connection between the feminist and abolitionist movement. Douglass' support for Truth and other feminists highlights his understanding of the double oppression faced by Black women.

5. Conclusion

The feministic views of Frederick Douglass, as reflected in his works and advocacy, are deeply rooted in his understanding of the intersectional nature of oppression relating to gender and race. His understanding of the oppression faced by women, especially enslaved women, shows his progressive and empathetic stance that aligns with his early feminist ideals. He was one of the few male voices of his time to openly address the gendered dimensions of slavery by highlighting sensitive issues like sexual violence, forced motherhood and emotional suffering of the enslaved women. Douglass tried to amplify the voices of the Black women who were often silenced in both the feminist and abolitionist discourses. Moreover, his support for women's rights extended beyond the abolition of slavery. Douglass was an active advocate for women suffrage which was evident in his participation in the Seneca Fall Convention, where he boldly declared that the right to vote was essential for women as it was essential for men. This research article supports the claim that Frederick Douglass was not only a fierce advocate for the abolition of slavery but also a very important companion in the struggle for women's rights. His feminist ideals were deeply rooted in his personal experiences of enslavement and his broader vision of equality. This study highlights the essential role that his feminist thoughts played in shaping his political and intellectual contributions. Through this research, we get a deeper understanding of his vision of emancipation which would dismantle both gender and racial oppression in the pursuit of a society that believed in social and political equality.

Reference:

[1] Blight, D. W. (2018), Frederick Douglass: Prophet of Freedom, Simon & Schuster.
[2] Davis, A. Y. (1981), Women, Race & Class, Vintage Books.
[3] Douglass, F. (1848), *The North Star*, Rochester.
[4] Douglass, F. (1845), *Narratives of the Life of Frederick Douglass, an American Slave*, Anti-Slavery Office.
[5] Douglass, F. (1855), *My Bondage and My Freedom*, Orton & Mulligan.
[6] Douglass, F. (1892), *Life and Times of Frederick Douglass*, Park Publishing.
[7] Foner, E. (2014), *Gateway to Freedom: The Hidden History of the Underground Railroad*, W. W. Norton & Company.
[8] Gates, H. L. Jr. (1988), *The Signifying Monkey: A Theory of African American Literary Criticism*, Oxford University Press.
[9] Krippendorff, K. (2018), *Content Analysis: An Introduction to Its Methodology*, SAGE Publications.
[10] Lawson, B. (2012), "Frederick Douglass: A Feminist before Feminism", Journal of African American History, 97 (3).
[11] McFeely, W. S. (1991), Frederick Douglass, W. W. Norton & Company.
[12] Mishra, R. et al. (2024), Locating the Self: An Analysis of Booker T. Washington's "Up from Slavery". Library Progress International, 44(3), 8622-8628.
[13] Mishra, R. et al. (2024), Booker T. Washington's Atlanta Compromise: An Integration of Blacks and Whites. Library Progress International, 44(3), 19690-19695
[14] Stanton, E. C. (1881), History of Woman Suffrage, Charles Mann.
[15] Stauffer, J. (2007), Giants: The Parallel Lives of Frederick Douglass and Abraham Lincoln, Twelve.

Transformation of Healthcare systems in Smart Cities using IoT and Big Data Analytics

Debasish Pradhan[1], Mamata Rath[2], Arup Kumar Mohanty[3], Sudeep Kumar Gochhhayat[4], Jayanta Kumar Mishra[5]
[1]Department of CSE, GITA Autonomous College, Bhubaneswar-752054, Odisha, India
Email: debasish2.cse @gmail.com
[2]Department of CSE, GITA Autonomous College, Bhubaneswar-752054, Odisha, India
Email: mamata.rath200@gita.edu.in
[3]Department of CSE, GITA Autonomous College, Bhubaneswar-752054, Odisha, India
Email: Arupkumohanty@gmail.com
[3]Department of CSE, GITA Autonomous College, Bhubaneswar-752054, Odisha, India
Email: sudeepku24@gmail.com
[3]Department of CSE, GITA Autonomous College, Bhubaneswar-752054, Odisha, India
Email: jayanta71980@gmail.com

*Corresponding Author's Email Id: debasish2.cse@gmail.com

Abstract

The rapid advancement of emerging technologies and industrial growth has significantly impacted lifestyles in smart cities, bringing both opportunities and challenges. Urban areas, characterized by high population density and evolving lifestyle patterns, face an increased prevalence of various health issues. The transition of cities into smart cities involves adopting automated systems across multiple sectors, including healthcare. This paper presents a comprehensive survey of health-related challenges in urban areas and explores innovative solutions leveraging Big Data Analytics, IoT, and smart applications. It proposes an advanced healthcare management system featuring smart ambulances integrated with enhanced security mechanisms to enable efficient and safe patient transport. By focusing on intelligent driving and swift emergency response, this approach aims to deliver reliable healthcare services, addressing critical health risks in the smart city environment effectively.

Keywords: Smart City, IoT, Big Data Analytics, Healthcare, Security

1. Introduction

The implementation of smart concepts such as smart homes, smart cities, and interconnected systems has positioned the Internet of Things (IoT) as a transformative field with immense impact, potential, and growth. The widespread adoption of the Internet has been a driving force behind this trend, enabling machines and smart devices to communicate, coordinate, and make decisions in real-world scenarios. The IoT revolution has accelerated rapidly, promising exponential growth in the number of Internet-connected devices. According to Cisco analysts, there were over 25 billion connected devices in 2015, with projections exceeding 50 billion by 2020. This explosion of

connectivity has paved the way for new business paradigms, resulting in a sharp rise in machine-to-machine (M2M) communications. This breakthrough moment marks a significant milestone, unlocking vast opportunities for enterprises and society as a whole. However, this rapid evolution also introduces serious security concerns. The increased connectivity has dramatically heightened the risk of cyber vulnerabilities, which could undermine the potential benefits of IoT technologies. For instance, a recent survey by HP revealed that 70% of IoT devices contain security vulnerabilities, underscoring the critical need for robust cybersecurity measures [1]. This section aims to provide an overview of current trends in cybersecurity within the IoT domain while offering insights into the challenges and opportunities that lie ahead as IoT continues to evolve.

1.1 Emergence of Internet of Things

The Internet of Things (IoT) has recently emerged as a pivotal research focus, integrating diverse sensors and devices to communicate autonomously without human intervention. The demand for large-scale IoT deployment is rapidly increasing, accompanied by significant security challenges. Detailed analysis that highlights the critical security threats and vulnerabilities in IoT systems, providing a comprehensive review of existing research in this domain [2]. A taxonomy of current IoT security threats is presented, categorized by application, architecture, and communication protocols.

1.2 Big data convergence with IoT

Simultaneously, we are living in the era of big data—a time characterized by the rapid collection and accumulation of vast amounts of ubiquitous data. Big data comprises enormous datasets and offers transformative potential across industries. From business optimization and economic forecasting to public administration, national security, and scientific research, big data is reshaping decision-making and operational strategies. For example, it has revolutionized customer behavior prediction, enabling businesses to fine-tune their approaches. One of the key contributors to big data is the rise of social networks, where a significant portion of data is generated [3]. The relationship between big data and social networks is both evident and complex. While social platforms provide a massive influx of data, managing and extracting meaningful insights remains a challenge. The true hurdle lies not in data collection but in its organization, analysis, and interpretation. Effective big data management requires balancing the benefits of its use against the costs of storage and maintenance. To address these challenges, numerous tools and methodologies are being developed to harness the power of big data for enhanced decision-making and business improvement. Researchers and practitioners continue to explore innovative ways to maximize the benefits of big data, ensuring its effective integration into various sectors while addressing the inherent challenges it presents.

1.3 The Role of IoT in Transforming Electronic Security Frameworks

The Internet of Things (IoT) is revolutionizing electronic security systems, offering transformative benefits for both business and residential applications. In many ways, traditional security products served as precursors to IoT technologies and continue to share key characteristics. However, the rapid decline in the cost of IoT devices and the anticipated installation of billions of new devices

in the next 5–10 years have positioned IoT as a game-changer in how electronic security systems are conceptualized and marketed [4].

IoT not only enhances the functionality of security systems but also redefines industry operations. Among consumers, security applications remain one of the most widely recognized and valued benefits of IoT adoption in homes. The integration of IoT devices into security frameworks increases their affordability, as the economics of the IoT market exert downward pressure on component costs. This trend enables consumers to access more advanced and feature-rich security solutions at lower prices, significantly increasing the value proposition for security buyers[5]. As IoT continues to evolve, its influence on the security sector will drive innovation and accessibility, making sophisticated electronic security systems more widespread and efficient than ever before.

1.4 Healthcare Innovation: Bridging Complexity and Advancement

Despite the intricate nature of human biology and the rigorous regulations governing medicine, the pace of innovation in healthcare remains extraordinarily rapid. Even in an era heavily influenced by science fiction, breakthroughs continue to captivate and redefine possibilities. Companies have achieved remarkable milestones, such as 3D-printing liver and kidney tissues, developing personalized prosthetics, and creating FDA-approved medications. Meanwhile, IBM Watson's artificial intelligence processes vast datasets to suggest optimal treatment options, and deep learning algorithms are poised to further transform diagnostics and patient care[6].

Wearable technologies are also revolutionizing the healthcare landscape. For instance, digital tattoos can track vital health metrics and provide timely alerts via smartphones when medical attention is required. Augmented reality tools, like Microsoft’s HoloLens, enhance surgical preparation by projecting digital overlays onto real-world scenarios, enabling surgeons to approach complex procedures with greater precision and confidence.

These advancements illustrate how innovation continues to bridge the complexity of healthcare with groundbreaking solutions, reshaping the future of medicine.

1.5 The Boundless Potential of Healthcare Innovation

Healthcare innovation appears limitless in its potential. For example, in 2020, startups delved into adherence technologies, embedding microchips into drug capsules to monitor when and whether patients take their medication. However, the vision of holographic data input devices remains largely underdeveloped, with most existing products still in their infancy and resembling toys rather than functional tools. Without substantial investment from major corporations, these technologies could take years before achieving mainstream adoption[7].

Nonetheless, some companies are leading the way. A prime example is L'Oréal, the global cosmetics giant, which has invested in a wearable sensor that alerts users when their sun exposure reaches dangerous levels. With such innovations, healthcare continues to evolve in groundbreaking ways, reshaping lives and challenging what we thought possible in the realm of medical technology.

1.6 The Expanding Impact of Big Data Across Sectors

Big data is pivotal in a wide range of research fields, such as healthcare, location-based services, satellite data analysis, online advertising, and retail marketing. With the ongoing growth of the Internet of Things (IoT), the global volume of data is set to increase exponentially, further expanding the reach and applications of big data. While numerous review papers have examined big data and its uses in specific domains like science, healthcare, geography, and the Internet, this paper provides a fresh perspective. It delves into recent advancements in big data, categorizing and analyzing its critical components, including data types, storage models, analytical frameworks, privacy concerns, security issues, and emerging applications [8]. By adopting a comprehensive approach, this paper highlights the dynamic evolution of big data and its transformative impact on various industries.

1.7 Exploring Emerging Technologies in Smart Healthcare Management

This research investigates the integration of emerging technologies, such as the Internet of Things (IoT), Cloud Computing, and Big Data Analytics, in the management of smart healthcare systems. Building on these advanced technologies, the second section of the chapter introduces a proposed Smart Healthcare Execution System (SHES), which utilizes soft computing and intelligent algorithms to optimize healthcare delivery. To assess the effectiveness of the planned framework, simulations were conducted using the NetSim Simulator. The results reveal significant performance improvements, including enhanced communication speed between smart healthcare centers and a notable increase in system throughput [9]. These findings underscore the potential of SHES to transform healthcare management by seamlessly combining smart intelligence with cutting-edge technological advancements.

2. Literature Review

2.1 The Role of Mobile Cloud Computing in Smart Healthcare for Smart Cities

Recently, the concept of Smart Cities has gained significant attention due to its potential to enhance the quality of life for urban residents. The concept encompasses various sectors, including Smart healthcare, Smart transportation, and Smart communities. In particular, Smart healthcare services in these cities rely heavily on the continuous sharing, processing, and analysis of Big Healthcare Data to enable informed decision-making. As a result, a robust wireless and mobile communication infrastructure is essential to connect and access Smart healthcare services, people, and sensors at any time, from anywhere[10].

In this context, Mobile Cloud Computing (MCC) plays a crucial role by offloading tasks related to Big Healthcare Data—such as sharing, processing, and analysis—from mobile applications to cloud resources. This ensures that the quality of service (QoS) requirements of end-users are met. Such resource migration, commonly referred to as Virtual Machine (VM) migration, is particularly effective in the Smart healthcare domain within Smart Cities, helping to optimize system performance and improve service delivery.

2.2 Improving Routing Protocols for Real-Time Data Transmission in Mobile Ad-Hoc Networks

The rapid growth of wireless communication has led to significant advancements in wireless networks and protocols, revolutionizing the global communication market. Unlike traditional cellular systems, these networks operate without fixed infrastructure, offering flexibility and scalability. Due to their decentralized nature, mobility, and multi-hop relaying capabilities, Mobile Ad-hoc Networks (MANETs) and other wireless networks are increasingly sought after for efficient recovery, vehicle tracking, and real-time management applications.

One of the key challenges in such networks is the dynamic nature of their topology, driven by the unpredictable movement of network nodes. This leads to difficulties in maintaining connectivity with neighboring entities, making reliable data delivery and ensuring adequate Quality of Service (QoS) a challenge. Routing protocols play a critical role in establishing end-to-end paths, as nodes are often not directly reachable from one another [11]. In such bandwidth-constrained networks, energy-efficient and robust routing strategies are crucial for ensuring network longevity.

2.3 Table Driven Approach of Protocol design

There are two primary types of routing protocols: table-driven and on-demand. Table-driven approaches, while proactive, flood the network with information even in the absence of actual traffic, resulting in significant overhead. This extra load is often unsustainable in wireless communication networks with limited bandwidth. On the other hand, on-demand protocols, such as Wireless Real-time protocols, only utilize network resources when required by the users, which helps conserve bandwidth and energy. These protocols remain idle until a demand for data transmission arises, at which point they initiate route discovery by sending out a Route Request packet. The packet traverses the network, reaching the destination, and creates a reverse route table [12]. The destination then replies with a Route Reply packet, which establishes the forward route for data packets.

However, the route discovery process can introduce delays, and some nodes may become overloaded due to frequent data handling. As a result, traditional routing methods are not immediately applicable to mobile ad-hoc networks due to their inherent limitations.Many research focus on refining the basic wireless routing protocol to address the aggressive QoS (Quality of Service) requirements of real-time network services in wireless communication. Real-time data transmission in wireless networks is challenging due to the self-organizing nature of mobile devices that form a network without centralized infrastructure. Nodes frequently change their positions and form networks that require careful consideration in protocol design, especially for time-sensitive applications.Key challenges faced in real-time data transmission include energy consumption, network mobility, efficient bandwidth utilization, resource reservation, minimizing connection failures, ensuring security, managing QoS, and adapting to the dynamically changing network topology. Many research seek to address these challenges through enhancements to existing routing protocols, aiming to optimize performance for real-time services in mobile ad-hoc networks.

3. Quality of Service in Health Care Systems

3.1 Advancements in Mobile Health Care through Network-Supported Systems

In recent years, electronic health care services have gained significant attention, driven by the rapid increase in high-performance computing devices connected to medical sensors and diagnostic systems via heterogeneous networking technologies. Mobile health care (mHealth) is a key subfield of eHealth, focusing on the use of mobile phones, wearable or embedded sensors, and Body Area Networks (BANs), along with a wide array of wireless communication technologies, to enhance traditional health care services.

3.2 Tele diagnosis and remote patient monitoring.

Advanced mobile technologies are playing an increasingly crucial role in health care systems, particularly in applications such as teleconferencing, telediagnosis, and remote patient monitoring. These mobile health care services typically require strict, therapeutic-level Quality of Service (QoS) and Quality of Experience (QoE) standards. Real-time use cases such as remote patient monitoring, telecare, and remotely guided surgeries demand even more stringent requirements, including minimal delay and jitter, quick response times, and low packet loss[13].

Many mobile health care applications rely on wearable body sensors (such as ECG monitors, heart rate sensors, and ultrasound devices) or the built-in sensors of modern smartphones (like high-definition cameras and gyroscopes). Given the diverse nature of mobile health care applications—each with its own unique network demands and QoS/QoE requirements—there is a need for sophisticated network management frameworks to ensure efficient service delivery. Many research aims to design and implement a network-assisted wireless access network selection system for mHealth services, using a multi-criteria decision engine to select the most appropriate available access network. Various research efforts have explored the use of Distributed Decision Engines (DDE) and Network Information Services (NIS) to provide both static and dynamic parameters of available health care communication networks. Additionally, some approaches have been developed for selecting the optimal network for Wi-Fi-based services[14]. E-health care systems also provide an effective platform for transmitting medical-quality data in various mobile health care scenarios.

4. Health Care in IoT Network and Smart Community

The importance of healthcare, alongside essential needs such as food and water, is widely acknowledged. In the development of a smart city, services like water management, energy management, building automation, and transportation all require the active participation of people within the "smart community." Therefore, prioritizing "smart healthcare" in 2015 is not just a luxury but a necessity. Despite popular belief that providing "smart healthcare" is entirely feasible, practical, and only requires minor adjustments to the software and hardware used for other "smart services," the key difference lies in the fundamental shift required in the mindset of both healthcare providers and recipients. Below are a few examples of Smart Healthcare (SHC) applications:

1. **Advancing healthcare education via eHealth**: Delivering verified, personalized healthcare information to a specific audience through mobile phones, and potentially leveraging public WiFi networks.
2. **Telemedicine-enabled pre-hospital care**: Smart ambulances equipped for emergency situations, trauma, and other medical needs.
3. **Remote healthcare monitoring at home**: Converting a home into a high-care ward using technology, reducing the need for hospital bed occupancy.
4. **Advanced diagnostic tools**: Today's glucometers, when combined with similar tests for liver, kidney, and heart function, will only require a few drops of blood and no paramedic involvement. Non-invasive sensors will eventually replace these, using biomarkers through the skin to analyze blood chemistry, and even urinary analysis for brain pathology [15].
5. **In-house SHC in large hospitals**: Providing smart healthcare within the hospital premises for its patients.
6. **In-house SHC for employees in large workplaces**: Offering healthcare services directly within the office.
7. **Virtual outpatient clinics**: Family doctors, specialists, and super-specialists can conduct virtual consultations at workplaces, shopping malls, or residential areas.
8. **24/7 access to Electronic Medical Records (EMR)**: This would significantly reduce the duplication of tests and provide fast access to a patient's entire medical history, improving healthcare quality.
9. **Data-driven healthcare assessments**: Real-time, statistical evaluations of healthcare outcomes, prevalence rates, and follow-up care would become possible.
10. **Healthcare integration in smart cities**: Healthcare should always be considered a vital component when planning a smart city. Whether addressing issues like pollution, transportation, or water management, input from healthcare professionals knowledgeable about technology and its behavioral implications is crucial.
11. **Future-ready healthcare**: Healthcare has historically been a retrofitted consideration, often added after the fact. With the rise of smart communities, we now have a unique opportunity to integrate healthcare from the outset.

5. Conclusion

The transformation of healthcare systems in smart cities through the integration of IoT and Big Data Analytics represents a significant shift in how healthcare services are delivered, managed, and optimized. IoT enables real-time monitoring and data collection from various sensors and devices, providing invaluable insights into patient health and environmental conditions. This data, when analyzed using Big Data Analytics, can lead to more informed decision-making, predictive healthcare, and personalized treatment plans. Smart healthcare systems can improve efficiency by reducing hospital readmissions, enhancing patient outcomes, and streamlining healthcare processes. Additionally, the use of IoT in smart ambulances, remote patient monitoring, and telemedicine empowers healthcare professionals to deliver timely care, even in emergencies or remote areas. Big Data Analytics facilitates proactive health management by identifying trends, risks, and preventive measures before problems escalate. With the ability to integrate vast amounts of data from multiple sources, healthcare providers can offer more precise and holistic care.

Despite these advancements, challenges such as data security, privacy concerns, and the need for robust infrastructure remain significant barriers. Nonetheless, the combination of IoT and Big Data Analytics promises to revolutionize healthcare delivery in smart cities, making it more accessible, efficient, and patient-centric. Ultimately, the future of healthcare in smart cities is poised for continuous innovation, aiming to improve the quality of life for urban populations.

References

[1.] Yanjun Li, Chung Shue Chen, Ye-Qiong Song, Zhi Wang, Real-Time Qos Support In Wireless Sensor Networks: A Survey, In Ifac Proceedings Volumes, Volume 40, Issue 22, 2007, Pages 373-380

[2.] Fatima Tul Zuhra, Kamalrulnizam Abu Bakar, Adnan Ahmed, Mohsin Ali Tunio, Routing protocols in wireless body sensor networks: A comprehensive survey, In Journal of Network and Computer Applications, Volume 99, 2017, Pages 73-97, ISSN 1084-8045,

[3.] Richard K. Lomotey, Joseph Pry, Sumanth Sriramoju, Wearable IoT data stream traceability in a distributed health information system, In Pervasive and Mobile Computing, Volume 40, 2017, Pages 692-707, ISSN 1574-1192,

[4.] H. J. F. Qiu, I. W. H. Ho, C. K. Tse and Y. Xie, "A Methodology for Studying 802.11p VANET Broadcasting Performance with Practical Vehicle Distribution," in IEEE Transactions on Vehicular Technology, vol. 64, no. 10, pp. 4756-4769, Oct. 2015.

[5.] Enji Sun, Xingkai Zhang, Zhongxue Li, “The Internet of Things (IOT) and cloud computing (CC) based tailings dam monitoring and pre-alarm system in mines” Safety Science,Vol 50 Pages 811–815,2012.

[6.] Bahar Farahani, Farshad Firouzi, Victor Chang, Mustafa Badaroglu, Nicholas Constant, Kunal Mankodiya, towards fog-driven IoT eHealth: Promises and challenges of IoT in medicine and healthcare, In Future Generation Computer Systems, Volume 78, Part 2, 2018, Pages 659-676, ISSN 0167-739X.

[7.] Mahmud Hossain, S.M. Riazul Islam, Farman Ali, Kyung-Sup Kwak, Ragib Hasan, An Internet of Things-based health prescription assistant and its security system design, Future Generation Computer Systems, Available online 2 December 2017, ISSN 0167-739X, https://doi.org/10.1016/j.future.2017.11.020.

[8.] Ahmed Harbouche, Noureddine Djedi, Mohammed Erradi, Jalel Ben-Othman, Abdellatif Kobbane, Model driven flexible design of a wireless body sensor network for health monitoring, In Computer Networks, Volume 129, Part 2, 2017, Pages 548-571, ISSN 1389-1286, https://doi.org/10.1016/j.comnet.2017.06.014.

[9.] Toni Adame, Albert Bel, Anna Carreras, Joan Melià-Seguí, Miquel Oliver, Rafael Pous, CUIDATS: An RFID–WSN hybrid monitoring system for smart health care environments, In Future Generation Computer Systems, Volume 78, Part 2, 2018, Pages 602-615, ISSN 0167-739X.

[10.] Jaime Lloret, Lorena Parra, Miran Taha, Jesus Tomás, An architecture and protocol for smart continuous eHealth monitoring using 5G, In Computer Networks, Volume 129, Part 2, 2017, Pages 340-351, ISSN 1389-1286, https://doi.org/10.1016/j.comnet.2017.05.018.

[11.] Sofoklis Kyriazakos, Vincenzo Valentini, Alfredo Cesario, Robert Zachariae, FORECAST - a cloud-based personalized intelligent virtual coaching platform for the well-being of cancer patients, In Clinical and Translational Radiation Oncology, 2017, , ISSN 2405-6308,

[12.] Olaniyi Olayinka, Michele Kekeh, Manasi Sheth-Chandra, Muge Akpinar-Elci, Big Data Knowledge in Global Health Education, In Annals of Global Health, 2017, , ISSN 2214-9996.

[13.] Bartha Maria Knoppers, Adrian Mark Thorogood, Ethics and Big Data in health, In Current Opinion in Systems Biology, Volume 4, 2017, Pages 53-57, ISSN 2452-3100, https://doi.org/10.1016/j.coisb.2017.07.001.

[14.] Md Ileas Pramanik, Raymond Y.K. Lau, Haluk Demirkan, Md. Abul Kalam Azad, Smart health: Big data enabled health paradigm within smart cities, In Expert Systems with Applications, Volume 87, 2017, Pages 370-383, ISSN 0957-4174, https://doi.org/10.1016/j.eswa.2017.06.027.

[15.] Yichuan Wang, LeeAnn Kung, William Yu Chung Wang, Casey G. Cegielski, An integrated big data analytics-enabled transformation model: Application to health care, In Information & Management, 2017, ISSN 0378-7206, https://doi.org/10.1016/j.im.2017.04.001.

Solving Fuzzy Number Travelling Salesman Problems with Linear Ranking Function

K.K. Mishra[1*],Rabindra Panda[2],Bijaya mishra[3]

[1]Department of Mathematics, GITA Autonomous College, Bhubaneswar-752054, Odisha,
Email:kkm.math1973@gmail.com
[2]Department of Mathematics, GITA Autonomous College, Bhubaneswar-752054, Odisha,
Email:rabip2005@gmail.com
[3] Department of Mathematics, GITA Autonomous College, Bhubaneswar-752054, Odisha,
Email: bijayamishra.math@gmail.com

Abstract

The goal of the classical traveling salesman model is to visit as many cities as possible from one's home city while keeping travel expenses to a minimum. A trapezoidal fuzzy number is used to represent travel expense in this paper. Using Maleki's suggested linear ranking function, TrFN is De-fuzzified. In order to resolve FNTSP, the classical traveling salesman model is enhanced.

Keywords: Trapezoidal fuzzy number, Linear Ranking function, traveling salesman

1. Introduction

In the nineteenth century, Irisl Mathematician W.R. Hamilton initially put up the Traveling Salesman Problem (TSP). The salesperson begins his journey from city 1, and the number of possible permutations of 2, 3, n represents the distance between each of the n cities. That means there are (n-1)! ways he could go on his tour. The trick is to figure out the best way to get where he needs to go.

TSP classifications:

(i) **Symmetrical:** Assuming that the direction of his journey has no effect on the distance between any two cities.

(ii) **Asymmetrical:** For some sets of cities, the distance varies depending on the direction. Time and money are not constants in the real world.

it may be due to:-

Present fuel consumptions impact trip costs; speed, in turn, is influenced by traffic conditions, which are external factors.Fuel prices are also subject to swings as a result of global events.Labor costs, which are based on average travel time, account for a disproportionately large share of transportation expenditures. As the transportation business requires a lot of cash, the timely usage of vehicles is a major concern.Fuzzy travelling salesman problems (FTSPs) arise when variables like time, distance, or cost are represented by fuzzy numbers.

2. Fundamental of Fuzzy Set Theory

The term "fuzzy" was proposed by Zadeh in 1962. In 1965, he published the paper "Fuzzy Sets".

Definition2.1: (Fuzzy Sets):

An ordered pair is a fuzzy set in X if X is a collection of items denoted generically by X. The membership function is located at this location.

Definition2.2 (Support):

Thesupport ofafuzzyset $\underline{A}$ is the crisps set defined by $\underline{A} = \{x \in X \mid \mu_{\underline{A}}(x) > 0\}$

Definition2.3:(core): Thecoreofafuzzyset $\underline{A}$

isthecrispsetofpoints $x \in X$ with $\mu_{\underline{A}} x = 1$.

Definition2.4: (Boundary): Figure 1 shows the area.

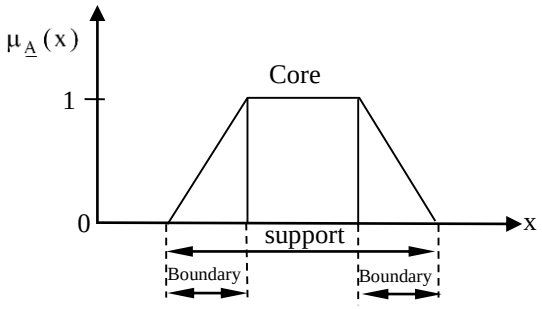

Fig.1: Shows The Area

Definition2.5: (Normality): Afuzzyset $\underline{A}$ is normal if and onlythereexists $x_i \in X$ suchthat $\mu_{\underline{A}}(x_i) = 1$.

Definition2.6: (Sub-normality): Afuzzyset $\underline{A}$ is sub normal if $\mu_{\underline{A}}(x) < 1$.

Definition2.7: (α -cut and strong α -cut). The α -cut of a fuzzy set $\underline{A}$ denoted by $[\underline{A}]_\alpha$ and is defined by $[\underline{A}]_\alpha = \{x \in X \mid \mu_{\underline{A}}(x) \geq \alpha\}$. If $\mu_{\underline{A}}(x) > \alpha$, then $[\underline{A}]_\alpha$ is called *strong* α -cut. It is clear that α -cut (strong α -cut) is a crisp set.

Definition2.8: (Convexity). A fuzzy set $\underline{A}$ on X is *convex* if for any $x_1, x_2 \in X$ and $\lambda \in [0,1], \mu_{\underline{A}}(\lambda x_1 + (1-\lambda)x_2 \geq \min\{\mu_{\underline{A}}(x_1), \mu_{\underline{A}}(x_2)\}$.

It is to be noted that a fuzzy set is convex if and only if its α –cut is convex.

Definition 2.9: (Fuzzy number). A fuzzy number is a fuzzy subset in universal set X which is both convex and normal.

Definition 2.10: A fuzzy number $\underline{A} = \{a, b, c, d\}$ is said to be a trapezoidal fuzzy number if its membership function is given by

$$\mu_{\underline{A}}(x) = \begin{cases} \dfrac{(x-a)}{(b-a)}, & a \leq x < b \\ 1, & b \leq x \leq c \\ \dfrac{(x-d)}{(c-d)}, & c < x \leq d \\ 0, & \text{othersiwe} \end{cases}$$

Definition 2.11: (Trapezoidal Fuzzy number). Let $\underline{A} = (a^L, a^U, \alpha, \beta)$ be the TrFN, where $(a^L - \alpha, a^U + \beta)$ is the support of $\underline{A}$ and $[a^L, a^U]$ is the core of $\underline{A}$.

Arithmetic on Trapezoidal Fuzzy Numbers

Let $\underline{a} = (a^L, a^U, \alpha, \beta)$ and $\underline{b} = \left(b^L, b^U, \gamma, \delta\right)\left(\frac{\pi}{2} - \theta\right)$ be two trapezoidal fuzzy numbers and $x \in R$. We define

$$x > 0, x \in R;\ \ x\underline{a} = \left(xa^L, xa^U, x\alpha, x\beta\right),$$

$$x < 0, x \in R;\ \ x\underline{a} = \left(xa^U, xa^L, -x\beta, -x\alpha\right),$$

$$\underline{a} + \underline{b} = (a^L + b^L, a^U + b^U, \alpha + \gamma, \beta + \delta),$$

$$\underline{a} - \underline{b} = (a^L - b^L, a^U - b^U, \alpha + \delta, \beta + \gamma).$$

RankingFunction

One efficient way to arrange fuzzy numbers is by ranking them. In order to solve linear programming issues including fuzzy parameters, several new kinds of ranking functions have been developed and put into use.

An effective approach for ordering the element of F(R)is to define a ranking function.

Let $\Re : F(R) \to (R)$. We define order on F(R) as follows:

1. $\underline{a} \geq_{\Re} \underline{b}$ iff $\Re(\underline{a}) \geq \Re(\underline{b})$,
2. $\underline{a} >_{\Re} \underline{b}$ iff $\Re(\underline{a}) > \Re(\underline{b})$,
3. $\underline{a} =_{\Re} \underline{b}$ iff $\Re(\underline{a}) = \Re(\underline{b})$
4. $\underline{a} \leq_{\Re} \underline{b}$ iff $\underline{b} \leq_{\Re} \underline{a}$.

Here $\Re$ is the ranking functions, s.t.

$$\Re\left(k\underline{a} + \underline{b}\right) = k\Re(\underline{a}) + \Re\left(\underline{b}\right) \qquad (1)$$

$\Re(\underline{a}) = \int_0^1 (\inf\ \underline{a}_\alpha + \sup \underline{a}_\alpha) d\alpha$ which reduced to

$$\Re(\underline{a}) = \left(a^L + a^U\right) + \frac{1}{2}(\beta - \alpha)$$

For any trapezoidal fuzzy numbers $\underline{a} = \left(a^L, a^U, \alpha, \beta\right)$ and $\underline{b} = (b^L, b^U, \gamma, \delta)$.

We have $\underline{a} \geq_{\Re} \underline{b}$ if and only if $a^L + a^U + \frac{1}{2}(\beta - \alpha) \geq b^L + b^U + \frac{1}{2}(\delta - \gamma)$ (2)

3. FORMULATION OF FUZZY NUMBER TRAVELLING SALESMAN PROBLEM AS FUZZY NUMBER ASSIGNMENT PROBLEMS

A traveling salesperson must stop in 'n' cities before making his way back to the beginning. He is limited to starting from a single city and can only visit each city once.

$$x_{ij} = \begin{cases} 1 \text{ if from city i to city j} \\ 0 \quad \text{otherwise} \end{cases}$$

$$\text{Min } \underline{Z} = \sum_{i=1}^{n} \sum_{j=1}^{n} \underline{C}_{ij} x_{ij}$$

S.C. $\sum_{j=1}^{n} x_{ij} = 1$ for i = 1, 2, ...,n

and $\sum_{i=1}^{n} x_{ij} = 1$ for j = 1, 2, ...,n

with $x_{ij} = 0$ or 1 for all i, j.

$\underline{C}_{ii} = \text{infinity}$.

However, all $\Re(\underline{C}_{ij}) > 0$ and $\underline{C}_{ij} + \underline{C}_{jk} \geq_{\Re} \underline{C}_{ik}$ for all i, j, k.

Table 1. Summarize the provided fuzzy traveling salesman

	1	**2**	**3**	**...**	**…**	**n**
1	∞	$\underline{C}_{12}$	$\underline{C}_{13}$	…	…	$\underline{C}_{1n}$
2	$\underline{C}_{21}$	∞	$\underline{C}_{23}$	...	...	$\underline{C}_{2n}$
3	$\underline{C}_{31}$		∞	…	…	$\underline{C}_{3n}$
M	M	M		...	...	
n	$\underline{C}_{n1}$	$\underline{C}_{n2}$	$\underline{C}_{n3}$	…	…	∞

Procedure

Step 1: Summarize the provided fuzzy traveling salesman issue using tables.

Step 2: Locate the fuzzy cost with the lowest value in each row of the cost matrix. Take each element in that row and deduct this least fuzzy cost element. The initial reduced fuzzy cost matrix is what this is referred to as.

Step 3: All the elements in that column should have this smallest fuzzy cost element subtracted from them. A second reduced fuzzy cost matrix is what this is known as.

Step 4: Put the second reduced fuzzy cost matrix into clear form using the linear ranking function.

Step 5: Choose the best assignment by following these steps:

(i) In order to find a row with exactly one zero, you must examine the rows in sequential order. Enclose the zero element in a box and remove all other zeros from its assigned cell. Continue doing so until you have checked every row. Skip that row and go on to the next one if it contains more than one zero.

(ii) Carry out the process again for each column of the expense reduction matrix. Select a row or column with the fewest zeros if none of the reduced matrix's rows or columns contain any zeros.

Step 6: When the number of cells assigned is equal to the number of rows and columns, we have identified the optimal assignment. There can be a different optimal solution if a zero cell is randomly selected. If there isn't a perfect answer (i.e., certain columns or rows that don't have an assignment), then go to the next step.

Step 7: Follow these steps to draw the smallest possible number of horizontal and/or vertical lines through all of the zeros:

(i) Mark (✓) to those rows where no assignment has been made.
(ii) Mark (✓) to those columns which have zeros in the marked rows.
(iii) Mark (✓) rows (not already marked) which have assignments in marked columns.
(iv) The process may be repeated until no more rows or columns can be checked.
(v) Draw straight lines through all unmarked rows and marked columns.

Step 8: An arbitrary allocation in the positions of the zeros not crossed in step 7 will yield the optimal solution if the minimal number of lines going through all the zeros is equal to the number of rows or columns. If not, proceed to the next section.

Step 9: Here is the updated fuzzy cost matrix:

(i) Identify the elements that are in the space between lines. At the intersection of the two lines, add the

smallest member from both sets and subtract it from all the uncrossed components.
(ii) Everything else that the lines intersect stays the same.

Step 10: When you have reached a good enough fuzzy answer, go back to Step 5 and keep going.

Step 11: If the traveling salesman problem's optimal fuzzy solution meets the route requirement, then step 10 is complete. After that, it provides the best answer to the fuzzy travelling salesman issue. If the current answer does not meet the requirements of the traveling salesman problem, the next best option will be assigned.

.

5. Numerical Examples

Example 1: Solve fuzzy number travelling salesman problem

To CityTable 2

		1	2	3	4
	1	∞	(1, 1.5, 1, 1)	(6, 9, 2, 3)	(2, 3,1, 2)
From City	2	(6,7,1,2)	∞	(9,11,3,4)	(5,5,1,1)
	3	(9,9,1,1)	(8,9,2, 4)	∞	(4, 4,3,2)
	4	(10,11,3,4)	(3,4,2,3)	(7,8,1,3)	∞

Step 1:

To CityTable 3

		1	2	3	4
	1	∞	(-0.5, 0.5,2,2)	(4.5,8,3,4,)	(0.5,2,2,3)
From City	2	(1, 2,2,3)	∞	(4, 6, 4, 5)	(0, 0, 2, 2)
	3	(5,5,3,3)	(4,5,4,6)	∞	(0,0, 4,4)
	4	(6, 8,6,6)	(-1,1,5,5)	(3,5,4,5)	∞

Step 2: Second reduced fuzzy cost matrix

To City Table4

		1	2	3	4
	1	∞	(-1.5, 1.5,7,7)	(-0.5,5,8,8)	(0.5,2,4,5)
From City	2	(-1,1,5,5)	∞	(-1,3,9,9)	(0,0,4,4)
	3	(3,4,6,5)	(3,6,9,11)	∞	(0,0,6,6)
	4	(4,7,9,8)	(-2,2,10,10)	(-2,2,9,9)	∞

Step 3:

To City Table 5

		1	2	3	4
	1	∞	0	4.5	3
From City	2	0	∞	2	0
	3	6.5	10	∞	0
	4	10.5	0	0	∞

Step 4: After you've made an assignment in the first row—which has one zero—and crossed (x) all of the zeros in that column, move on to the next row and examine it in the same manner. The process is the same for each column; after you've made an assignment in the first two columns, cross (x) all the other zeros in that row.

To City Table 6

From City	1	2	3	4
1	∞	[0]	4.5	3.7
2	[0]	∞	2	~~0~~
3	6	11	∞	[0]
4	10	~~0~~	[0]	∞

Optimal solution is

Table 7

City → / City↓	1	2	3	4
1	∞	[–1.5,1.5,7,7]	(-0.5,5,8,8)	(0.5, 2, 4, 5)
2	[–1,1,5,5]	∞	(-1, 3, 9, 9)	~~(0,0,4,4)~~
3	(3, 4, 6, 5)	(3, 6,9, 11)	∞	[0,0,6,6]
4	(4,7,9,8)	~~(–2,2,10,10)~~	[–2,2,9,9]	∞

Table 8

City → / City↓	1	2	3	4
1	∞	~~–1.5,1.5,7,7~~	[–0.5,5,8,8]	(0.5, 2, 4, 5)
2	[–1,1,5,5]	∞	(-1, 3, 9, 9)	~~(0,0,4,4)~~
3	(3, 4, 6, 5)	(3, 6,9, 11)	∞	[0,0,6,6]
4	(4,7,9,8)	[–2,2,10,10]	~~(–2,2,9,9)~~	∞

The optimum solution is

Table 9

City → / City↓	1	2	3	4
1	∞	(1,1.5,1,1)	[6,9,2,3]	(2, 3, 1, 2)
2	[6,7,1,2]	∞	(9,11, 3, 4)	(5, 5, 1, 1)
3	(9, 9, 1, 1)	(8, 9,2, 4)	∞	[4,4,2,2]
4	(10,11,3,4)	[3,4,2,3]	(7, 8, 1, 3)	∞

The optimal route is 1→3→4→2→1and the fuzzy minimum cost is (19, 24, 7,10).

Example 2:

To City Table 10

From City	1	2	3	4
1	∞	(9, 10, 1, 3)	(6, 8, 3, 5)	(8, 9,1, 3)
2	(9,10,2,4)	∞	(10,11,3,1)	(4,5,1,3)
3	(7,8,1,3)	(10,11,3, 4)	∞	(7, 8,2,3)
4	(9,10,3,5)	(10,11,3,4)	(6,8,1,5)	∞

Ans. Step 1:

To City Table 11

		1	2	3	4
From City	1	∞	(1, 4, 6, 6)	(-2,2,8, 8)	(10,3,6,6)
	2	(4,6,5,5)	∞	(5,7,6,2)	(-1,1,4,4)
	3	(-1,1,4,5)	(2,4,6, 6)	∞	(-1, 1,5,5)
	4	(1,4,8,6)	(1,5,8,5)	(-2,2,6,6)	∞

Step 2: Second reduced fuzzy cost matrix

To CityTable 5.12

		1	2	3	4
From City	1	∞	(-4,3,11, 14)	(-4,4,14,14)	(9,4,10,10)
	2	(3, 7,10,9)	∞	(3,9,12,8)	(-2,2,8,8)
	3	(-2,2,9,9)	(-3,3,11,14)	∞	(-2,2,9,9)
	4	(0,5,13,10)	(-4,4,13,13)	(-4,4,12,12)	∞

Step 3:

To City Table 13

		1	2	3	4
From City	1	∞	0.5	0	13
	2	9.5	∞	10	0
	3	0	1.5	∞	0
	4	3.5	0	0	∞

Step 4: After you've made an assignment in the first row—which has one zero—and crossed (x) all of the zeros in that column, move on to the next row and examine it in the same manner. The second row also has a zero, so you'll need to assign a value to it and then cross (x) all the zeros in its column. The process is the same for each column

This leads us to the conclusion,

To CityTable 14

		1	2	3	4
From City	1	∞	2	[0]	13
	2	9	∞	8	[0]
	3	[0]	3	∞	~~0~~
	4	8	[0]	~~0~~	∞

Table 15

City →	**1**	**2**	**3**	**4**
City↓				
1	∞	(-4,3,11,14)	[–4,4,14,14]	(9,4, 10, 10)
2	(3, 7, 10,9)	∞	(3, 9, 12, 8)	[–2,2,8,8]
3	[–2,2,9,9]	(-3, 3,11, 14)	∞	~~(–2,2,9,9)~~
4	(0,5,13,10)	[–4,4,13,13]	~~(–4,4,12,12)~~	∞

Table 16

City →	**1**	**2**	**3**	**4**

City↓				
1	∞	–4,3,11,14	~~–4,4,14,14~~	(9,4, 10, 10)
2	(3, 7, 10,9)	∞	(3, 9, 12, 8)	–2,2,8,8
3	–2,2,9,9	(-3, 3,11, 14)	∞	~~(–2,2,9,9)~~
4	(0,5,13,10)	~~–4,4,13,13~~	–4,4,12,12	∞

Table 17

City →	1	2	3	4
City↓				
1	∞	9,10,1,3	(6,8,3,5)	(8,9, 1,3)
2	(9,10, 2,4)	∞	(10,11,3,1)	4,5,1,3
3	7,8,1,3	(10,11,3, 4)	∞	(7,8,2,3)
4	(9,10,3,5)	(9,11,3,4)	6,8,1,5	∞

The optimal route is 1→2→4→3→1and the fuzzy minimum cost is (26, 31, 4,14).

6. Conclusion

The classical approach to addressing the travelling salesman issue forms the basis of the proposed solution for handling the fuzzy number travelling salesman problem. When compared to the current method, the results from examples 8.1 and 8.2 are comparable. You can use this proposed technique to solve real-world problems because it is effective and straightforward to understand.

References

[1.] Dubois, D. and H. Prade, *Fuzzy Sets and Systems -- Theory and Application* (Academic, New York, 1980).

[2.] Jones, A., A. Kaufmann and H.-J. Zimmermann (eds.), *Fuzzy Sets Theory and Applications* (D. Reidel, Dordrecht, 1985).

[3.] Kaufmann, A. and M.M. Gupta, *Introduction to Fuzzy Arithmetic: Theory and Applications* (Van Nostrand Reinhold, New York, 1985).

[4.] Zimmermann, H.-J., *Fuzzy Set Theory and Its Applications* (Kluwer-Nijhoff, Hinghum, 1985).

[5.] T. J. Ross, Fuzzy Logic with Engineering Applications, John Wiley and Sons, 2004.

[6.] Bellman RE, Zadeh LA .1970. *Decision-making in a fuzzy environment*, Manage. ci., 17: 141-164.

[7.] Hannan EL 1981. *Linear programming with multiple fuzzy goals*. Fuzzy Sets Syst., 6: 235-248

[8.] Hansen MP 2000. *Use of substitute Scalarizing Functions to guide Local Search based Heuristics:* The case of MOTSP, J. Heuristics, 6: 419-431

[9.] Jaszkiewicz A 2002. *Genetic Local Search for Multiple Objectives Combinatorial Optimization*. Eur. J. Oper. Res., 137(1): 50-71.

[10.] Yan Z, Zhang L, Kang L, Lin G 2003. *A new MOEA for multi-objective TSP and its convergence property analysis*. Proceedings of Second International Conference, Springer Verlag, Berlin, pp. 342-354.

[11.] Angel E, Bampis E, Gourvès, L 2004. *Approximating the Pareto curve with Local Search for Bi-Criteria TSP (1, 2) Problem*, Theor. Comp.Sci., 310(1-3): 135-146.

[12.] Paquete L, Chiarandini M, Stützle T 2004. *Pareto Local Optimum Sets in Bi-Objective Traveling Sales man Problem: An Experimental Study*. In: Gandibleux X., Sevaux M., Sörensen K. and Tkindt V. (Eds.), Metaheuristics for Multi-Objective Optimization. Lect. Notes Ec on. Math. Syst., Springer Verlag, Berlin, 535: 177-199.

[13.] Liang TF 2006. *Distribution planning decisions using interactive fuzzy multi-objective linear programming.* Fuzzy Sets Syst., 157: 1303-1316.
[14.] Rehmat A, Saeed H, Cheema MS 2007. *Fuzzy Multi-objective Linear Programming Approach for Traveling Salesman Problem*. Pak. J. Stat. Oper. Res., 3(2): 87-98.
[15.] Javadia B, Saidi-Mehrabad M, Haji A, Mahdavi I, J olai F, Mahdavi-Amiri .N 2008. *No-wait flow shop scheduling using fuzzy multi-objective linear programming*. J. Franklin Inst., 345: 452-467.
[16.] Tavakoli-Moghaddam R, Javadi B, J olai F, Ghodratnama A 2010. *The use of a fuzzy multi-objective linear programming for solving a multi-objective single-machine scheduling problem*. Appl. Soft Comput., 10: 919-925.
[17.] Mukherjee S. and Basu, K. 2010. *Application of fuzzy ranking method for solving assignment problems with fuzzy costs*. International Journal of Computational and Applied Mathematics, 5: 359-368.
[18.] Chaudhuri A, De K 2011. *Fuzzy multi-objective linear programming for traveling sales man problem*. Afr. J. Math. Comp. Sci. Res., 4(2): 64-70.
[19.] Majumdar J, Bhunia AK 2011. *Genetic algorithm for asymmetric traveling salesman problem with imprecise travel times*. J. Comp. Appl. Math., 235: 3063-3078.
[20.] SepidehFereidouni 2011. *Travelling salesman problem by using a fuzzy multi-objective linear programming.* African Journal of mathematics and computer science research 4(11) 339-349
[21.] Amit Kumar and Anil Gupta, 2012. *Assignment and Travelling salesman problems with co-efficient as LR fuzzy parameter*. International Journal of applied science and engineering 10(3) 155-170.
[22.] R.R.Yager, 1981. *A procedure for ordering fuzzy subsets of the unit interval*. Information Sciences, 24, 143-161
[23.] Zadeh LA 1965. *Fuzzy Logic and its Applications*, Academic Press, New York.
[24.] H.R. Maleki, Ranking functions and their applications to fuzzy linear programming, Far East J. Math. Sci. (FJMS) 4 (2002), 283-301.

Morphometric Analysis of a Small River Basin in Coastal Plain of Odisha

Joygopal Jena[1], Prajna Roul[2], B.M.Behera[3], B. Samal[4], Priyadarshini Swain[5]

[1]Dept. of Civil Engineering, GITA Autonomous College, Bhubaneswar,
jenajoygopal@gmail.com
[2]Dept. of Civil Engineering, GITA Autonomous College, Bhubaneswar,
prajnaroul@gmail.com
[3]Dept. of Civil Engineering, GITA Autonomous College, Bhubaneswar,
beherabibhumahima@gmail.com
[4]Dept. of Civil Engineering, GITA Autonomous College, Bhubaneswar,
biswajitsamal293@gmail.com
[5]Dept. of Civil Engineering, GITA Autonomous College, Bhubaneswar,
Priyadarshiniswain.priya@gmail.com

Abstract

Morphometric Analysis is a fundamental means to describe the geo-morphological characteristics and terrain behaviour of river basins. The paper envisages Morphometric Analysis of a small coastal river, the Budhabalanga River in Odisha State in India. In the study ten sub-basins covering 65% of the whole basin has been considered. Traditional simple techniques of utilizing the survey maps of Geological Survey of India (GSI) (topo-sheets) have been used to assess the morphometric parameters for example drainage pattern, channel orde*r* basin shape, area of basin and relief etc. Fundamentals of the Morphometric constraints have been described in details. The analysis demonstrates the feasibility and effectiveness of conducting Morphometric study without the assistance of Geographic Information System (GIS). The key findings of the study include hierarchical orders of the streams, spatial dissemination of the stream pattern and variations in geo-morphological features of land forms. The findings thus obtained from the study results helps in better presentations of hydrological parameters and surface erosion potential.

Key Words: Linear aspects, Morphometric Parameters, Relief aspects, Areal aspects, Budhabalanga Basin

1. Introduction

Morphometry involves the measurement and mathematical evaluation of the Earth's surface configuration, including the shape and dimensions of its landforms (Clarke, 1966). This process is conducted by analyzing the aerial, linear, and relief characteristics of basins and slopes (Nag and Chakraborty, 2003). At the watershed level, morphometric characteristics provide critical insights into its formation and evolution, as all hydrological and geomorphic activities take place within the watershed boundary (Singh, 1992). The morphometric analysis offers a quantitative approach to describing the drainage system, which plays a crucial role in watershed characterization (Strahler, 1964). Over the years, geomorphology has focused on developing quantitative methods to understand the formation and behavior of surface drainage systems (Horton, 1945). This type of analysis is particularly valuable in watershed management, helping to classify natural features such as mountain ranges, plains, groundwater resources, land elevation, slope, and soil quality. Through this approach, key elements like and relief properties are assessed to evaluate the surface characteristics of drainage basins and their networks.To evaluate the basin properties of the basin, measurements in the context of fractions and non-dimensional entities are important for statistical analysis which provides near accurate information independent scale. Morphometric analysis provides in general the followings. These are: (1) Explanation of different characteristics inside the drainage basin, (2) Effective study of physical conditions inside the drainage basin and (3) Detailed report of the useful parameters of the drainage basin.

2. Study Area

Figure 1 shows its various river basins of Odisha. **T**here are eleven river basins. Out of these Mohanadi river basin is the largest and the Bahuda river basin is the smallest one. The present study encompasses the Budhabalanga river basin only.

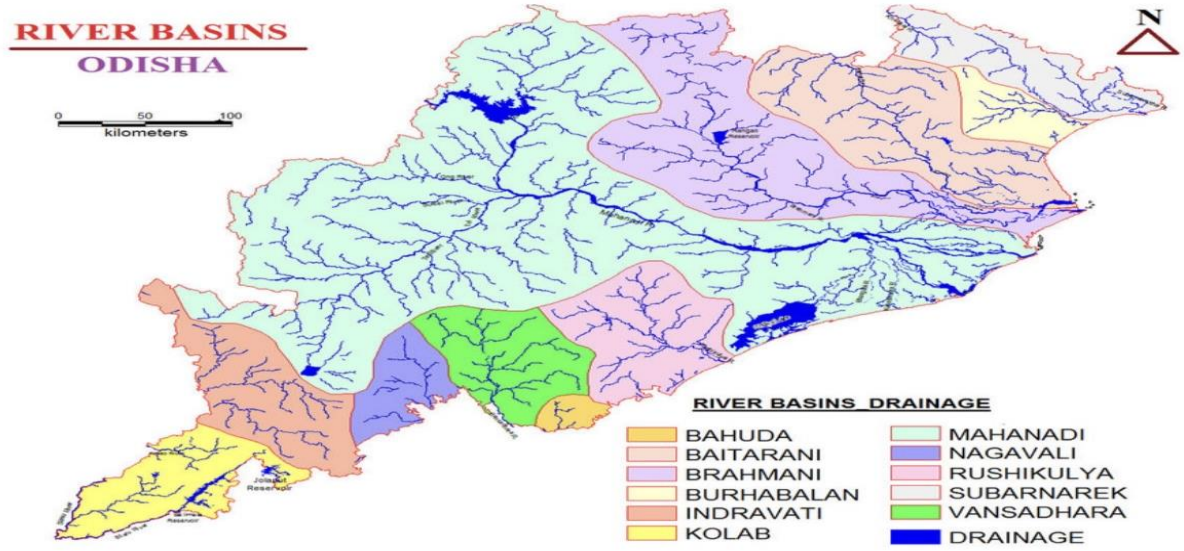

Figure -1 River Basins Map of Odisha

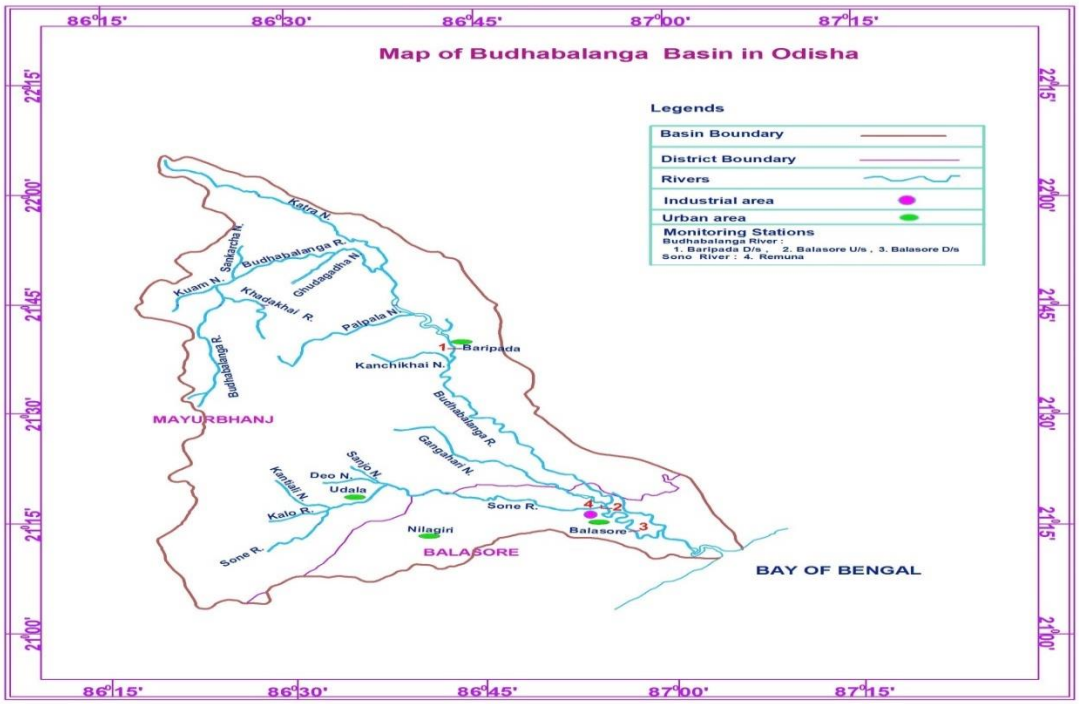

Figure- 2 Map of Budhabalanga River Basin

Figure 2 shows the map of Budhabalanga River basin. In this study various sub-bsins of Budhabalanga river namely Deoriver, Katra river, Khadkhai river, Kuam river, Palpala river, Gharagoddha river, Badajore Nala. Madhabi river and Tangana river were considered totally covering about 65% of the basin area.

The Budhalanga River, originating from the Similipal Hills, cascades through Barehipani Falls, India's second-highest waterfall in Simlipal National Park. Flowing northward to Karnjipal in Bangiriposi, it shifts northeast along the railway track to Jhankapahadi, then turns south to join the Katra Nala. Tributaries like Palpala and Chipat, both hill streams from Similipal, merge with it. Passing through Baripada, the river continues through Balasore district before emptying into the Bay of Bengal.

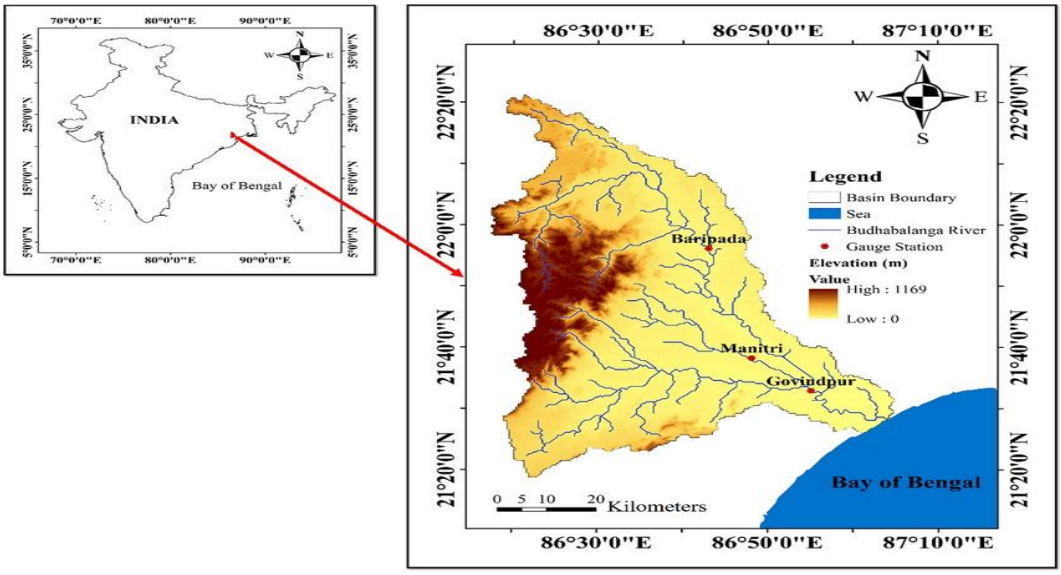

Figure 3. Satellite Map of the Budhabalanga river Basin

Figure 3 shows satellite Map of the said Basin. The Budhabalanga River is about 175km long covering catchment of 4840sqkm. It is bounded by geographical coordinates of north latitudes between $21^0$22'to 22^0 20' and ast longitude $86^0$20' to $87^0$05'. Its major tributaries are: Sone, Gangadhar, and Katra etc.

3. Materials and Methods

3.1 Morphometric Parameters:

Three aspects of morphometric parameters are categorized for analysis, those includes areal, linear and relief aspects. Details of the Parameters are stated briefly as under.

3.1.1 Linear aspects

Linear aspects include of many parameters, which shows measurements of linear aspects of the drainage; such as, basin length, perimeter, stream number, stream order, stream length, mean stream length, ratio of stream length and bifurcation ratios.

3.1.1.1 Basin length (Lb)

The measurement of extent of drainage catchment is known as basin length. It is the maximum length of catchment within a circle of maximum area around the boundary of the basin, that is parallel to the main-stream.

3.1.1.2. Perimeter (P)

In morphometric analysis, catchment perimeter refers to the total length of the boundary that encloses the river's drainage basin. It is a key parameter used to characterize shape and size of basin, providing insights into hydrological and geomorphic processes. Catchment perimeter influences water flow and basin dynamics.

3.1.1.3. Stream order

The classification of stream orders serves as the foundational step in drainage watershed analysis. Initially introduced by Horton (1945) in the United States and later refined by Strahler (1964), this system establishes a hierarchical framework for understanding the connections between various stream segments that comprise a drainage network. In this system, streams are ranked based on their connectivity and tributary relationships.

According to Strahler's method, first-order streams are the smallest and most sensitive branches in a drainage system, characterized by the absence of tributaries. When two first-order streams converge, they form a second-order stream. Similarly, the merging of two second-order streams creates a third-order stream, and this hierarchical process continues for higher orders. The application of this ranking method in the study area provides a systematic approach to analyzing the structure and behavior of the drainage network.

3.1.1.4. Stream number (Nu)

Morphometric stream analysis involves quantifying physical features like length, width, and slope to understand a stream's characteristics. Calculating the stream number, often using Strahler or Shreve methods, assigns a numerical order to each stream based on its tributary pattern. Smaller streams are given a lower order, and when two streams of equal order converge, the resulting stream is assigned the next order. This hierarchical numbering aids in studying watershed organization and stream network complexity, providing valuable insights into hydrological systems and landscape

3.1.1.5. Stream Length (Lu)

Stream length refers to the length of streams within each order in a drainage watershed. It can be measured using ArcGIS software, as per the stream length law proposed by Horton (1945). The total length of streams in a given order is calculated by summing up the lengths of all streams of that specific order.

3.1.1.6. Mean Stream Length (MLu)

Mean stream length is calculated by dividing the total length of streams of a particular order by the number of streams in that order. It is noted that mean stream length tends to increase with stream order, indicating a direct relationship. The formula for calculating mean stream length is as follows:

$$MLu = \frac{\sum_{i=1}^{N} Lu}{Nu} \quad (1)$$

Where:

MLu: Mean stream length

Lu: Total length of streams in the given order

Nu: Total number of streams in the given order

3.1.1.7. Stream Length Ratio (RLu)

Stream length ratio is determined by dividing the total length of streams in a given order (Lu) by the total length of streams in the next lower order. The formula used for this calculation is:

$$RLu = \frac{Lu}{Lu-1} \quad (2)$$

Where MLu is mean stream length, Lu is total length of stream order, and Nu is total number of stream orders. This ratio helps to understand the relationship between stream lengths of consecutive orders.

3.1.2. Areal aspects

This includes drainage strictures those belong to areal features for example, stream frequency, area elongation ratio, drainage density, circularity ratio, drainage texture, constant of channel maintenance and length of surface flow.

3.1.2.1. Basin area (A)

Catchment area of a river, also known as a watershed or drainage basin, is the land surface that contributes water to the river and its tributaries. The catchment area is defined by natural topographic boundaries such as hills and ridges. Its role is crucial role in hydrological processes, inducing water quantity and quality of rivers. Understanding the catchment area is vital for managing water resources, assessing environmental impacts, and planning development of river basins.

3.1.2.2. Stream frequency (Sf)

The stream frequency is demarcated as the ratio between total number of streams of the catchment and the catchment area, and the ratio was first proposed by Horton (1945). The stream frequency is calculated by the following formula;

$$sf = \frac{\sum_{i=1}^{N} Nu}{A} \quad (3)$$

Where $\sum_{i=1}^{N}$ Nu is the total stream number of the watershed,

A is watershed area and Sf is Stream frequency.

3.1.2.3. Drainage density (Dd)

The drainage density is calculated by dividing total length of streams of all orders to the total watershed area by the equation as follows:

$$Dd = \frac{\sum_{i=1}^{N} Lu}{A} \quad (4)$$

Where $\sum_{i=1}^{N} Lu$ is total streams length of all orders,

A is the area of watershed and Dd is Drainage density (km/km2).

3.1.2.4. Drainage texture (Dt)

The drainage texture is one of the most important factor in morphometric study. The drainage texture defined as total stream number of all orders divided by perimeter of the basin.

$$Dt = \frac{Nu}{P} \quad (5)$$

Where Nu is total stream number

P is the parameter of the basin

3.1.2.5. Elongation ratio (Re)

It is the ratio between the diameter of the circle having the same extent as of the watershed and to the maximum length of the watershed.

$$Re = \frac{1.128\sqrt{A}}{Lb} \quad (6)$$

Where, Re is elongation ratio,

A is an basin area, and Lb is the maximum basin Length

3.1.2.6. Circularity ratio (Rc)

The Parameter, circularity ratio is dimensionless and is used as a quantitative method for evaluating and determining the shape of the catment and ranges from zero to one for elongated basin and the spherical catchment. Circularity ratio is computed by the formula below:

$$Rc = \frac{4\pi A}{P^2} \quad (7)$$

Where:

Rc is circularity ratio

A is basin area, and P is basin perimeter

3.1.2.7. Form factor (Ff)

The form factor can be described as number obtained by dividing area of catchment by maximum length square of the same catchment. The shape of the catchment is computed by the equation stated as under.

$$Ff = \frac{A}{L_b^2} \quad (8)$$

Where; Rf, is Form factor which is indicated in catchment area is labelled by A, and Lb is length of the catchment

2.2.8. Constant of channel maintenance (C)

Channel maintenance constant of the catchment can be represented by inverse of drainage density, and is computed by the equation stated under. This constant specifies the area of watershed in km2 required for improving and sustenance of an one km long stream. The formula as stated above:

$$C = \frac{1}{Dd} \quad (9)$$

Where;

C is channel maintenance constant, and Dd is drainage density.

3.1.2.9. Length of overland flow (Lg)

The length of surface flow is defined (Horton, 1945) as a length of path surface flow of rain water on the surface of earth prior to be merged into well-defined channels. It is a significant hydrologic and physiographic parameter that affects the evolution of drains of the, The length of surface flow can be computed by the equation as stated under:

$$Lg = \frac{1}{2 \times Dd} \quad (10)$$

Where;

Lg is the length of surface flow, and

Dd is drainage density.

3.1.2.10. Rho factor (p)-

The rho factor (p) in hydrology a dimensionless factor used for assessing shape of complex river basin. A higher ρ value indicates a more complex basin shape. It's is computed by the formula

$$\rho = \frac{P}{\sqrt{A}} \quad (11)$$

Where;

P is the basin's perimeter and

A is its area.

3.1.2.11. Shape Index (Sw)

The Shape Index Sw of basin of a river indicates its elongation. A higher value signifies a greater elongated shape. Sw is computed by the formula as stated under

$$S_W = \frac{L_b}{W} \quad (12)$$

P is the basin's perimeter

A is its area.

3.1.2.12. Shape factor (R_s)-

The shape factor (R_s) of a river basin characterizes its geometry. This factor helps in estimating the basin's elongation, impact on hydrological activities and land use planning. It is computed using the formula

$$R_s = \frac{L_b^2}{A} \quad (13)$$

Where;

A is the basin's area, and

P is its perimeter.

3.1.3. Relief aspects

Different parameters are important in morphometric analysis those are included relief aspects. They are mainly utilised to understand denudation and development of the catchment. The direction of the water is detected by these factors for example; relief ratio, basin relief, slope of watershed and ruggedness number.

3.1.3.1. Basin relief (Rb)

The basin relief is defined as the level difference between the maximum and minimum altitudes of any location within the catchment. The value of elevation is obtained from the GSI toposheet; by the equation stated as under:

$$Rb = H - h \quad (14)$$

3.1.3.2. Relief ratio (Rr)

The term relief ratio is defined is as ratio of total watershed relief divided by the maximum catchment length adjacent to the main stream path. Higher value of relief indicates steep slope and high relief basin, whereas, lower value specifies hard rock and very gentle slope. Relief Ratio is computed by the equation stated as under:

$$Rr = Rb/Lb \quad (15)$$

Where Rr is relief ratio,

Rb is relief of watershed, and

Lb is basin length.

3.1.3.3. Dissection index (Di)

The dissection index explains the formation of terrains of any basin. The dissection index value varies from 0 to 1. Near zero value specifies a total absence of erosion in vertical direction and dissection indicating the area as flat surface, Vertical cliffs, ridges, and hill slopes or seashore is indicated by higher value of near 1 dissection index. Dissection index computed as per the formula stated below:

$$Di = Rb/aRb \quad (16)$$

Where Di is dissection index, Rb is basin relief, and Rb is absolute basin relief.

3.1.3.4. Ruggedness Number (Rn)

Ruggedness Number is the obtained by multiplying drainage density with watershed relief. It is used for steeper gradient and slope of the catchment. It is also used to define the vulnerability of catchment towards soil erosion. This is calculated by the equation stated below:

$$Rn = Rb \times Dd \quad (17)$$

Where;

symbol Rn is ruggedness number

Rb, watershed relief, and.

Dd is denoted as drainage density

3.2 Methods

This study revolves around the finding various morphometric parameters those includes Areal, Linear, and Relief aspects. Budhabalanga basin of Odisa state is considered for detailed study. All total of ten sub-basins of the said basin are considered. These are: Katra river, Madhabi river, Khadkhai river, Deo river, Palpala river, Badajore Nala. Kuam river, Tangana river and Gharagoddha river. The study area is covered by GSI Topo sheets No 73J/7, 73K/7, 73K/8, 73K/6, 73J/11, 73K/10 3J/12, 73K/9, 73K/11, 73K/13, 73K/14, 73O/2, 73O/3 and 73K/15 with the scale 1:50,000. GIS Topo sheets were used for determining the data of surface features, as the basin is very small comparatively to others and the non-GIS method was used for its easiness. After obtaining the information from the topo-sheets other various aspects are calculated by the stated mathematical formulae.

4.0 Results and Analysis:

The results of morphometric analysis with various parameters such as linear, aerial and the relief parameters for catchments of different sub-basins are presented in Table-1. Drainage area which is very important characteristics that shows the water volume that can be acquired by rainfall. Ten sub-basins have been considered for this study. All total 4840 km2 of drainage area of the sub-basins covered and their total perimeter is 713.5 km. The determination of order and the fluvial hierarchy is the first and foremost significant step in the morphometric characterization of basin. It is always based on the criteria of reference for determining the order of the channels and uses geo-processing methods to determine basin drainage network, that is characterized as 7th order. The watershed area of the Budhabalanga basin has a total length of 214.95 km, including all of its channels. Extensive channels are present throughout the basin. The drain length is directly linked to the topography of channels.

Table 1 Details of Morphometric Parameters

S.N.	Parameters	Units	**Details of Badhabalanga River Sub-basins**									
			Deo Basin	Katra Basin	Sanakacha basin	KhadKhai Basin	Kuam Basin	Palpala Basin	Ghoragadha Basin	Barajora Basin	Madhabi Basin	Tangana Basin
Linear Aspects												
1	Basin Lenth		32.6	44.3	11.25	14.2	10.8	24.15	18.2	18.15	15.65	25.65
2	Basin Perimeter		107.7	128.25	48.9	42.1	45.4	95.4	64.8	48.5	43.15	89.3
3	Maximum Catchment Width		21.3	12.4	13.75	6.6	8.35	11.3	10.7	6.5	6.92	13.65
4	Highest order of Catchment Stream		5	5	4	5	4	5	6	3	4	5
5	Cumulative StreamcSegment		1008	703	225	164	185	520	291	48	70	809
6	Cumulative Stream Length		1415.9	577.75	224.49	187.1	247.05	492.2	508	104.15	168.53	922.3

7	Mean stream length		1.4	0.82	1	1.14	1.34	0.95	1.75	2.17	2.41	1.14
8	Mean stream length Ratio		0.54	0.79	0.55	0.54	0.44	0.58	0.66	0.48	0.38	0.6
9	Mean bifurcation Ratio		11.42	5.73	5.89	3.55	5.9	4.77	2.99	6.44	4.26	4.91
Areal Aspects												
1	Basin Area		382.3	295.2	71.6	76.38	59.3	196.47	135.8	65.54	74.3	154.4
2	Stream Frequency		2.64	2.38	3.14	2.15	3.12	2.65	2.14	0.73	0.94	5.24
3	Drainage Density		3.7	1.96	3.14	2.45	4.17	2.51	3.74	1.59	2.27	5.97
4	Drainage texture		9.36	5.48	46	3.9	4.07	5.45	4.49	0.99	1.62	9.06
5	Elongation Ratio		0.68	0.44	0.85	0.69	0.8	0.65	0.72	0.5	0.62	0.55
6	Circulatory ratio		0.41	0.23	0.38	0.54	0.36	0.27	0.41	0.35	0.5	0.24
7	Form Factor		0.36	0.15	0.57	0.38	0.51	0.34	0.41	0.2	0.3	0.23
8	Constant for Channel Maintenance		0.27	0.51	0.32	0.41	0.24	0.4	0.27	0.63	0.44	0.17
9	Length of Overland flow		0.14	0.26	0.16	0.2	0.12	0.2	0.13	0.31	0.22	0.08
10	Rho Factor		5.51	7.46	5.78	4.82	5.9	6.81	5.56	5.99	5.01	7.19
11	Shape Index		1.53	3.57	0.82	2.15	1.29	2.14	1.7	2.79	2.26	1.88
12	Shape factor		2.78	6.65	1.77	2.64	1.97	2.97	2.44	5.03	3.3	4.26
Relief Aspects												
1	Maximum Elevation of Basin		1080	659	820	1012	870	960	835	-	390	-
2	Minimum Elevation of Basin		50	60	160	180	160	40	90	-	40	-
3	Basin Relief		1030	599	660	832	710	920	745	-	350	-
4	Relief Ratio		31.59	13.52	58.67	58.59	6574	38.11	40.93	-	22.36	-
5	Dissection Index		0.95	0.9	0.8	0.82	0.81	0.95	0.89	-	0.89	-
6	Ruggedness Number		3811	1174.04	2072.4	2038.4	2960.7	2309.2	2786.3	-	794.5	-

5. Conclusion

It is concluded from this investigation of morphometric variables that the said watershed i.e., Budhabalanga basin has low susceptibility for flood. The geological structure, that consists primarily of sandstones and is seen with the presence of quartz accompanying with mountainous relief which is favorable for the erosion of surface by water. The morphometric characterization result indicates important variables, in particular with comparison to horizontal and vertical dissection cards which may help in planning, designing, and management of water resources of the watershed which helps the rural settlement complexity.

References:

[1] Biswas, S., Sudhakar, S. and Desai, V.R. (1999). "Prioritization of Sub watersheds based on Morphometric Analysis of Drainage Basin: A Remote Sensing and GIS Approach. Journal of the Indian Society of Remote Sensing, 27(3): 155-166.

[2] Chakraborti, A.K. (1991 a). Sediment Yield prediction and Prioritization of Watersheds Using Remote Sensing Data. Proe. 12 th Asian Conference on Remote Sensing, Singapore, pp. Q-3-1 to Q-3-6.

[3] Chinnamani, S. (199l). Estimation of Sediment Yield using Remote Sensing., Jalvigyan, Sammeksha. V: 13-18.

[4] Durbuda, D.Cx Purandara, B.K. and Sharma, A. (2001). Estimation Surface Run-off Potential of a Watershed in Semi-Arid Environment- A Case Study. Jour. of Ind. Soc, of Remote Sensing, 29(1&2): 47-58.

[5] Elias Rodrigues da Cunha, Vitor Matheus Bacani (2016) "Morphometric Characterization of a Watershed through SRTM Data and Geoprocessing Technique" Journal of Geographic Information System, 2016, 8, 238-247

[6] Kuldeep Pareta and Upasana Pareta (2011) "Quantitative Morphometric Analysis of a Watershed of Yamuna Basin, India using ASTER (DEM) Data and GIS" International Journal of Geomatics and Geosciences Volume 2, No 1, 2011

[7] Kartic Bera and Jatisankar Bandyopadhyay (2013) "Prioritization of Watershed using Morphometric Analysis through Geoinformatics technology: A case study of Dungra subwatershed, West Bengal, India" Int. Journal of Advances in Remote Sensing and GIS, Vol. 2, No. 1, 2013

[8] Mani, P. Kumar, R. and Chatterjee, C. (2003), Erosion Study of a Part of Majuli River - Island Using Remote Sensing Data. Journal of the Indian Society of Remote Sensing, 31(1): I 1-18.

[9] Murthy, K.S.R. (2000). Groundwater Potential in a Semi-Arid Region of Andhra Pradesh-A GIS Approach. Int. J. of Remote Sensing, 21(9): 1867-1884.

[10] Strahler A. (1952a). Dynamic Basis of Geomorphology. Bull. Geol. Soc. Am., 67: 571-596.

[11] Sarita Gajbhiye, Meshram and S. K. Sharma1 (2017) "Prioritization of watershed through morphometric parameters: a PCA-based approach" Appl Water Sci (2017) 7:1505–1519

[12] Tribhuvan, P.R. and Sonar, M.A. (2016) "Morphometric Analysis of a Phulambri River Drainage Basin (Gp8 Watershed), Aurangabad District (Maharashtra) using Geographical Information System" International Journal of Advanced Remote Sensing and GIS 2016, Volume 5, Issue 6, pp. 1813-1828

[13] V. B. Rekha, A. V. George and M. Rita (2011) "Morphometric Analysis and Micro-Watershed Prioritization of Peruvanthanam Sub-watershed, the Manimala River Basin, Kerala, South India" Environmental Research, Engineering and Management, 2011. No. 3(57), P. 6 – 14